

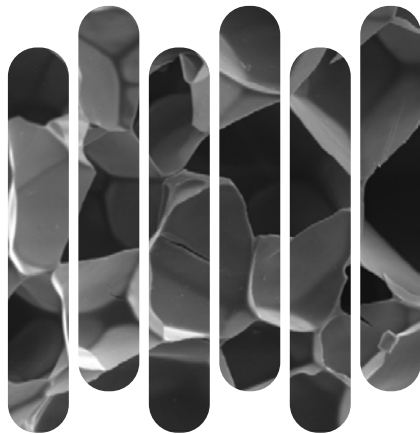


**UNIVERSIDADE ESTADUAL PAULISTA “JÚLIO DE MESQUITA FILHO”
FACULDADE DE ENGENHARIA
CAMPUS DE ILHA SOLTEIRA**

ADHEMAR WATANUKI FILHO

**“PHYSICAL AND MECHANICAL CHARACTERIZATION OF
CEMENT-MORTARS INTERNALLY CURED WITH HYBRID
NANOCOMPOSITES BASED ON HYDROGEL AND NANOCCLAY”**

Ilha Solteira, SP
2021



Ph.D. Thesis

“Physical and mechanical characterization of cement-mortars internally cured with hybrid nanocomposites based on hydrogel and nanoclay.”

Ph.D. thesis presented to the School of Engineering Ilha Solteira/SP as part of the requirements to obtain the Ph.D. degree in Materials Science.

Concentration area: Materials Science and Engineering.

Adhemar Watanuki Filho

Advisor: Prof. Dr. Fauze Ahmad Aouada

FICHA CATALOGRÁFICA

Desenvolvido pelo Serviço Técnico de Biblioteca e Documentação

Watanuki Filho, Adhemar.

W324p Physical and mechanical characterization of cement-mortars internally cured with hybrid nanocomposites based on hydrogel and nanoclay / Adhemar Watanuki Filho. -- Ilha Solteira: [s.n.], 2021
146 f. : il.

Tese (doutorado) - Universidade Estadual Paulista. Faculdade de Engenharia de Ilha Solteira. Área de conhecimento: Ciência e Engenharia dos Materiais, 2021

Orientador: Fauze Ahmad Aouada
Inclui bibliografia

1. Hydrogel. 2. Absorbent polymer. 3. Hybrid nanocomposite. 4. Civil construction. 5. Internal curing. 6. Cloisite Na+.

Rafael de Silva Santos
Rafael de Silva Santos

UNIVERSIDADE ESTADUAL PAULISTA
FACULDADE DE ENGENHARIA DE ILHA SOLTEIRA
SERVIÇO TÉCNICO DE BIBLIOTECA E DOCUMENTAÇÃO
ILHA SOLTEIRA - SP



UNIVERSIDADE ESTADUAL PAULISTA

Câmpus de Ilha Solteira

CERTIFICADO DE APROVAÇÃO

TÍTULO DA TESE: Physical and mechanical characterization of cement-mortars internally cured with hybrid nanocomposites based on hydrogel and nanoclay

AUTOR: ADHEMAR WATANUKI FILHO

ORIENTADOR: FAUZE AHMAD AOUADA

Aprovado como parte das exigências para obtenção do Título de Doutor em CIÊNCIA DOS MATERIAIS, área: Ciência e Engenharia dos Materiais pela Comissão Examinadora:

Prof. Dr. FAUZE AHMAD AOUADA (Participação Virtual)
Departamento de Física e Química / Faculdade de Engenharia de Ilha Solteira - UNESP

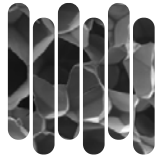
Prof. Dr. MAURO MITSUUCHI TASHIMA (Participação Virtual)
Departamento de Engenharia Civil / Faculdade de Engenharia de Ilha Solteira - UNESP

Prof. Dr. JORGE LUIS AKASAKI (Participação Virtual)
Departamento de Engenharia Civil / Faculdade de Engenharia de Ilha Solteira - UNESP

Prof. Dr. JOÃO VICTOR FAZZAN (Participação Virtual)
Departamento de Construção Civil / Instituto Federal de Educação, Ciência e Tecnologia de São Paulo - IFSP

Prof. Dr. EDUARDO RADOVANOVIC (Participação Virtual)
Departamento de Química / Universidade Estadual de Maringá - UEM

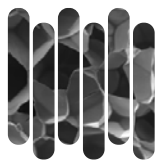
Ilha Solteira, 29 de julho de 2021



Dedication

*Dedico esta tese a meus pais, **Rosária** e **Adhemar** por estarem sempre ao meu lado me apoiando em todas as minhas decisões pessoais, pelas palavras de incentivo, por serem meu exemplo de perseverança e por todo o amor incondicional que me foi concedido.*

*Dedico também a minha amada e companheira **Cássia** pela paciência e amor por toda esta jornada.*



Acknowledgments

A cada ciclo que se encerra ou se inicia devemos ser gratos a tudo que nos conduziu durante esta jornada, por isso, faço uso da palavra “Obrigado” de tamanho singelo, contudo de nobre significado para expor toda minha gratidão:

À Deus, pelo dom da vida, bênçãos concedidas, conhecimentos e ser meu refúgio espiritual em todos os momentos.

Aos meus pais Rosária e Adhemar, pelo exemplo de caráter, honestidade, perseverança e amor incondicional. Por serem meu porto seguro e sempre me incentivar a novos desafios, ir além, desbravar o desconhecido e ter coragem para seguir com humildade e bondade nos caminhos da vida. A vocês todo meu amor e gratidão!

Aos meus irmãos Eduardo e Elys, pelo amor e incentivo! Pela torcida e admiração recíproca, mesmo que as vezes distante. E a toda minha família que sempre ficou na torcida.

Aos meus “pequenos” José Eduardo, Felipe e André, meu afilhado e sobrinhos queridos, que tornaram essa trajetória mais leve, através de um simples sorriso, uma palavra de carinho ou um abraço apertado. A vocês meu orgulho de tê-los como sobrinhos e todo meu amor.

À Cássia por entender minhas ausências neste período, pelo carinho, atenção, amor e parceria. Agradeço a você por me ensinar o verdadeiro sentido do amor e do respeito, por estar ao meu lado em decisões importantes da minha vida, sempre me apoiando com muita delicadeza e acolhimento junto a sua família, ao qual estendo todo meu carinho, respeito e gratidão.

Aos meus amigos de outrora, Adimitri, Fernando, Leticia Nascimbem, Paula Amed, Nilton Pimenta, Rosemeire, Fatinha, Renata Nassar pela torcida e por estarem ao meu lado para o der e vier.

Aos “amigos irmãos” que a pesquisa me presenteou Ana Paula, Elaine, Danilo, Fabricio, Kely, Renan, Uilian, Vanessa Solfa, muito obrigado pelos “cafés com ciência” regados à sorrisos e lágrimas, pela convivência diária, ensinamentos sobre a vida e ciência, e por permitir sonhar, compartilhar e viver tudo isso junto com vocês. Muito obrigado!

Aos alunos de iniciação científica Sabrina, Vitor, Murillo, Giovanna e Lais pela amizade e contribuições. Enfim, ao nosso “nanogrupo” de pesquisa, obrigado.

Ao Prof. Dr. Fauze Ahmad Aouada, por toda orientação, confiança e parceria estabelecida durante esses anos. Obrigado por todas as orientações nos caminhos da Química, vida acadêmica e científica. Agradeço por contribuir na minha formação sem hesitar em compartilhar conhecimento. Ao professor externo toda minha admiração e profunda gratidão!

A todos integrantes do grupo de pesquisa Grupo de Compósitos e Nanocompósitos Híbridos (GCNH) pelo apoio e companheirismo. E a Prof.^a Dr.^a Marcia Regina de Moura Aouada pelo apoio e parceria.

Aos professores Prof. Dr. Mauro Mitsuuchi Tashima e Prof. Dr. Jorge Luís Akasaki por todo apoio dado durante a realização desta pesquisa. Por disponibilizar, laboratórios,

equipamentos e acima de tudo tempo, para que esta pesquisa se concretizasse. Aos professores muito obrigado.

Ao Grupo de Polímeros (GPol) pela utilização do laboratório para as análises de difração de raios-X (DRX), em especial ao professor Dr. José A. Malmonge.

A Universidade Estadual Paulista “Júlio de Mesquita Filho” (UNESP), Faculdade de Engenharia de Ilha Solteira (FEIS), Programa de Pós-Graduação em Ciência dos Materiais (PPGCM), pela oportunidade.

Aos professores e funcionários do Departamento de Física e Química (DFQ) da Faculdade de Engenharia de Ilha Solteira (FEIS).

Aos professores e funcionários do Departamento de Engenharia Civil da Faculdade de Engenharia de Ilha Solteira (FEIS), por disponibilizar acesso a toda infraestrutura de laboratórios do departamento. Em especial, aos técnicos de laboratório Gilson, Flávio e Natália por todo apoio na execução de alguns ensaios.

Aos professores e funcionários do Departamento de Engenharia Elétrica da Faculdade de Engenharia de Ilha Solteira (FEIS), em especial ao Prof. Dr. Ricardo Tokio pelo apoio nas medidas e análises de ultrassom.

Ao Instituto Federal de Educação, Ciência e Tecnologia de São Paulo (IFSP) pelo apoio concedido durante todo o período de afastamento. E ao programa de formação doutoral docente (PRODOUTORAL) pelo incentivo. Aproveito ainda para agradecer ao Prof. Dr. João Fazzan (campus Ilha Solteira) pelo apoio e atenção de sempre!

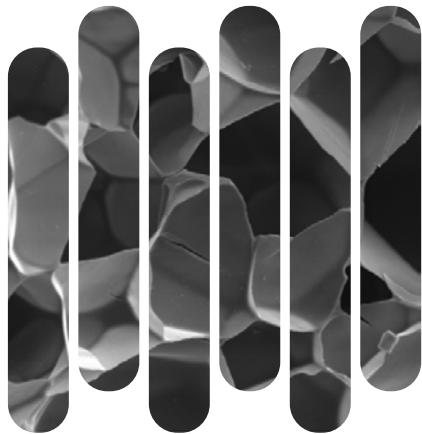
A Embrapa Instrumentação, São Carlos, pela ajuda e apoio científico prestado ao GCNH.

À Coordenação de Aperfeiçoamento de Pessoal de Nível Superior (CAPES) pelo incentivo para realização desta pesquisa.

O presente trabalho foi realizado com apoio da Coordenação de Aperfeiçoamento de Pessoal de Nível Superior - Brasil (CAPES) - *Código de Financiamento 001*.

*“Descobri como é bom chegar quando se tem paciência.
E para se chegar, onde quer que seja, aprendi que não é preciso dominar a força, mas a
razão. É preciso, antes de mais nada, querer” [Amyr Klink].*

*“Existe um limite na mente das pessoas sobre quão longe é seguro ir. Após cruzar essa linha
é impossível voltar atrás” [Fiódor Dostoiévski].*



SCIENTIFIC

PRODUCTION

BOOK CHAPTER

FERNANDES, R. S.; TANAKA, F. N.; ANGELOTTI, A. M.; F JUNIOR, C. R.; YONEZAWA, U. G.; **WATANUKI FILHO, A.**; MOURA, M. R. de ; AOUADA, F. A. Properties, synthesis, characterization, and application of hydrogel and magnetic hydrogels: A concise review. *Advances in Nano-Fertilizers and Nano-Pesticides in Agriculture*, 1 (2021), 437-457, <https://doi.org/10.1016/B978-0-12-820092-6.00017-3> (**Published**)

PAPERS

CILLI, S. L., SILVA, H. C., **WATANUKI FILHO, A.**, AOUADA, M. R. D. M., AOUADA, F. A., Otimização de metodologia de obtenção de pastas cimentícias contendo hidrogéis. *J. Exp. Tech. Instrum.* 2, 1 (2019), 1-9, DOI: 10.30609/jeti.2019-7474. (**Published**).

SIQUERI, V. A., **WATANUKI FILHO A.**, MOURA, M. R. de, AOUADA F. A., Effect of hydrogel nanocomposites on the fresh and hardened properties of cementitious pastes, *Macromol. Symp.*, 394, 1 (2020), 2000047, doi.org/10.1002/masy.202000047 (**Published**).

CALESCO, M. A. F., **WATANUKI FILHO A.**, MOURA, M. R. de, AOUADA F. A., Melhoria das propriedades dos estados frescos e endurecido de argamassas cimentícias ocasionada pela presença de nanocompósito híbridos baseados em hidrogéis de polissacarídeos e nanoargila, *Cerâmica* (2021) (**Under review/ Accepted**)

PUBLICATIONS IN EVENTS

WATANUKI FILHO, A., CILLI, S. L., AKASAKI, J. L., TASHIMA, M. M., DE MOURA, M. R., AOUADA, F. A., Obtenção de argamassas cimentícias com a inserção de hidrogéis de poliacrilamida (PAAm), carboximetilcelulose (CMC) e nanoargila do tipo Cloisita Na⁺. In: *IV Encontro de Pesquisadores em Ciência e Engenharia de Materiais – EPCEM, Ilha Solteira: UNESP, 2018.*

CILLI, S. L., COLLETI SILVA, H., **WATANUKI FILHO, A.**, DE MOURA, M. R., AOUADA, F. A., Otimização de compósitos obtidos a partir de hidrogéis e cimento Portland: investigação mecânica e morfológica. In: *IV Encontro de Pesquisadores em Ciência e Engenharia de Materiais – EPCEM, Ilha Solteira: UNESP, 2018.*

WATANUKI FILHO, A., DE MOURA, MARCIA R; AOUADA, F. A. Propriedades mecânicas de argamassas produzidas com nanocompósitos híbridos baseados em hidrogéis e cimento Portland. In: *23º CBECIMAT – Congresso Brasileiro de Engenharia e Ciência dos Materiais, Foz do Iguaçu, 2018.*

CILLI, S. L., **WATANUKI FILHO, A.**, DE MOURA, M. R., AOUADA, F. A., Analysis of the physical properties of cement pastes containing hydrogels. In: *1º SPIMF – Simpósio de Pesquisa e Inovação em Materiais Funcionais - SPIMF, São Carlos, 2019.*

SIQUERI, V. A., **WATANUKI FILHO A.**, MOURA, M.R. de, AOUADA F. A., Effect of the application of nanocomposites on the bulk density and slump test of cement pastes. In: *1º SPIMF – Simpósio de Pesquisa e Inovação em Materiais Funcionais - SPIMF, São Carlos, 2019.*

WATANUKI FILHO, A., DE MOURA, MARCIA R; AOUADA, F. A. Water absorption, kinetic and structural characterizations of polymeric hydrogels containing Cloisite Na⁺ using cement Portland and water as swelling medium. In: V Reunião Anual sobre Argilas Aplicadas, Franca: UNIFRAN, 2019.

CALESCO, M. A. F., **WATANUKI FILHO, A., MOURA, M. R.; AOUADA, F. A.** Efeito da relação água/cimento sobre as propriedades mecânicas de nanocompósitos baseados em hidrogel polimérico e argamassas cimentícias. In: 61. Congresso Brasileiro do Concreto - IBRACON, Fortaleza, 2019.

WATANUKI FILHO, A., MOURA, M. R., AOUADA, FAUZE A. Efeito da aplicação de nanocompósitos híbridos baseados em hidrogéis e nanoargila nas propriedades mecânicas de argamassas. In: 15º Congresso Brasileiro de Polímeros - CBPOL, Bento Gonçalves, 2019.

CILLI, SABRINA L., **WATANUKI FILHO, A., MOURA, M. R.; AOUADA, F. A.,** Efeito de hidrogel polimérico sobre as propriedades mecânicas e índice de consistência de pastas cimentícias. In: 15º Congresso Brasileiro de Polímeros - CBPOL, Bento Gonçalves, 2019.

SIQUERI, V. A., **WATANUKI FILHO, A., DE MOURA, MARCIA R.; AOUADA, F. A.,** Efeito de nanocompósito sobre as propriedades no estado fresco e endurecido de pastas cimentícias. In: 15º Congresso Brasileiro de Polímeros - CBPOL, Bento Gonçalves, 2019.

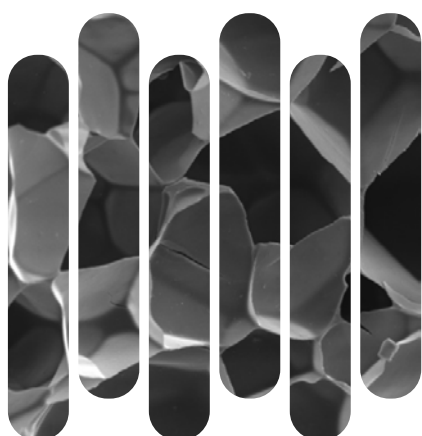
WATANUKI FILHO, A., MOURA, M. R., AOUADA, FAUZE A. Application of hybrid biodegradable nanocomposites based on hydrogel and nanoclay in cement mortars. In: II Encontro de Polímeros Naturais, Ilha Solteira (on line), 2020.

OLIVEIRA, A. P. S., **WATANUKI FILHO, A., MOURA, M. R., AOUADA, F. A.,** Translucent cementitious composites based on mortars and polymeric optical fiber as sustainable alternatives for energy saving. In: II Encontro de Polímeros Naturais, Ilha Solteira (on line), 2020.

BONFIM, K. S., **WATANUKI FILHO, A., AOUADA, F. A, MOURA, M. R.** Effect of oxidation reaction time on water retention properties (WRV) of bacterial cellulose nanofibers. In: II Encontro de Polímeros Naturais, Ilha Solteira (on line), 2020.

CILLI, SABRINA L., **WATANUKI FILHO, A., MOURA, M. R.; AOUADA, F. A.** Technological potential of hydrogels in cementitious pastes: a possible application as an internal curing agent. In: II Encontro de Polímeros Naturais, Ilha Solteira (on line), 2020.

TANAKA, F. C., **WATANUKI FILHO, A., MOURA, M. R.; AOUADA, F. A.** Influence of morphology and Ph on the swelling degree and diquat released properties from methylcellulose-based nanocomposite hydrogels. In: II Encontro de Polímeros Naturais, Ilha Solteira (on line),2020.



ABSTRACT

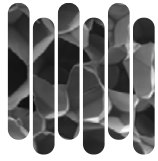
Cement-based materials are the most produced in civil construction due to their versatility and durability. However, new admixtures have been widely studied and applied for better performance, especially when it comes to curing processes. The hybrid nanocomposite hydrogels, characterized by their hydrophilic characteristics of water absorption and release, stand out as promising agents for internal curing in cementitious matrices. This study proposed to analyze the physical, chemical, and morphological properties of hydrogels based on polyacrylamide, carboxymethylcellulose, and three different concentrations of Cloisite Na⁺ in two different swelling media (distilled water and filtered solution of water+Portland cement) and to evaluate the effect of applying 0.5% (wt/wt_{cement}) of these presoaked hydrogels on the fresh and hardened state properties of cementitious mortars (1:2.16 and 0.40 w/c ratio). The results showed that the hydrogels provided reductions in slump flow of up to 4.8% for AHN20 mortars and exudation rate for the fresh state. These observations allowed us to evaluate that the increased concentration of nanoclay in the polymer interferes directly in the kinetic parameters of hydrogels and contributes to greater water retention, which may reflect better hydration and reduction of pathologies. As for the results in the hardened state, it was possible to evaluate that the type of curing of the samples was an important factor since there were no variations in densities (2.18 ± 0.02 g/cm³) of all samples, indicating that the hydrogels were partially or fully swollen during the tests. Loss of mechanical strength was observed, but at 28 days for AHN20 mortars, the results were similar to the control, which corroborates the percentage of voids found. In this case, both mortars had a lower rate of voids when compared to AHN0 and AHN10 mortars and consequently better performances in their mechanical properties. The concentration of nanoclay in the hydrogel controls water release, as observed from the results of mass loss and plastic shrinkage that reduced as this concentration increased. The SEM images allowed us to evaluate that the more uniform matrices with higher mechanical properties, with few pores or micro-cracks. It is concluded that hybrid hydrogel nanocomposites can be applied as internal curing agents, especially those produced with 20% (wt/wt of CMC+AAm) nanoclay. Because its more controlled release allowed reducing porosity, water absorption, shrinkage, and significantly acting on the mechanical properties thus, this type of polymeric additive can be an innovative material for water control improvements in cementitious materials technology.

Keywords: Absorbent polymer, hybrid nanocomposite, civil construction, Cloisite Na⁺, internal curing.

RESUMO

Os materiais de base cimentícia são os mais produzidos na construção civil devido a sua versatilidade e durabilidade. Contudo, para melhores desempenhos, novos aditivos vêm sendo amplamente estudados e aplicado, principalmente ao que se refere aos processos de cura. Destacam-se então os hidrogéis nanocompósitos híbridos caracterizados por suas características hidrofílicas de absorção e liberação de água, como promissores agentes de cura interna em matrizes cimentícias. Este estudo se propôs analisar as propriedades físicas, químicas e morfológicas de hidrogéis baseados em poliacrilamida, carboximetilcelulose e três concentrações diferentes de Cloisita-Na⁺ em dois meios diferentes de intumescimento (água destilada e solução filtrada da mistura de água+cimento Portland), e avaliar o efeito da aplicação de 0,5% (m/m_{cimento}) destes hidrogéis pré-intumescido nas propriedades do estado fresco e endurecido de argamassas cimentícias (1:2,16 e relação a/c=0,40). Os resultados demonstraram que para estado fresco os hidrogéis proporcionaram reduções no *slump flow* de até 4,8% para argamassas AHN20, além de menor taxa de exsudação. Estas observações permitiram avaliar que o aumento da concentração de nanoargila no polímero interfere diretamente nos parâmetros cinéticos dos hidrogéis e contribui para maior retenção de água, o que pode refletir em melhor hidratação e redução de patologias. Quanto aos resultados no estado endurecido, foi possível avaliar que o tipo de cura das amostras interferiu nos resultados, já que não ocorreram variações nas densidades ($2,18 \pm 0,02 \text{ g/cm}^3$) de todas as amostras, indicando que os hidrogéis encontravam-se parcialmente ou totalmente intumescidos durante a realização dos ensaios. A perda de resistência mecânica foi observada, contudo aos 28 dias para as argamassas AHN20 os resultados foram similares ao controle, o que corrobora com a porcentagem de vazios encontrada. Neste caso, ambas argamassas tiveram menor porcentagem de vazios, em relação as argamassa AHN0 e AHN10, e consequentemente melhores desempenhos em suas propriedades mecânicas. Destaca-se também, que a concentração de nanoargila no hidrogel controla a liberação de água, sendo observado a partir dos resultados de perda de massa e retração plástica que reduzem à medida que esta concentração aumentava. As imagens de SEM permitiram avaliar que as matrizes com maiores propriedades mecânicas são mais uniformes, com poucos poros ou microfissuras. Conclui-se que os hidrogéis híbridos nanocompósitos podem ser potencialmente aplicados como agentes de cura interna, em destaque para os produzidos com 20% (massa/ massa de CMC+AAM) de nanoargila, uma vez que sua liberação mais controlada permitiu reduzir aspectos como porosidade, absorção de água, retração e atuar significativamente nas propriedades mecânicas. Assim, este tipo de aditivo polimérico pode ser um material inovador no para melhorias no controle de água na área da tecnologia de materiais cimentícios.

Palavras-chaves: Polímero absorvente, nanocompósito híbrido, construção civil, Cloisita Na⁺, cura interna.



List of figures

| | |
|---|----|
| Figure 1.1 – Representative chemical structure of acrylamide (AAm) monomer..... | 6 |
| Figure 1.2 – Representative chemical structure of carboxymethylcellulose..... | 7 |
| Figure 1.3 – Structure of MMT Cloisite- Na^+ nanoclay, adapted from Bao et.al, 2015. [70]..... | 8 |
| Figure 1.4 – Type of mineral clay dispersion in hydrogel, adapted from Bensadoun et. al [76]..... | 8 |
| Figure 2.1 – Schematic representation of the hybrid nanocomposite hydrogels synthesis (Source: Author’s own graphical)..... | 21 |
| Figure 2.2 – Graphical representation of the mortar preparation (Source: Author’s own graphical). ... | 24 |
| Figure 3.1 – Graphical representation of the solution from the filtrate of the water+cement mixture preparation (Source: Author’s own graphical)..... | 28 |
| Figure 3.2 - FTIR spectra of PAAm/ MBAAm/ CMC + Cloisite Na^+ swollen in (a) distilled water, and (b) solution from the filtrate of the water+cement mixture..... | 32 |
| Figure 3.3a - X-ray diffraction for PAAm/ MBAAm/ CMC + Cloisite Na^+ swollen in distilled water. | 34 |
| Figure 3.3b - X-ray diffraction for PAAm/ MBAAm/ CMC + Cloisite- Na^+ swollen in solution from the filtrate of the water+cement mixture..... | 35 |
| Figure 3.4 - SEM micrographs (5000x magnification) of hydrogel swelled in distilled water: (a) PAAm+CMC, (b) PAAm+CMC+10% Cloisite Na^+ , (c) PAAm+CMC+20% Cloisite Na^+ | 37 |
| Figure 3.5 - SEM micrographs (500x and 10000x magnification) of hydrogel swelled solution from the filtrate of the water+cement mixture: (a-b) PAAm+CMC, (c-d) PAAm+CMC+10% Cloisite Na^+ , (e-f) PAAm+CMC+20% Cloisite Na^+ | 38 |
| Figure 3.6 - Swelling curves as a function of time for hydrogels with different Cloisite Na^+ concentration in (a) distilled water and, (b) solution from the filtrate of the water+cement mixture. ... | 40 |
| Figure 3.7 - Effect of the amount of Cloisite Na^+ on the equilibrium swelling degree..... | 41 |
| Figure 4.1 – Density in the fresh state for mortars produced with different Cloisite Na^+ nanoclay hydrogels and water/cement of 0.40. | 57 |
| Figure 4.2 – Relation between density in the fresh state and air content (%) for mortars produced with different Cloisite Na^+ nanoclay hydrogels. | 58 |
| Figure 4.3 – Comparative of the water retention for mortars containing nanocomposites prepared from different Cloisite Na^+ nanoclay amount and water/cement of 0.40..... | 60 |
| Figure 4.4 – Comparative of the consistency index for mortars with different water/cement ratios (a); different Cloisite Na^+ nanoclay hydrogels and water/cement of 0.40 (b). | 62 |
| Figure 4.5 – Exudation index as the function of time for cement-mortars with different Cloisite Na^+ nanoclay hydrogels and water/cement of 0.40. | 65 |
| Figure 5.1 – Comparative of the evolution of bulk density over time for mortars control and mortars produced with 0, 10, and 20% Cloisite Na^+ nanoclay hydrogels. | 79 |
| Figure 5.2 – Flexural strength of control and mortars produced with 0, 10, and 20% Cloisite Na^+ nanoclay hydrogels at various ages..... | 80 |
| Figure 5.3 – Tensile strength mortars control and mortars produced with 0, 10, and 20% Cloisite Na^+ nanoclay hydrogels at various ages..... | 82 |

Figure 5.4 – Evolution of compressive strength over time for mortars produced with 0, 10, and 20% Cloisite Na⁺ nanoclay hydrogels.83

Figure 5.5 – Dynamic elastic modulus at 7 and 28 d obtained by ultrasonic velocity for mortars produced with 0, 10, and 20% Cloisite Na⁺ nanoclay hydrogels.86

Figure 5.6 – Elastic modulus at 7 and 28 d for mortars produced with 0, 10, and 20% Cloisite Na⁺ nanoclay hydrogels. *Average with their respective standard deviation values, followed by equal letters do not differ statistically from each other following the Tukey test with a 95% confidence level.87

Figure 5.7 – Volume of permeable pore space (voids) at 28 d for mortars produced with 0, 10, and 20% Cloisite Na⁺ nanoclay hydrogels, in two different conditions: (a) dry and (b) wet curing.*Average with their respective standard deviation values, followed by equal letters do not differ statistically from each other following the Tukey test with a 95% confidence level.89

Figure 6.1 – Effect of hydrogels with different Cloisite Na⁺ concentrations in water absorption (%) of cement-mortars over time. *Average with their respective standard deviation values, followed by equal letters do not differ statistically from each other following the Tukey test with a 95% confidence level.100

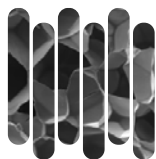
Figure 6.2 – Capillarity coefficient (g/dm²*min^{0.5}) of mortars at 28 days produced without or with different nanocomposites hydrogels. *Average with their respective standard deviation values, followed by equal letters do not differ statistically from each other following the Tukey test with a 95% confidence level.102

Figure 6.3 – Relation between relative humidity variation (%) and weight loss (g) of mortars produced without or with different nanocomposites hydrogels, over time.104

Figure 6.4 – Evolution of dry shrinkage (mm/m), over time, of cement mortars without and with hydrogel nanocomposites in different curing media (a) wet curing (35+2°C and 98% RHexternal); (b) Controlled curing (35+2°C and 55% RHexternal); (c) External curing (30+2°C and 46% RHexternal). *Average followed by equal letters does not differ statistically from each other following the Tukey test with a 95% confidence level.106

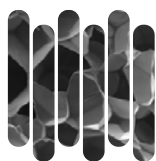
Figure 6.5 – Relation between drying shrinkage (mm/m) and mass variation (%) of the cement mortars without and with hydrogel nanocomposites in different curing media (a, b) wet curing (35+2°C and 98% RHexternal); (c, d) Controlled curing (35+2°C and 55% RHexternal); (e, f) External curing (30+2°C and 46% RHexternal). *Average followed by equal letters does not differ statistically from each other following the Tukey test with a 95% confidence level.110

Figure 6.6 – SEM images of the cement mortars (a) ACTR (control) at 7 days, (b) ACTR (control) at 28 days, (c) AHN0 at 7 days, (d) AHN0 at 28 days, (e) AHN10 at 7 days, (f) AHN10 at 28 days, (g) AHN20 at 7 days and (h) AHN20 at 28 days.112



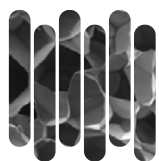
List of tables

| | |
|---|-----|
| Table 2.1 - Chemical composition of cement Portland CII-Z-32 [1]..... | 22 |
| Table 2.2 - Physical properties of cement Portland CII-Z-32 [2] | 23 |
| Table 2.3 - Design of mix proportion of mortars samples | 23 |
| Table 3.1 - Main FTIR spectroscopic assignments PAAm/MBAAm/CMC + Cloisite Na ⁺ FTIR (distilled water or water + Portland cement solution as swelling medium) | 31 |
| Table 3.2 - Values of k and n obtained for different concentrations of Cloisite Na ⁺ in the hydrogels swelled in distilled water and solution from the filtrate of the water+cement mixture media. | 43 |
| Table 4.1 - Average value and standard deviation to physical properties in the fresh state to different mortars..... | 66 |
| Table 6.1 - Average value and standard deviation to mechanical properties in the hardened state to different mortars. *Average followed by equal letters does not differ statistically from each other following the Tukey test with a 95% confidence level. | 113 |
| Table 6.2 - EDX analysis for mortars produced with and without nanocomposite hydrogel. | 114 |



List of abbreviations and symbols

| | |
|---|--|
| AAm | Acylamide |
| C ₂ S | Calcium disilicate or belite |
| C ₃ A | Tricalcium aluminate or aluminat |
| C ₃ S | Calcium trisilicate or alite |
| C ₄ AF | Tetracyclic iron or ferrite |
| Ca(OH) ₂ | Calcium hydroxide |
| CMC | Carboxymethylcellulose |
| C-S-H | Hydrated calcium silicate |
| EDX | Energy Dispersive X-Ray Analysis |
| FTIR | Fourier-transform infrared spectroscopy |
| <i>k</i> | Diffusion coefficient |
| KBr | Potassium bromide |
| MBAAm | N'-N-Methylenebisacrylamide |
| MMT | Montmorillonite |
| MW | Molecular Weight |
| <i>n</i> | Diffusion exponent |
| N ₂ | Elemental nitrogen gas |
| Na ₂ S ₂ O ₈ | Sodium Persulfate |
| PAAm | Polyacrilamide |
| RH | Relative Humidity |
| SAP | Superabsorbent Polymer |
| SD | Sweeling degree |
| SEM | Scanning Electron Microscopy |
| TEMED | N,N,N',N'-tetramethyl-ethylenediamine |
| w/c | water/cement ratio |
| wt | weight |
| XDR | X-Ray Diffraction |
| XRF | X-Ray fluorescence |
| θ | Incidence angle between the incident beam and sample plane |
| λ | Wavelength of the beam incident on the sample |
| \varnothing | Diameter |



Contents

| | |
|---|----|
| CHAPTER 1 - INTRODUCTION | 1 |
| 1.1 OVERVIEW | 2 |
| 1.2 HYDROGELS | 4 |
| 1.3 HYBRID HYDROGELS | 5 |
| 1.4 MOTIVATIONS AND JUSTIFICATIONS | 9 |
| 1.5 OBJECTIVES | 11 |
| 1.6 THESIS STRUCTURE | 12 |
| 1.7 REFERENCES | 13 |
| CHAPTER 2 – MATERIAL AND GENERAL METHODOLOGY | 20 |
| 2.1 HYDROGEL SYNTHESIS | 21 |
| 2.2 MORTAR PREPARATION | 22 |
| 2.3 REFERENCES | 24 |
| CHAPTER 3 - HYDROGELS | 26 |
| 3.1 OVERVIEW | 27 |
| 3.2 EXPERIMENTAL | 28 |
| 3.2.1 PAAm/ CMC and Cloisite Na ⁺ nanocomposites synthesis | 28 |
| 3.2.2 Water + Portland cement type CII-Z-32 solution preparation | 28 |
| 3.2.3 Fourier transform infrared spectroscopy (FTIR) | 29 |
| 3.2.4 X-ray diffraction (XRD) | 29 |
| 3.2.5 Scanning electron microscopy (SEM) | 29 |
| 3.2.6 Swelling degree (SD) in distilled water or water + Portland cement solution | 29 |
| 3.2.7 Kinetic parameters | 30 |
| 3.2.8 Statistical analysis | 30 |
| 3.3 RESULTS AND DISCUSSION | 31 |
| 3.3.1 Fourier transform infrared spectroscopy (FTIR) | 31 |
| 3.3.2 X-ray diffraction (XRD) | 34 |
| 3.3.3 Scanning electron microscopy (SEM) | 36 |
| 3.3.4 Swelling degree (SD) | 39 |
| 3.3.5 Kinetic parameters | 43 |
| 3.4 CONCLUSIONS | 44 |
| 3.5 REFERENCES | 45 |
| CHAPTER 4 – FRESH PROPERTIES OF MORTARS | 50 |
| 4.1 OVERVIEW | 51 |
| 4.2 EXPERIMENTAL | 53 |
| 4.2.1 Hydrogel synthesis and mortar preparation | 53 |
| 4.2.2 Density in the fresh state | 53 |
| 4.2.3 Air content | 54 |
| 4.2.4 Water retention | 54 |
| 4.2.5 Consistency index | 55 |
| 4.2.6 Exudation test | 56 |
| 4.2.7 Statistical analysis | 56 |

| | |
|--|-----|
| 4.3 RESULTS AND DISCUSSION | 56 |
| 4.3.1 Density in the fresh state | 56 |
| 4.3.2 Air content..... | 58 |
| 4.3.3 Water retention..... | 60 |
| 4.3.4 Consistency index | 61 |
| 4.3.5 Exudation index | 64 |
| 4.4 CONCLUSIONS | 66 |
| 4.5 REFERENCES..... | 67 |
| | |
| CHAPTER 5 – HARDENED PROPERTIES OF MORTARS: PART 1..... | 74 |
| 5.1 OVERVIEW | 75 |
| 5.2 EXPERIMENTAL | 75 |
| 5.2.1 Hydrogel synthesis and mortar preparation..... | 75 |
| 5.2.2 Bulk density | 76 |
| 5.2.3 Flexural strength..... | 76 |
| 5.2.4 Tensile strength | 76 |
| 5.2.5 Compressive strength | 77 |
| 5.2.6 Dynamic elastic modulus | 77 |
| 5.2.7 Elastic modulus | 78 |
| 5.2.8 Volume of permeable voids spaces | 78 |
| 5.2.9 Statistical analysis | 79 |
| 5.3 RESULTS AND DISCUSSION | 79 |
| 5.3.1 Bulk density | 79 |
| 5.3.2 Flexural strength..... | 80 |
| 5.3.3 Tensile strength | 81 |
| 5.3.4 Compressive strength | 83 |
| 5.3.5 Dynamic elastic modulus | 85 |
| 5.3.6 Elastic modulus | 87 |
| 5.3.7 Volume of permeable pore space (voids)..... | 88 |
| 5.4 CONCLUSIONS..... | 90 |
| 5.5 REFERENCES..... | 90 |
| | |
| CHAPTER 6 – HARDENED PROPERTIES OF MORTARS: PART 2..... | 94 |
| 6.1 OVERVIEW | 95 |
| 6.2 EXPERIMENTAL | 96 |
| 6.2.1 Hydrogel synthesis and mortar preparation..... | 96 |
| 6.2.2 Water absorption | 96 |
| 6.2.3 Capillarity coefficient..... | 97 |
| 6.2.4 Weight loss..... | 98 |
| 6.2.5 Drying shrinkage | 98 |
| 6.2.6 Scanning electron microscopy (SEM) and Energy-Dispersive X-Ray (EDX) Spectroscopy .. | 99 |
| 6.2.7 Statistical analysis | 100 |
| 6.3 RESULTS AND DISCUSSION | 100 |
| 6.3.1 Water absorption | 100 |
| 6.3.2 Capillarity coefficient..... | 102 |
| 6.3.3 Weight loss..... | 104 |
| 6.3.4 Dry shrinkage and mass variation | 105 |
| 6.3.5 SEM-EDX analysis | 111 |
| 6.4 CONCLUSIONS..... | 114 |

6.5 REFERENCES.....115

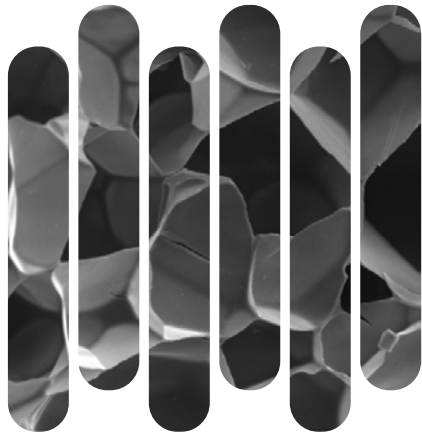
CHAPTER 7 – FINAL CONSIDERATIONS121

7.1 FINAL CONSIDERATIONS122

7.2 FUTURE PERSPECTIVES123

7.3 IMPACTS AND ECONOMIC, SOCIAL RELEVANCE124

7.4 ACKNOWLEDGMENTS..... 125



CHAPTER 1

INTRODUCTION

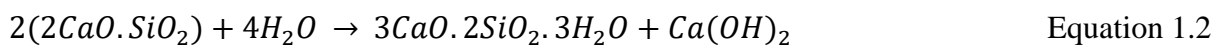
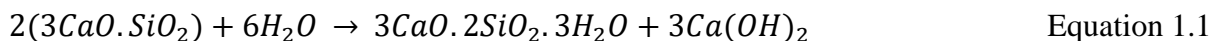
1.1 OVERVIEW

Cement-based materials are defined as some products obtained from the use of a cementitious medium [1]. These are generally characterized by the basic mixture of a hydraulic binder with the presence or not of aggregates [2], whose chemical reactions of setting and hardening occur in water presence [3-5].

Portland cement is widely used as a binder [6], confirmed by the high global production of approximately 4100 Mt in 2019 [7]. Recent data showed that cement production in Brazil was about 4.7 Mt in February 2021, representing an increase of around 14% compared to the same period in 2020 [8]. Thus, it is important to know that cement production is complex. It involves four main stages, such as crushing and grinding of raw materials, homogenization of the materials (limestone, clay, iron oxides, etc.) [9] in the correct proportions, burning the prepared mix in a rotary kiln at 1450 °C [9], and grinding clinker together with gypsum.

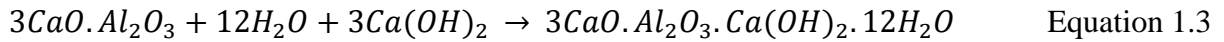
Calcium sulfate or gypsum is added to the clinker in small concentrations (~5%) to control the setting time due to the high clinker reactivity with water [8]. Elemental clinker chemistry composition presents around 67% CaO, 22% SiO₂, 5% Al₂O₃, 3% Fe₂O₃, and 3% other compounds. Four phases are denominated calcium trisilicate or alite (C₃S), calcium disilicate or belite (C₂S), tricalcium aluminate or aluminite (C₃A), and tetracyclic iron or ferrite (C₄AF) are formed. They are responsible for the hardening and strength increase because of the reaction these with water [10].

Thus, C₃S and C₂S silicates are important compounds for cement materials because their contact with water is responsible for forming hydration products, such as hydrated calcium silicate (C₃S₂H₃) or C-S-H gel. In addition, some amounts of crystalline calcium hydroxide Ca(OH)₂ or portlandite [1], whose chemical reactions are expressed by Equations 1.1 and 1.2 [6, 10]:

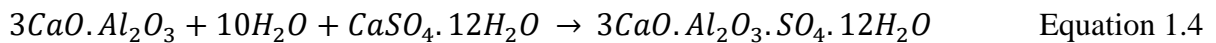


C₃A presence in Portland cement contributes poorly to strength development, but it can be beneficial in manufactured types of cement where they facilitate silica and limestone combinations [11]. It should be noted that C₃A reactions with water (Equation 1.3) are fast

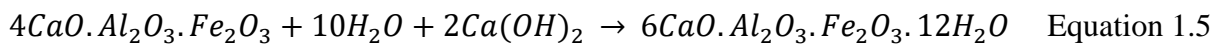
and could cause a quick hardening that can be prevented with the gypsum addition to the clinker [6].



Its reaction with the gypsum results in ettringite crystals, as presented by Equation 1.4 [10].



C₄AF is also present in cement in small quantities compared to the other three compounds, and it does not significantly affect the cement-paste behavior. However, C₄AF reacts with the gypsum resulting in calcium sulfoferrite that can accelerate the hydration of silicates [1, 11]. C₄AF reactions with water (Equation 1.5) are slower concerning C₃A, and these can result in a final compound based on iron (III) oxide or hydroxide.



Although the chemical reactions involved in the hardening and strength gain are complex, aspects such as easier handling, good mechanical properties, and durability, performance satisfactory [12] of pastes, mortars, or concretes, depending on their combination or not with aggregates [13], make Portland cement the second material most used in the civil construction world rank [14].

Pastes, mortars, and concretes as main cement products are widely researched to obtain materials with satisfactory properties in their fresh and hardened states [15]. The main purpose is to develop cementitious composites to reduce pathological manifestations such as plastic shrinkage, cracking, increased permeability and porosity, and improve their durability and performance [16] over time. In this way, the development of new admixtures contributes to the insertion of chemical concepts in the construction industry to produce special cementitious materials [17] with better physical properties, such as increased setting time, reduced water/binder ratio, porosity, and shrinkage reduction [18].

Several mitigations strategies to avoid pathologies are based on the use of admixtures. Thus, these are most frequently applied to aid in controlling the dosage of water, once it is one of the elements that can change the properties of cementitious materials in their fresh and

hardened states. Water control in cementitious materials is important because the hydration degree changes the mechanical behavior since effective cement particles' hydration results in a homogeneous microstructure [19, 20] and, consequently, a denser matrix.

In this way, hydrogels acting as a polymeric additive can contribute to the internal hydration of cement-matrix and act as small reservoirs of slow-release water.

1.2 HYDROGELS

Hydrogels are also known as hydrophilic absorbent polymers. They are three-dimensional (3D) cross-linked chain materials [21, 22] synthesized from synthetic, semi-synthetic, or natural raw materials whose main function is to absorb large amounts of water or other fluid [23] and release it later. Some authors define hydrogel as polymeric systems capable of swelling in water and retaining a significant fraction (>20%) of water inside their 3D structure without dissolving in this medium [21, 24]. The water storage of the hydrogels occurs from polymeric chain expansion due to the repulsion from the hydrophilic groups present on polymeric chains such as -OH-, -NH₂-, -COOH-, -CONH₂-, -SO₃H- [25, 26].

The interaction between chain networks and water is through capillary, osmotic, and hydration forces causing expansion of these chains [21, 27]. Thus, when the osmotic and hydration forces are counter-balanced with the elastic forces, the hydrogel no longer absorbs more water, reaching its swelling equilibrium [28, 21]. Such equilibrium state of these absorbent polymers determines some properties, such as internal transport, diffusion characteristic, and mechanical strength [29].

Hydrogels can be classified from the chemical nature of their side groups, the type of the chemical crosslinking, the type of raw material, etc. According to the side groups, hydrogels can be neutral when the side groups have no electrical charge or ionic, when side groups dissociate and they interact with other elements, i.e., they have positive (anion) or negative (cation) charges [30-33]. Classification from the crosslinking process is based on the type of three-dimensional networks established by polymer synthesis, which allows these to be denominated chemical, physical [34], or biochemical hydrogels [35]. Chemical-type hydrogels are characterized by chemical cross-links (covalent bonds). They can no longer be undone [36, 37] because the covalent bonding introduces mechanical integrity and degradation resistance to the hydrogel. While physical hydrogels are formed by physical interactions such as van der Waals forces and hydrogen bonds, their networks can be undone through a change in environmental conditions such as pH changes, temperature, or saline

solution [38, 39]. In biochemical hydrogels, biological agents like enzymes or amino acids participate in the gelation process [35]. As mentioned, another important classification of hydrogels is about the constituent raw material of their matrices, which can be based on natural, semi-synthetic, or synthetic polymers. Natural hydrogels are synthesized from biodegradable materials such as polysaccharides [40], alginate [41], cellulose and their derivatives, pectin, gelatin, chitosan [42], etc., and they are considered as ‘ecologically-friendly products due to their renewable and non-toxic sources [43]. All of these materials are naturally abundant. They present satisfactory characteristics to their synthesis, such as biocompatibility [41, 44], water-solubility, a high swelling degree that permits a wide range of chemical structures [45]. On the other hand, this hydrogel type presents a low mechanical resistance, but the association with synthetic raw materials during the synthesis process can improve it [45].

Remarkably, some natural hydrogel applications are in drug delivery systems, tissue engineering [46], and agricultural field due to their unique characteristics such as satisfactory hydrophilic network and adsorption capacity [47], low-cost and straightforward synthesis, non-toxicity of the final material, and easy application [48].

Synthetic hydrogels are materials commonly applied in numerous fields due to their interesting properties, such as large water absorption capacity and reasonable strength and cost [21]. Typically, synthetic hydrogels are obtained from raw materials like poly(hydroxyalkyl methacrylates), polyacrylates, poly(acrylic acid), polyacrylamide, and polymethacrylamide and its derivatives as poly(N-vinyl-2-pyrrolidone) and poly(vinyl alcohol), among others [21]. In addition, these polymers are applied in effluents treatment [42], as drug release systems, and medical field [49].

Sometimes, it is necessary to develop blends using natural and synthetic materials to obtain polymeric matrices that include the properties of natural and synthetic polymers simultaneously. First, however, it is important to understand the interaction between the two components so that the semi-synthetic hydrogel obtained can satisfy the application needs [50].

1.3 HYBRID HYDROGELS

Hybrid hydrogels are polymers composed of chemically, functionally, and morphologically distinct blocks, including natural, synthetic raw materials or nano/microstructures interconnected via physical or chemical means. In this way, the type-

hydrogel has been developed to improve existing formulations and to expand the range of applications [51]. Thus, this research is based on applying nanocomposite hybrid hydrogel based on polyacrylamide (PAAm), carboxymethylcellulose polysaccharide (CMC) Cloisite Na⁺ nanoclay in cementitious matrices. The choice for this hybrid hydrogel was based on the properties of each component to obtain a hybrid nanocomposite with appropriate characteristics to be applied as an internal curing agent for cementitious materials.

Firstly, it is important to understand the contribution of each raw material used in hydrogel formulations and its impact on the final behavior of the polymer obtained. Hydrogels based on polyacrylamide (PAAm) have been applied frequently in several areas (agricultural, biomedical, pharmaceutical area) [52] due to their properties, such as high hydrophilicity and good mechanical behavior. They are synthesized from synthetic acrylamide (AAm) monomer (Figure 1.1).

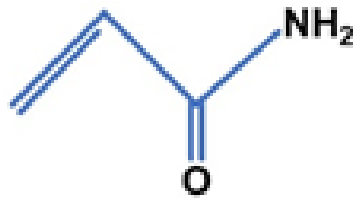


Figure 1.1 – Representative chemical structure of acrylamide (AAm) monomer.

Polyacrylamide hydrogels consist of a covalent polymer network and water; under ordinary conditions, the polyacrylamide network is stable, and water is mobile into the polymer network [53]. Because of their mechanical properties and hydrophilicity, this type-hydrogel has been widely used as the main base in developing new types of absorbent polymers [54].

Another interesting type of absorbent polymer widely researched is the polysaccharide-based hydrogel due to its biocompatibility, biodegradability, high water absorption capacity, and production from renewable raw materials [55,56]. Carboxymethylcellulose (CMC) (Figure 1.2) is a cellulose derivative [57], and its main properties are water-soluble anionic polysaccharide, non-toxicity, biodegradability [58], and owing its features, CMC is used in various areas such as food packaging [59], drug delivery [60] and tissue engineering.

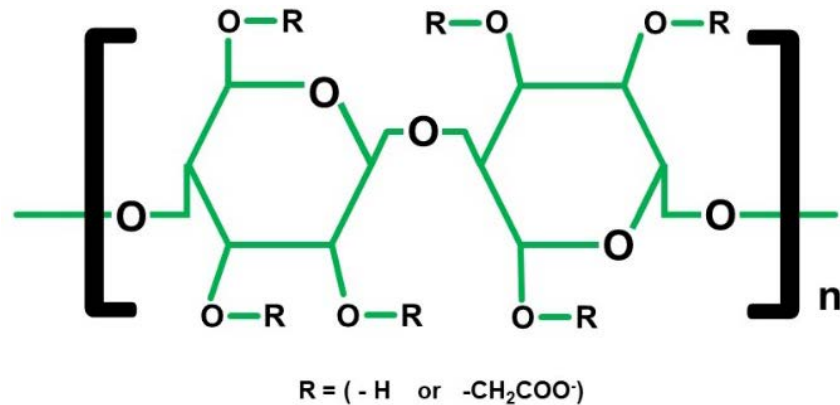


Figure 1.2 – Representative chemical structure of carboxymethylcellulose.

Moreover, CMC can be obtained by reacting cellulose with sodium hydroxide [61] and monochloroacetic acid. This procedure is necessary because cellulose is hydrophilic but insoluble in water due to the polymeric chain more crystalline. Their derivatives such as methylcellulose (MC), carboxymethylcellulose (CMC), hydroxypropylcellulose (HPC) acquire high water solubility because there is a partial substitution of the hydroxyl groups present in the cellulose chains by methyl, carboxyl, and hydroxypropyl groups, respectively, reducing the dense packing and causing physicochemical changes compared to cellulose [62].

CMC-based hydrogels have a high degree of swelling in water due to the repulsion of the functional carboxylate groups (COO⁻). However, to improve the mechanical stability of these hydrogels, it is common to synthesize them with synthetic raw materials [63] and to add reinforcing agents such as clay minerals.

Combining these natural and synthetic materials with mineral clay allows the development of hybrid nanocomposites, as reported in the literature [64]. A mineral clay-type often used in nanocomposite hydrogels synthesis is the Cloisite Na⁺ [65-67], a type of montmorillonite (MMT) sodium nanoclay.

Cloisite Na⁺ nanoclay has a chemical structure compound by an octahedral alumina sheet between two tetrahedral silica sheets [68], as shown in Figure 1.3, and it can be used due to their excellent cation-exchange capacity, high specific surface area, functional swelling capacity, high platelet aspect ratio, and easy surface modification [69].

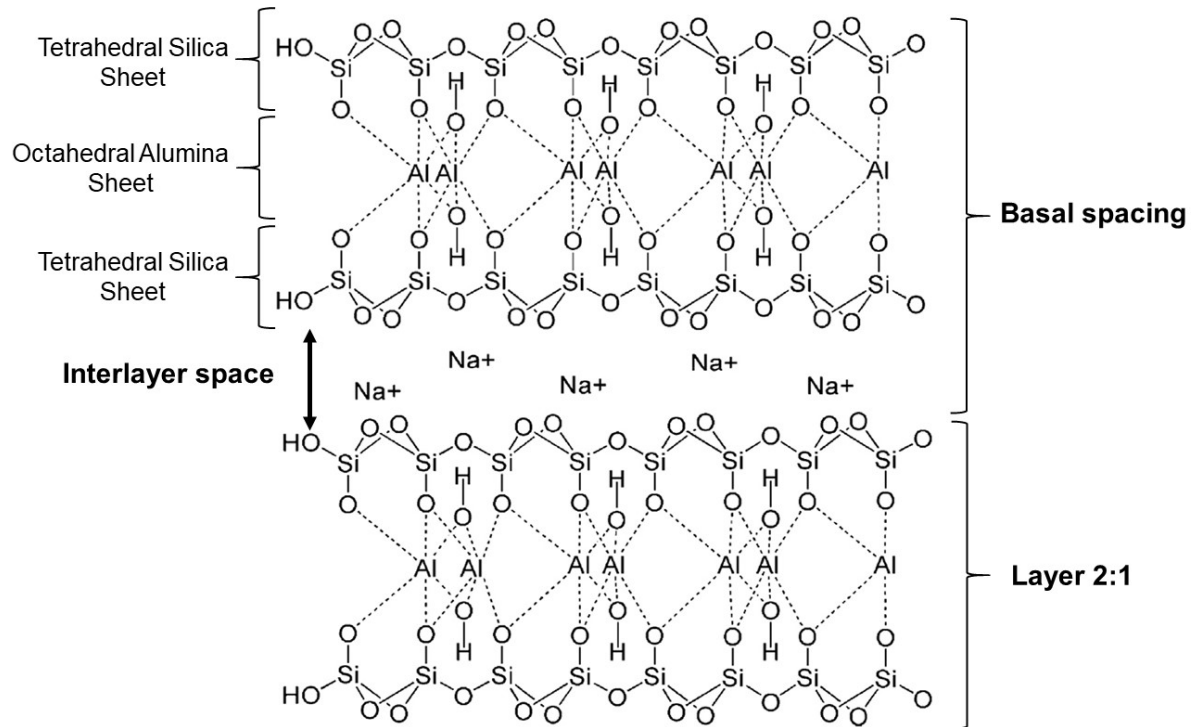


Figure 1.3 – Structure of MMT Cloisite- Na^+ nanoclay, adapted from Bao et.al, 2015. [70]

During the nanocomposite synthesis, three different configurations can be obtained concerning the dispersion of clay nanostructures into hydrogel (Figure 1.4): (i) Intercalated, in which the hydrogel chains are penetrated among the clay platelets, without affecting its structure [69, 71]; (ii) Exfoliated, when the clay platelets are completely dispersed in the polymeric matrix [72, 73]; (iii) Intercalated-exfoliated: junction of both [74, 75]. The most interesting dispersion to nanocomposites is the exfoliated configuration because it increases the polymer-clay interactions.

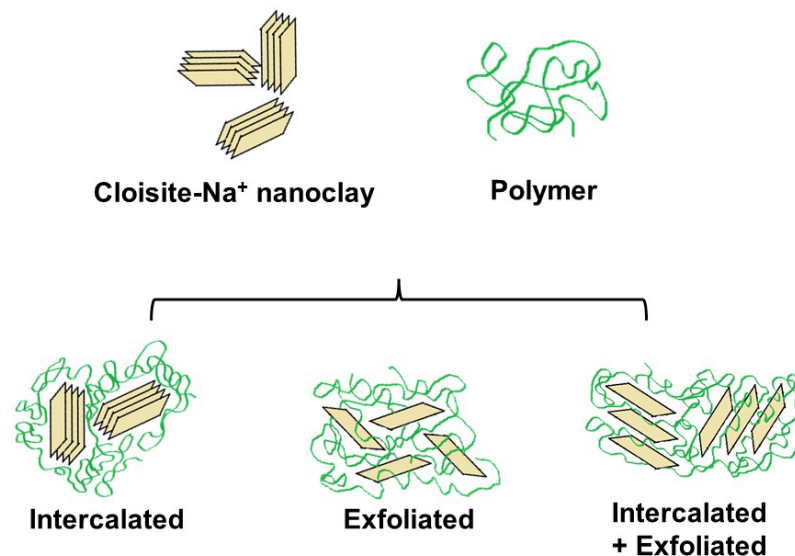


Figure 1.4 – Type of mineral clay dispersion in the hydrogel, adapted from Bensadoun et al. [76]

Notably, the manner as the clay is dispersed in the hydrogel matrix can modify the behavior of these nanocomposites. For instance, Cloisite Na⁺ nanoclay in the polymer demonstrated that it releases kinetics slower while its concentration increases in the polymer matrix [77]. Thus, the nanoclay presence on the polymeric matrix provides an increase in physical crosslinks, reducing both the amount of water released over time and the release time of the hydrogels [78]. In addition, mineral clay, when is associated with a polysaccharide, as carboxymethylcellulose (CMC) or others [79], can also improve the hydrophilic properties of these systems [80].

In this way, semi-synthetic hydrogel modified with nanoclays is a technological and innovative material for future application in construction civil, whereas their good properties of water retention and release are very interesting to the internal curing process in cement materials.

1.4 MOTIVATIONS AND JUSTIFICATIONS

The construction industry is an essential economic field that continues to grow worldwide due to housing shortages and population growth [81]. This expansion allows new materials to be developed to improve aspects such as durability and building performance.

Noteworthy is the high consumption of cement in pastes, mortars, and concretes since these are materials present good mechanical properties and easy handling and application. In this aspect, mortars as heterogeneous composite materials [82] can have multiple applications, either as a binding material for sealing elements (blocks, bricks, and stones) or as surface coatings and ceramic tile bases [83].

However, this cementitious composite has some characteristics that compromise its mechanical performance, such as low resistance to cracking, small deformation, and low flexural strength compared to compressive strength [84]. Some mortars can present porous microstructure, facilitating the transport of water inside and thus cause chemical damage to the structure due to the transport of some ions [82]. Thus, new materials have been developed and applied to improve the physical and mechanical properties and therefore ensure the reduction of pathologies of these cementitious materials [16].

One of the strategies to overcome these disadvantages is applying chemical additives as an integral part of the dosages of these materials [12]. Because one of its advantages lies in the fact that its use can alter the water/binder ratio without modifying the dosage of the other

constituent materials to improve the mechanical properties and maintain its workability [18, 85].

The purpose of developing and applying an auxiliary alternative to the traditional curing procedures of cementitious materials, commonly performed externally, through the application of coatings or wet curing by immersion [20] is one of the justifications for applying this type of hydrogel in cementitious matrices. Furthermore, the application of hydrogels as a component of cementitious materials is a way to ensure that part of the dosage water is stored in its polymeric matrix to be later released, besides increasing the internal moisture and assisting in the hydration of cement particles.

Several studies [25, 85, 86] in the literature indicate the application of commercial superabsorbent polymers (SAP) in cementitious matrices. The innovation of this thesis is in developing a semi-synthetic hybrid nanocomposite based on a polysaccharide and a mineral clay with hydrophilic, biodegradable, and mechanical characteristics suitable for more controlled release kinetics [86].

The application of polysaccharides like carboxymethylcellulose (CMC) is a good option for the preparation of hydrogels because it has ionizable carboxylic groups in its chemical structure, increasing the hydrophilicity [47] of the polyacrylamide (PAAm)-based nanocomposite.

Clay minerals in nano and micro scale are commonly present in the constitution of nanocomposites because they provide high thermal stability, good gas barrier properties [87], good mechanical resistance, high degree of swelling, and adsorption capacity [47]. Thus, these nanoclays can improve the water release process [87] inside the cement matrix due to its improvements in the hydrogel's hydrophilic properties [88].

The motivation for this study is because the semi-synthetic hydrogels based on PAAm, CMC, and Cloisite Na⁺ nanoclay may present similar or better behaviors to commercial synthetics when applied in cementitious matrices, which make these polymers technology attractive to the construction industry, as smarties internal curing agents. For this, the analysis of the behavior in the fresh and hardened states of mortars produced with these hybrid nanocomposite hydrogels was performed and discussed in detail in this thesis.

As hydrogels can absorb and release water as an internal curing agent, this can lead to the swelling of the polymer particles, which causes changes in the porous structure of the cementitious materials, affecting their properties in the hardened state. In this sense, the synthesis of the hybrid nanocomposite hydrogel took into account three different

concentrations of Cloisite Na⁺ nanoclay to verify the influence of this component in the process of water release by the polymer in aspects such as hydration of the cement and the changes of the mechanical properties of the mortar.

Thus, the guarantee that cementitious composites can have good physical and mechanical properties throughout their useful life, such as improvements in water retention [89], modifications in workability [16], reduction of shrinkage and cracking by water evaporation [90] from adequate hydration of the cement particles, assumes that it is necessary to establish greater control over the availability of water in the cement matrix [91], and this condition can be remedied with the application of a controlled release absorbent polymer.

1.5 OBJECTIVES

The general objective of this study was to evaluate the effect of the application of hybrid nanocomposites based on hydrogel and Cloisite Na⁺ nanoclay on the properties of cementitious mortars in fresh and hardened states. For this, the following specific objectives were proposed:

- ✓ To analyze the physical, chemical, and morphological properties of hybrid hydrogels containing different concentrations of Cloisite Na⁺ nanoclay, having two different swelling media, i.e., distilled water or in solution from the filtrate of the water+cement mixture.
- ✓ To develop cement mortars (dosage 1:2.16 and w/c ratio = 0.40) based on cement, sand, water, and 0.50% (wt/wt concerning cement) of the pre-soaked hydrogels their hybrid nanocomposites. Remarkably, 4 different systems have been used: - reference system or only cement mortar; - mortars containing different concentrations of Cloisite Na⁺ nanoclay (0, 10 and 20% wt/wt acrylamide + CMC) in their polymeric matrices;
- ✓ To determine the effect of the different types of hydrogels, in the proposed systems, on the physical, mechanical and structural properties of the mortars, in their fresh (workability, density, incorporated air, water retention, exudation index) and hardened state (strength compressive, tensile and flexural, bulk density, dynamic and estatic elastic moduli, voids, capillarity index, water absorption, loss, and mass variation);
- ✓ To verify the effect of hydrogels, as potential agents of internal cure, in the control of plastic shrinkage and morphology (SEM) of the microstructure of the cement matrix.

1.6 THESIS STRUCTURE

For a better presentation and discussion of the results, this thesis was structured into 7 chapters:

CHAPTER 1: Overview of the main concepts of the thesis, besides the presentation of justifications and proposed objectives.

CHAPTER 2: Material and methodology for hydrogel synthesis and mortar productions.

CHAPTER 3: Main definitions and analyses about water absorption behavior, kinetic properties, and structural characterizations of polymer hydrogels containing Cloisite Na⁺ nanoclay, using distilled water and solution filtered of Portland cement + water as swelling media, will be presented.

CHAPTER 4: At this moment, the properties in the fresh state of cement mortars produced with the addition of hybrid nanocomposites based on hydrogel and nanoclay will be analyzed. The results obtained for the physical properties of workability, the density of the mortar in the fresh state, incorporated air, water retention, and exudation index will also be discussed.

CHAPTER 5: This chapter will present the mechanical properties of cementitious mortars cured internally with hybrid nanocomposites based on hydrogel and nanoclay. The approach is based on discussing the results obtained for the properties of compressive strength, tensile and flexural, density in the hardened state, dynamic and elastic moduli.

CHAPTER 6: The effect of applying hybrid nanocomposites based on hydrogel and nanoclay will be presented as a potential application for shrinkage reduction, water absorption in cementitious materials, and its effect on capillarity properties, water absorption by immersion, mass loss and variation, and scanning electron microscopy (SEM);

CHAPTER 7: Finally, the most relevant final considerations on the application of these hydrogels as internal curing agents of cementitious mortars and their effect on the properties of the fresh and hardened states will be exposed in this chapter.

1.7 REFERENCES

- [1] F. A. Neville, J. J. Brooks, *Tecnologia do concreto*. Bookman, Porto Alegre, RS, Brazil, 2013.
- [2] S. Tang, J. Huang, L. Duan, L., P. Yu, E. Chen, A review on fractal footprint of cement-based materials. *Powder Technol.*, 230 (2020), 237-250.
- [3] American Society for Testing and Materials (ASTM), *Standard Terminology Relating to Hydraulic and Other Inorganic Cements*, ASTM C219-20a, ASTM International, West Conshohocken, PA, 2020.
- [4] H. Zhang, Y. Xu, Y. Gan, Z. Chang, E. Schlangen, B. Šavija, Microstructure informed micromechanical modelling of hydrated cement paste: Techniques and challenges, *Constr. Build. Mater.*, 251 (2020), 1-20.
- [5] H. Cheng-Yong, L. Yun-Ming, M. M. A. B. Abdullah, K. Hussin, Thermal Resistance Variations of Fly Ash Geopolymers: Foaming Responses. *Sci. Repor.*, 7 (2017), 1-11.
- [6] M. S. Mamlouk, J. P. Zaniewski, *Materials for civil and construction engineers*. Upper Saddle River, NJ: Pearson Prentice Hall, 2006.
- [7] International Energy Agency, *Global cement production, 2010-2019*, IEA, Paris, France, 2020. <https://www.iea.org/data-and-statistics/charts/global-cement-production-2010-2019>. (accessed 15 August 2020).
- [8] Associação Brasileiro de Cimento Portland, *Indústria do cimento mantém vendas em alta*, ABCP, São Paulo, Brazil, 2021. <https://abcp.org.br/imprensa/industria-do-cimento-mantem-vendas-em-alta/> (accessed 4th April 2021).
- [9] W. Kurdowski, *Cement and concrete chemistry*. Springer Science & Business, Kraków, Poland, 2014.
- [10] H. F. Taylor, *Cement Chemistry*, Thomas Telford, London, UK, 1997.
- [11] G. C. Bye, *Portland cement – Third Edition*, ICE Publishing: Thomas Telford Limited, London, UK, 2011.
- [12] P. K. Mehta, P. J. Monteiro, *Concrete microstructure, properties and materials*, McGraw Hill, USA, 2017.
- [13] A. Mignon, D. Snoeck, P. Dubruel, S. Van Vlierberghe, N. De Belie, Crack mitigation in concrete: superabsorbent polymers as key to success? *Mater.* 10, 3 (2017), 237-262.
- [14] Á. Salesa, J. A. Pérez-Benedicto, D. Colorado-Aranguren, P. L. López-Julián, L.M. Esteban, L. J. Sanz-Baldúz, D. Olivares, Physico-mechanical properties of multi-recycled concrete from precast concrete industry. *J. Clean. Prod.*, 141 (2017), 248-255.
- [15] J. J. Biernacki, J. W. Bullard, G. Sant, K. Brown, F. P. Glasser, S. Jones, T. Prater, Cements in the 21st century: Challenges, perspectives, and opportunities. *J. Am. Ceram. Soc.*, 100 (2017), 2746–2773.
- [16] V. Mechtcherine, E. Secrieru, C. Schröfl, Effect of superabsorbent polymers (SAPs) on rheological properties of fresh cement-based mortars—Development of yield stress and plastic viscosity over time. *Cem. Concr. Res.* 67, 1 (2015), 52-65.

- [17] SAP, RILEM TC. Application of Superabsorbent Polymers (SAP) in Concrete Construction. RILEM State-of-the-Art Report Prepared by Technical Committee, 1 (2012), 165.
- [18] L. G. Li, A. K. Kwan, A. K. Effects of superplasticizer type on packing density, water film thickness and flowability of cementitious paste. *Constr. Build. Mater.*, 86 (2015), 113-119.
- [19] M. Valcuende, C. Parra, E. Marco, A. Garrido, E. Martínez, J. Cánoves, J. Influence of limestone filler and viscosity-modifying admixture on the porous structure of self-compacting concrete. *Constr. Build. Mater.*, 28 (2012), 122-128.
- [20] X. Y. Liu, C. H. Huang, C. H. Zhuang, K. C. Hsu, C. H. Huang, An amphoteric hydrogel: Synthesis and application as an internal curing agent of concrete, *J. Appl. Polym. Sci.*, 132 (2015), 1-9.
- [21] K. Varaprasad, G. M. Raghavendra, T. Jayaramudu, M. M. Yallapu, R. Sadiku, A mini-review on hydrogels classification and recent developments in miscellaneous applications. *Mater. Sci. Eng. C*. 79, 11 (2017), 958-971.
- [22] F. Wahid, X. J. Zhao, S. R. Jia, H. Bai, C. Zhong, Nanocomposite hydrogels as multifunctional systems for biomedical applications: Current state and perspectives. *Compos. B. Eng.*, 1 (2020), 108208.
- [23] F. Ullah, M. B. H. Othman, F. Javed, Z. Ahmad, A. M. Akil, Classification, processing, and application of hydrogels: A review. *Mater. Sci. Eng. C*, 57 (2015), 414–433.
- [24] M.J. Zohuriaan-Mehr, K. Kabiri, Superabsorbent polymer materials: a review, *Iran. Polym. J.* 17 (2008), 451.
- [25] M. T. Hasholt, O. M. Jensen, K. Kovler, S. Zhutovsky, Can superabsorbent polymers mitigate autogenous shrinkage of internally cured concrete without compromising the strength? *Constr. Build. Mater.*, 31 (2012), 226-230.
- [26] C. R. F. Junior, M. R. de Moura, F. A. Aouada, Synthesis and characterization of intercalated nanocomposites based on poly(methacrylic acid) hydrogel and nanoclay Cloisite- Na^+ for possible application in agriculture. *J. Nanosci. Nanotechnol.* 17 (2017), 5878-5883.
- [27] S. Sharma, S. Tiwari, Shachi. A review on biomacromolecular hydrogel classification and its applications. *Int. J. Biol. Macromol.*, 162 (2020), 737-747.
- [28] W. E. Roorda, H. E. Bodde, A. G. De Boer, H. E. Junginger, Synthetic hydrogels as drug delivery systems. *Pharm. Weekbl.*, 8 (1986), 165-189.
- [29] U. G. Yonezawa, M.R. de Moura, F.A. Aouada, Hybrid bionanocomposites formed from polysaccharide hydrogels and nanoclay II: incorporation in substrate to seedling improving. *Cult. Agron.* 26 (2017), 82-94.
- [30] S.J. Buwalda, K.W.M. Boere, P.J. Dijkstra, J. Feijen, T. Vermonden, W.E. Hennink, Hydrogels in a historical perspective: from simple networks to smart materials, *J. Control. Release*, 190 (2014), 254.
- [31] N. A. Peppas, P. Bures, W. Leobandung, H. Ichikawa, Hydrogels in pharmaceutical formulations. *Eur. J. Pharm. Biopharm.*, 50 (2000), 27-46.

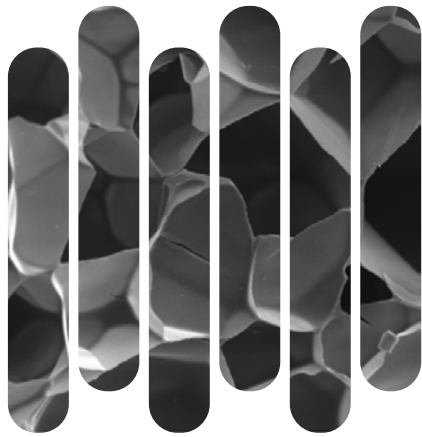
- [32] G. R. Bardajee, Z. Hooshyar. One-pot synthesis of biocompatible superparamagnetic iron oxide nanoparticles/hydrogel based on salep: Characterization and drug delivery. *Carbohydr. Polym.*, 101 (2014), 741–751.
- [33] F. N. Tanaka, C. R. F. Junior, M. R. de Moura, F. A. Aouada, F.A. Water absorption and physicochemical characterization of novel zeolite-PMAA-co-PAAm nanocomposites. *J. Nanosci. Nanotechnol.* 18 (2018), 7286-7295.
- [34] P. Liu, et al. Synthesis of covalently crosslinked attapulgite/poly (acrylic acid-co-acrylamide) nanocomposite hydrogels and their evaluation as adsorbent for heavy metal ions. *J. Ind. Eng. Chem.*, 23 (2015), 188-193.
- [35] S. B. Majee, Emerging concepts in analysis and applications of hydrogels. *BoD–Books on Demand.* 1 (2016).
- [36] F. A. Aouada, L. H. C. Mattoso, Hidrogéis biodegradáveis: uma opção na aplicação como veículos carreadores de sistemas de liberação controlada de pesticidas. *Embrapa Instrumentação-Boletim de Pesquisa e Desenvolvimento (Infoteca-E)*, 2009.
- [37] C. Ghobril, M. W. Grinstaff, M. W. The chemistry and engineering of polymeric hydrogel adhesives for wound closure: a tutorial. *Chem. Soc. Rev.*, 44 (2015), 1820–1835.
- [38] R. S. Fernandes, R. S., F. N. Tanaka, M. R. de Moura, F. A. Aouada, Development of alginate/starch-based hydrogels crosslinked with different ions: Hydrophilic, kinetic and spectroscopic properties. *Mater. Today Commun.*, 21 (2019), 100636.
- [39] J. A. F. Garcia, M. R. de Moura, F. A. Aouada. Efeito do pH, espécie e concentração iônica na absorção de água de hidrogéis bionanocompósitos constituídos de CMC/PAAM/LAPONITA RDS. *Quim. Nova*, 42 (2019), p. 831-837.
- [40] D. Pasqui, M. de Cagna, R. Barbucci. Polysaccharide-based hydrogels: the key role of water in affecting mechanical properties. *Polymers*, 4 (2012), 1517-1534.
- [41] R. da Silva Fernandes, M. R. de Moura, G. M. Glenn, F. A. Aouada, F. A. Thermal, microstructural, and spectroscopic analysis of Ca^{2+} alginate/clay nanocomposite hydrogel beads. *J. Mol. Liq.*, 265 (2018), 327-336.
- [42] Y. Zhou, S. Fu, L. Zhang, H. Zhan, M. V. Levit. Use of carboxylated cellulose nanofibrils-filled magnetic chitosan hydrogel beads as adsorbents for Pb (II). *Carbohydr. Polym.*, 101 (2014), 75-82.
- [43] W. Xu, X. He, M. Zhong, X. Hu, Y. Xiao. A novel pH-responsive hydrogel based on natural polysaccharides for controlled release of protein drugs. *RSC Adv.*, 5 (2015), 3157-3167.
- [44] S. S. Stalling, S. O. Akintoye, S. B. Nicoll. Development of photocrosslinked methylcellulose hydrogels for soft tissue reconstruction. *Acta Biomater.*, 5 (2009), 1911-1918.
- [45] P. Mohammadzadeh Pakdel, S. J. Peighambaroust, A review on acrylic-based hydrogels and their applications in wastewater treatment. *J. Environ. Manage.*, 217 (2018), 123–143.
- [46] M. R. Singh, S. Patel, D. Singh. Natural polymer-based hydrogels as scaffolds for tissue engineering. In *Nanobiomaterials in soft tissue engineering*, William Andrew Publishing, (2016), 231-260.

- [47] A. T. Paulino, L. A. Belfiore, L. T. Kubota, E. C. Muniz, E. B. Tambourgi, Efficiency of hydrogels based on natural polysaccharides in the removal of Cd^{2+} ions from aqueous solutions. *Chem. Eng. Technol.*, 168 (2011), 68-76.
- [48] A. T. Paulino, M. R. Guilherme, E. A. de Almeida, A. G. Pereira, E. C. Muniz, E. B. Tambourgi, One-pot synthesis of a chitosan-based hydrogel as a potential device for magnetic biomaterial. *J. Magn. Magn. Mater.*, 321 (2009), 2636-2642.
- [49] R. Cruz-Acuna, A. J. García. Synthetic hydrogels mimicking basement membrane matrices to promote cell-matrix interactions. *Matrix Biol.*, 57 (2017), 324-333.
- [50] Y. Berkovitch, D. Seliktar, Semi-synthetic hydrogel composition and stiffness regulate neuronal morphogenesis. *Int. J. Pharm.* 523 (2017), 545-555.
- [51] R. da Silva Fernandes, F. N. Tanaka, A. M. Angelotti, C. R. F. Júnior, U. G. Yonezawa, A. Watanuki Filho, M. R. de Moura, F. A. Aouada, Properties, synthesis, characterization and application of hydrogel and magnetic hydrogels: A concise review. *Advances in Nano-Fertilizers and Nano-Pesticides in Agriculture*, Elsevier, 1 (2021), 437-457.
- [52] L. L. Palmese, R. K. Thapa, M. O. Sullivan, K. L. Kiick, Hybrid hydrogels for biomedical applications. *Curr. Opin. Chem. Eng.*, 24 (2019), 143-157.
- [53] M. J. Caulfield, G. G. Qiao, D. H. Solomon, D. H. Some aspects of the properties and degradation of polyacrylamides. *Chem. Rev.*, 102 (2002), 3067-3084.
- [54] C. Yang, T. Yin, Z. Suo, Polyacrylamide hydrogels. I. Network imperfection. *J. Mech. Phys. Solids*, 131 (2019), 43-55.
- [55] C. E. Kadow, P. C. Georges, P. A. Janmey, K. A. Beningo, K. A. Polyacrylamide hydrogels for cell mechanics: steps toward optimization and alternative uses. *Methods Cell Biol.*, 83 (2007), 29-46.
- [56] I. Cicha, R. Detsch, R. Singh, S. Reakasame, C. Alexiou, A. R. Boccaccini, Biofabrication of vessel grafts based on natural hydrogels. *Curr. Opin. Biomed. Eng.* 2 (2017), 83-89.
- [57] R. Jin, L. M. Teixeira, A. Krouwels, P. J. Dijkstra, C. A. Van Blitterswijk, M. Karperien, J. Feijen, Synthesis and characterization of hyaluronic acid-poly (ethylene glycol) hydrogels via Michael addition: An injectable biomaterial for cartilage repair. *Acta Biomater.*, 6 (2010), 1968-1977.
- [58] B. K. Bozođlan, O. Duman, S. Tunç, Preparation and characterization of thermosensitive chitosan/carboxymethylcellulose/scleroglucan nanocomposite hydrogels. *Int. J. Biol. Macromol.*, 162 (2020), 781-797.
- [59] A. M. Youssef, S. El-Sayed, M. Samah. Bionanocomposites materials for food packaging applications: Concepts and future outlook. *Carboh. Polym.*, 193 (2018), 19-27.
- [60] S. Abdurrahmanoglu, V. Can, O. Okay, Design of high-toughness polyacrylamide hydrogels by hydrophobic modification. *Polym. Oxford*, 50 (2009), 5449-5455.
- [61] S. Javanbakht, A. Shaabani, Carboxymethyl cellulose-based oral delivery systems. *Int. J. Biol. Macromol.*, 133 (2019), 21-29.

- [62] F. A. Aouada, Síntese e caracterização de hidrogéis de poliacrilamida e metilcelulose para liberação controlada de pesticidas. Doctoral thesis. Federal University of São Carlos (UFSCar), São Carlos, 2009.
- [63] B. Mandal, S. K. Ray, Removal of safranin T and brilliant cresyl blue dyes from water by carboxy methyl cellulose incorporated acrylic hydrogels: Isotherms, kinetics and thermodynamic study. *J. Taiwan Inst. Chem. Eng.*, 60 (2016), 313–327.
- [64] M. Irani, H. Ismail, Z. Ahmad, Preparation and properties of linear low-density polyethylene-g-poly (acrylic acid)/organo-montmorillonite superabsorbent hydrogel composites. *Polym. Test.* 32 (2013), 502-512.
- [65] S. Tunç, O. Duman, Preparation and characterization of biodegradable methyl cellulose/montmorillonite nanocomposite films. *Appl. Clay Sci.*, 48 (2010), 414–424.
- [66] P. H. Camani, J. P. M. Toguchi, A. P. S. Fiori, D. dos Santos Rosa, Impact of unmodified (PGV) and modified (Cloisite20A) nanoclays into biodegradability and other properties of (bio) nanocomposites. *Appl. Clay Sci.*, 186 (2020), 105453.
- [67] A. Cojocariu, L. Profire, M. Aflori, C. Vasile, In vitro drug release from chitosan/Cloisite 15A hydrogels. *Appl. Clay Sci.*, 57 (2012), 1–9.
- [68] S. Mallakpour, M. Dinari, Preparation and characterization of new organoclays using natural amino acids and Cloisite Na⁺. *Appl. Clay Sci.*, 51 (2011), 353-359.
- [69] I. Hackman, L. Hollaway, Epoxy-layered silicate nanocomposites in civil engineering. *Compos. A.*, 37 (2016), 1161–1170.
- [70] X. Bao, F. Zhang, Q. Liu, Q. Sulfonated poly (2, 5-benzimidazole) (ABPBI)/MMT/ionic liquids composite membranes for high temperature PEM applications. *Int. J. Hydrog. Energy*, 40 (2015), 16767-16774.
- [71] D. S. Dlamini, J. Li, B. B. Mamba, Critical review of montmorillonite/polymer mixed-matrix filtration membranes: Possibilities and challenges. *Appl. Clay Sci.*, 168 (2019), 21-30.
- [72] C. Wolf, H. Angellier-Coussy, N. Gontard, F. Doghieri, V. Guillard, How the shape of fillers affects the barrier properties of polymer/non-porous particles nanocomposites: A review. *J. Membr. Sci.*, 556 (2018), 393-418.
- [73] T. B. Sharmila, E. P. Ayswarya, B. T. Abraham, P. S. Begum, E. T. Thachil, Fabrication of partially exfoliated and disordered intercalated cloisite epoxy nanocomposites via in situ polymerization: Mechanical, dynamic mechanical, thermal and barrier properties. *Appl. Clay Sci.*, 102 (2014), 220-230.
- [74] A. R. Ramadan, A. M. Esawi, A. A. Gawad, Effect of ball milling on the structure of Na⁺-montmorillonite and organo-montmorillonite (Cloisite 30B). *Appl. Clay Sci.*, 47 (2010), 196-202.
- [75] C. K. Hong, M. J. Kim, S. H. Oh, Y. S. Lee, C. Nah, C., Effects of polypropylene-g-(maleic anhydride/styrene) compatibilizer on mechanical and rheological properties of polypropylene/clay nanocomposites. *J. Ind. Eng. Chem.*, 14 (2008), 236-242.
- [76] F. Bensadoun, F., N. Kchit, C. Billotte, F. Trochu, E. Ruiz, A comparative study of dispersion techniques for nanocomposite made with nanoclays and an unsaturated polyester resin. *J. Nanomater.*, 2011 (2011), 1-13.

- [77] D. W. S. Nascimento, M. R. de Moura, L. H. C. Mattoso, F. A. Aouada, Hybrid Biodegradable Hydrogels Obtained from Nanoclay and Carboxymethylcellulose Polysaccharide: Hydrophilic, Kinetic, Spectroscopic and Morphological Properties. *J. Nanosci. Nanotechnol.*, 17 (2017), 821–827.
- [78] M. G. Hernández, J. J. Anaya, M. A. G. Izquierdo, L. G. Ullate, Application of micromechanics to the characterization of mortar by ultrasound. *Ultrasonics*, 40 (2012), 217-221.
- [79] Q. Chen, W. Y. Wen, F. X. Qiu, J. C. Xu, H. Q. Yu, M. L. Chen, D. Y. Yang, Preparation and application of modified carboxymethyl cellulose Si/polyacrylate protective coating material for paper relics. *Chem. Pap.*, 70 (2016), 946-959.
- [80] M. I. Syakir, N. A. Nurin, N. Zafirah, M.A. Kassim, H. A. Khalil, Nanoclay reinforced on biodegradable polymer composites: Potential as a soil stabilizer. In *Nanoclay Reinforced Polymer Composites* Springer, Singapore, 1 (2016), 329-356.
- [81] P. S. Oliveira, M. L. P. Antunes, N. C. da Cruz, E. C. Rangel, A. R. G. de Azevedo, S. F. Durrant, Use of waste collected from wind turbine blade production as an eco-friendly ingredient in mortars for civil construction. *J. Clean. Prod.*, 274 (2020).
- [82] ([1] M. Liu, Y. Hu, Z. Lai, T. Yan, X. He, J. Wu, Z. Lu, S. Lv, Influence of various bentonites on the mechanical properties and impermeability of cement mortars. *Constr. Build. Mater.* 241, 12 (2020), 118015
- [83] H. A. Jaber, R. S. Mahdi, A. K. Hassan, Influence of eggshell powder on the Portland cement mortar properties. *Mater. Today: Proceedings* 20, 4 (2020), 391.
- [84] R. Bagherzadeh, H. R. Pakravan, A. H. Sadeghi, M. Latifi, A. A. Merati, An investigation on adding polypropylene fibers to reinforce lightweight cement composites (LWC). *J. Eng. Fibers Fabr.* 7, 4 (2012), 1.
- [85] V. A. S. Siqueri, A. Watanuki Filho, M. R. de Moura, F.A. Aouada, Effect of Hydrogel Nanocomposites on the Fresh and Hardened Properties of Cementitious Pastes *Macromol. Symp.* 394 (2020), 2000047.
- [86] A. Bortolin, F. A. Aouada, L. H. Mattoso, C. Ribeiro, Nanocomposite PAAm/methyl cellulose/montmorillonite hydrogel: evidence of synergistic effects for the slow release of fertilizers, *J. Agric. Food Chem.*, 61, 31 (2013), 7431-7439.
- [87] Q. Zhao, J. Sun, Y. Lin, Q. Zhou, Study of the properties of hydrolyzed polyacrylamide hydrogels with various pore structures and rapid pH-sensitivities. *React. Funct. Polym.*, 70 (2010), 602-609.
- [88] M. I. Syakir, N. A. Nurin, N. Zafirah, M. A. Kassim, H. A. Khalil, Nanoclay reinforced on biodegradable polymer composites: Potential as a soil stabilizer. In *Nanoclay Reinforced Polymer Composites*, 329-356, Springer, Singapore, 2016.
- [89] J. R. Tenório Filho, E. Mannekens, K. Van Tittelboom, D. Snoeck, N. de Belie, Assessment of the potential of superabsorbent polymers as internal curing agents in concrete by means of optical fiber sensors. *Constr. Build. Mater.* 238, 9 (2020) 1-8.
- [90] L. Dudziak, V. Mechtcherine, V. Enhancing early-age resistance to cracking in high-strength cement-based materials by means of internal curing using super absorbent polymers. In: *RILEM Proc. PRO. 2010.* p. 129-139.

[91] V. Mechtcherine, Use of superabsorbent polymers (SAP) as concrete additive, RILEM Technical Letters, 10 (2016), 81-87.



CHAPTER 2

**MATERIAL AND GENERAL
METHODOLOGY FOR HYDROGEL,
NANOCOMPOSITE, AND MORTARS
PREPARATION**

z

2.1 HYDROGEL SYNTHESIS

Three types of hybrid nanocomposite hydrogels composed of polyacrylamide (PAAm), biodegradable polysaccharide carboxymethylcellulose (CMC), and Cloisite Na⁺ nanoclay were obtained through free radical polymerization (Figure 2.1), following the procedures described by Aouada et al. [3] and Nascimento et al. [4].

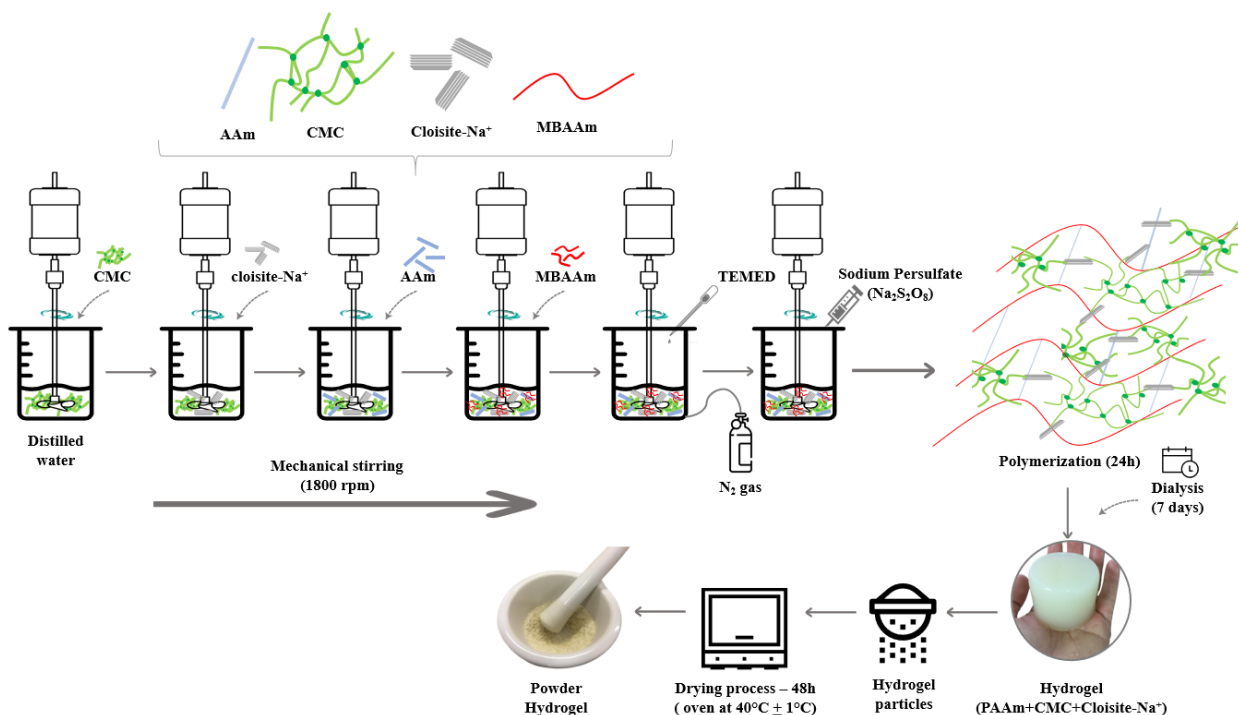


Figure 2.1 – Schematic representation of the hybrid nanocomposite hydrogels synthesis (Source: Author's own graphical).

These hybrid nanocomposite hydrogels were synthesized using 6.0% (wt/v) acrylamide (AAm) monomer (Sigma-Aldrich 99%, C₃H₅NO MW = 71.08 g/mol) in an aqueous solution containing 1% (wt/v) of polysaccharide carboxymethylcellulose (CMC) (Synth P.A, M_v = 114.000 g/mol), different Cloisite Na⁺ (Southern Clay Products) contents: 0% (reference), 10% and 20% (mass% concerning to AAm + CMC mass).

It was used 2.0% (mol relative to AAm monomer) of N'-N'-methylenebisacrylamide (MBAAm) as crosslinking agent (Sigma-Aldrich 99%, C₇H₁₀N₂O₂, MW = 154.17 g/mol), 6.67 mmol/L of N, N, N', N'- tetramethylethylenediamine (TEMED) (Sigma-Aldrich 99%, (CH₃)₂NCH₂CH₂N(CH₃)₂, MW = 116.20 g/mol) as reaction catalyst, and 3.50 mmol/L of sodium persulfate (Sigma-Aldrich > 98%, Na₂S₂O₈, MW = 238.10 g/mol) as reaction initiator.

To improve the efficiency of hydrogel polymerization was necessary to applied nitrogen gas (N₂), after TEMED addition, for 10 minutes. After this stage, sodium persulfate

solution was added under stirring into the polymeric solution to initiate the polymerization process. Finally, the hydrogel-forming solution was stored for 24 hours at a temperature of 25°C until complete polymerization.

Hybrid nanocomposite hydrogels were subjected to the dialysis process, i.e., changing the storage water daily for 7 days to eliminate the reagents that were not consumed. For this procedure, it was not necessary to use any membrane. Subsequently, hydrogels were ground into microparticles and subjected to the drying process in an oven at 40 ± 1 °C for approximately 48 hours or until achieving constant mass (variation < 0.50%). With the material completely dry, it was again ground and stored until its application. All concentrations of the required reagents were pre-established by our research group GCNH (Grupo de Compósitos e Nanocompósitos Híbridos) [5].

These hydrogels present values of swelling degree of 34.7 ± 1.9 ; 27.2 ± 1.3 ; and 24.4 ± 0.8 g.g⁻¹ for 0%, 10% and 20% Cloisite Na[±] nanoclay concentrations, respectively. The swelling degree in distilled water and kinetic properties of the hydrogels will be presented in section 3.3.4, Chapter 3. The values are used to calculate the amount of water necessary to produce the mortars without modifying the water/binder ratio. Details about the dispersion of the nanoclay in the solution can be seen in Chapter 3, where it was found to be dispersed intercalated in distilled water medium and possibly exfoliated when swelled in solution from the filtrate of the water+cement mixture.

2.2 MORTAR PREPARATION

Mortars-cement production followed the NBR 16541 [6] and NBR 7215 [7] recommendations. A composite cement type CII-Z-32 (Ciplan Planalto Cimentos S. A.[®]) was used in their preparation. The choice for this type of cement is because it is one of the most used types of cement in civil construction in Brazil and due to its high availability in the Brazilian market. The physical and chemical compositions of the cement are presented in Tables 2.1 and 2.2. The chemical composition was determined by X-ray fluorescence (XRF), according to Spósito et al. [1].

Table 2.1 - Chemical composition of cement Portland CII-Z-32 [1]

| Element | CaO | SiO ₂ | SO ₃ | Fe ₂ O ₃ | K ₂ O | TiO ₂ | SrO | MnO | Others |
|-----------------|-------|------------------|-----------------|--------------------------------|------------------|------------------|------|------|--------|
| Composition (%) | 75.29 | 16.19 | 3.70 | 3.11 | 1.11 | 0.25 | 0.24 | 0.04 | 0.07 |

Table 2.2 - Physical properties of cement Portland CII-Z-32 [2]

| Loss on ignition (%) | Setting time | | Surface area (m ² /kg) | Compressive Strength (MPa) | | | |
|-------------------------|------------------|----------------|--------------------------------------|----------------------------|-------|-------|-------|
| | Initial (min) | Final (min) | | 1 d | 3 d | 7 d | 28 d |
| 7.10 | 141 | 214 | 463.40 | 14.60 | 22.10 | 26.40 | 33.10 |

Siliceous sand (Castilho city, São Paulo-Brazil) was used as fine aggregate (fineness modulus of 2.05 and a specific gravity of 2650 kg.m⁻³) to produce all mortars.

The choice of the reference dosages proposed (Table 2.3) was based on the production parameters of the mortar for the test to determine the compressive strength of cylindrical samples presented by NBR 7215 [7]. The variation of the type of hybrid nanocomposite hydrogel allowed to define 4 mortar systems, designated as ACTR, AHN0, AHN10, and AHN20, where ACTR represent the mortar control (without hydrogel or nanocomposite), and 0, 10, or 20 indicates the absence or the nanoclay amount into nanocomposites, respectively.

Table 2.3 - Design of mix proportion of mortars samples

| Mix ID | CII-Z-32 cement (kg/m ³) | Siliceous sand (kg/m ³) | Water (l/m ³) | | | w/c ratio | | Hydrogel (%) | |
|--------|--|---|---------------------------|-----------|--------|----------------------|-----------------------------|---------------|--------|
| | | | Dosage | Hydrogel* | Total | a/c _{total} | a/c _{effective} ** | Pre-soaked*** | Dry*** |
| ACTR | 649.81 | 1403.59 | 259.93 | - | 259.93 | 0.40 | - | - | - |
| AHN0 | 649.81 | 1403.59 | 256.77 | 3.16 | 259.93 | 0.40 | 0.39 | 0.50 | 0.015 |
| AHN10 | 649.81 | 1403.59 | 256.80 | 3.13 | 259.93 | 0.40 | 0.39 | 0.50 | 0.018 |
| AHN20 | 649.81 | 1403.59 | 256.81 | 3.12 | 259.93 | 0.40 | 0.39 | 0.50 | 0.021 |

* Amount of water corresponding to absorbed and stored water by the hydrogel.

** Water/cement ratio of dosage without considering stored water by the hydrogel

*** Percentage established concerning the mass of cement used.

The hydrogel concentration (0.5% wt/wt concerning cement mass) was determined according to the results obtained in previous researches [5, 8]. It is important to mention that all the hydrogels were pre-soaked, until the equilibrium state (48 hours), before being applied. Then, the amount of water absorbed by the polymer was removed from the dosage water to maintain the w/c = 0.40 constant.

For the preparation of all mortars, a mechanical mixer (total volume 20 L) was used for 5 minutes (Figure 2.2). First, cement, water, and pre-soaked hydrogel were mixed for 60 seconds with minimum rotation (125 rpm around the main axis and 62 rpm of the planetary rotation). Then, without stopping the mortar mixer, all sand quantity was added for 30 seconds, and the rotation was increased to maximum (220 rpm around the main shaft and 125

rpm planetary rotation) for more than 30 seconds. After this agitation period, the mortar mixer was then stopped for removing and mixing the materials adhered to the sidewalls of the container. The mortar remained at rest for 60 seconds and mixed again at maximum rotation for 90 seconds.

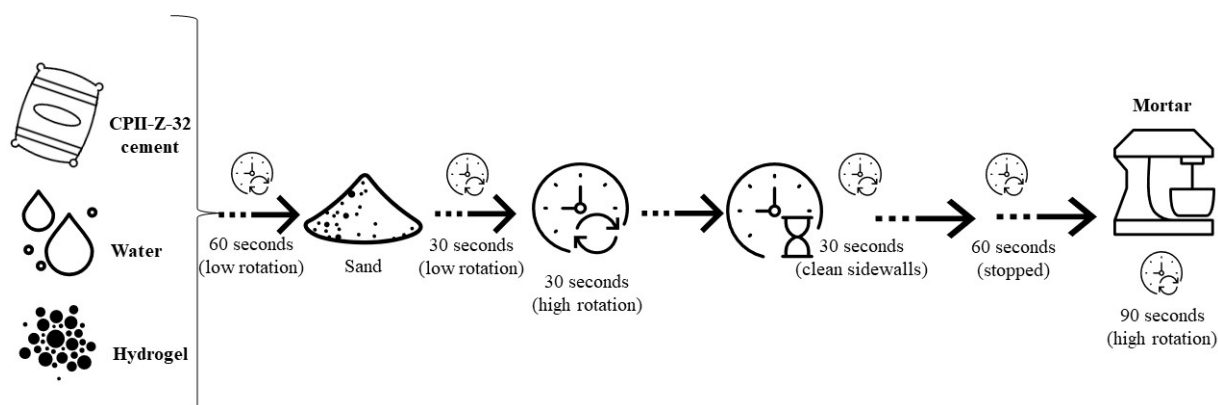


Figure 2.2 – Graphical representation of the mortar preparation (Source: Author’s own graphical).

The mortars were casting in different molds according to tests realized. They were manually or mechanically densified (vibrated table SOLOTEST®, Brazil) to eliminate incorporated air bubbles during the mechanical mix. The type of densification was determined in function of the mold and testing realized.

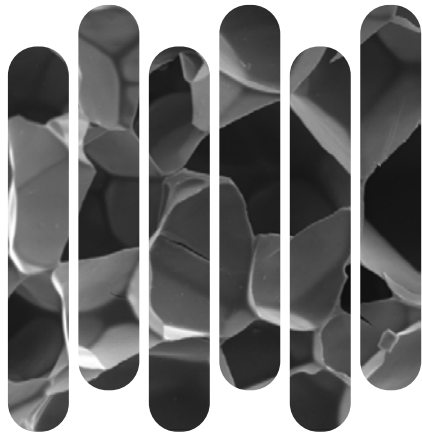
2.3 REFERENCES

- [1] F. A. Spósito, R. T. Higuti, M. M. Tashima, J. L. Akasaki, J. L. P. Melges, C. C. Assunção, C. F. Fioriti, Incorporation of PET wastes in rendering mortars based on Portland cement/hydrated lime. *J. Build. Eng.*, 32, 5 (2020), 1-38.
- [2] Ciplan Cimento Planalto S/A, Ficha de Informações de Segurança de Produtos Químicos - FISQ, Ciplan Cimento Planalto S/A, Sobradinho, Federal District, Brazil, 2020. http://www.ciplan.com.br/fispq/FISPQ_CIMENTO_CIPLAN.pdf. (accessed 15 January 2020)
- [3] F. A. Aouada, Síntese e caracterização de hidrogéis de poli(acrilamida e metilcelulose para liberação controlada de pesticidas. Doctoral thesis. Federal University of São Carlos (UFSCar), São Carlos, 2009.
- [4] D.W. Nascimento, M. R. de Moura, L. H. Mattoso, F. A. Aouada, Hybrid biodegradable hydrogels obtained from nanoclay and carboxymethylcellulose polysaccharide: hydrophilic, kinetic, spectroscopic and morphological properties. *J. Nanosci. Nanotechnol.* 17, 1 (2017), 821-827.
- [5] J. C. D. Santos, M. M. Tashima, M. R. de Moura, F. A. Aouada, Obtainment of hybrid composites based on hydrogel and Portland cement. *Química Nova*, 39, 1 (2016), 124-129.

[6] Associação Brasileira de Normas Técnicas (ABNT), Argamassa industrializada para assentamento de paredes e revestimentos de paredes e tetos: preparo da mistura para realização de ensaios. NBR 16541, Rio Janeiro 2016.

[7] Associação Brasileira de Normas Técnicas (ABNT), Cimento portland: Determinação da resistência à compressão, NBR 7215, Rio de Janeiro 1996.

[8] L. Cilli, H. C. Silva, A. Watanuki Filho, M. R. D. M. Aouada, F. A. Aouada, Otimização de metodologia de obtenção de pastas cimentícias contendo hidrogéis. J. Exp. Tech. Instrum. 2, 1, (2019), 1-9.



CHAPTER 3

HYDROGELS

“Water absorption, kinetic and structural characterizations of polymeric hydrogels containing Cloisite Na⁺ nanoclay in distilled water or solution from the filtrate of the water+cement mixture.”

3.1 OVERVIEW

Hydrogels can be classified as hydroretentor materials [1] with great applicability as internal curing additives of cementitious materials. They can act as water inclusions (macropores) that continuously moisturize the cementitious matrix to reduce its shrinkage and microcracks during the hardening process [2, 3]. However, it is essential to ensure that these alternative solutions to self-desiccation do not result in new pathologies [4]. Because by releasing all water contained in its structure, the hydrogels can change the cementitious microstructure porosity and modify their mechanical properties [5,6].

On the other hand, the addition of mineral clay during hydrogel synthesis to obtain a hybrid nanocomposite [7] is a promissory alternative. Clay mineral–polymer nanocomposites are of particular interest because of the enhancement of some physical properties as well as the biodegradability of polymers or polymer matrices [8-10]. Furthermore, the hybrid hydrogel nanocomposites containing nanoclay exhibit improved mechanical properties due to the increased physical crosslinking caused by the presence of the mineral into the polymer matrix and have their absorption and release properties modified [11]. It reduces the amount of water released over time while increasing the release time of the hydrogels [12].

In this sense, the “smart” water coming from swollen hydrogels inside the microstructure of the cementitious material can be a potential technological application of these nanocomposites as an internal curing agent.

This study is aimed at investigating the effect of hydrogels prepared from different concentrations of Cloisite Na⁺ nanoclay (0, 10, and 20% wt/wt concerning AAm + CMC) on the water absorption by swelling degree measurements, morphological, kinetic, and structural properties of the hydrogels, using a solution from the filtrate of the water+cement mixture (water/cement ratio of 0.40), and distilled water as the swelling medium.

This investigation in the different swelling media is essential to understand how hydrogels can behave when applied in cementitious matrices. Moreover, due to their characteristics, the hybrid nanocomposites application becomes an alternative for cementitious materials to attenuate problems related to retraction; besides, they can assist the cement hydration procedures.

3.2 EXPERIMENTAL

3.2.1 PAAm/ CMC and Cloisite Na⁺ nanocomposites synthesis

All materials and details about hybrid nanocomposite hydrogel synthesis have been presented in sections 2.1 and 2.2, Chapter 2.

3.2.2 Water + Portland cement type CII-Z-32 solution preparation

The solution from the filtrate of the water+cement mixture (CII-Z-32) was obtained from mixing distilled water and Portland cement type CII-Z-32 at a water/cement ratio (w/c) of 0.40. All physical and chemical properties of cement used have been present in section 2.1, Chapter 2.

Initially, the Portland cement was mixed with water in a mechanical stirrer for 60 seconds at minimum rotation (250 rpm). Then, the agitation was stopped for removing the materials adhered to the sidewalls of the beaker. The velocity of the mechanical stirrer was then increased to medium rotation (1000 rpm) until to complete 5 minutes, according to Figure 3.1.

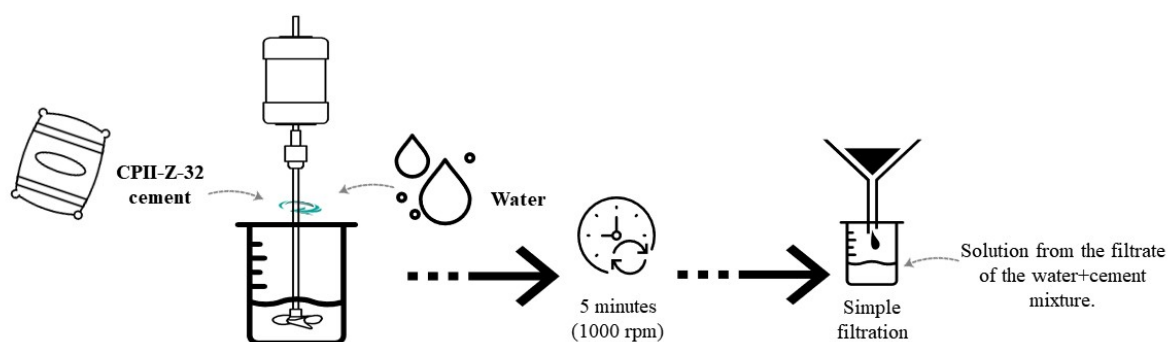


Figure 3.1 – Graphical representation of the solution from the filtrate of the water+cement mixture preparation (Source: Author's own graphical).

After this procedure, the liquid phase of the cementitious paste was separated by simple filtration. It is noteworthy that possibly the filtration process has changed the initial w/c ratio, but for its use as a swelling medium, only the characteristics similar to the pore solution is being considered, simulating the behavior of the hydrogel inside the cementitious material. This solution was stored in hermetic flasks to avoid the carbonatation process until its utilization.

3.2.3 Fourier transform infrared spectroscopy (FTIR)

FTIR spectra of the nanocomposite hydrogels were recorded using a Nicolet–NEXUS 670 FTIR spectrophotometer with 2 cm^{-1} resolution. KBr pellet technique (0.5 mg of sample in 100 mg of KBr) was applied for monitoring changes in the IR spectra of the samples in the range of $4000\text{--}400\text{ cm}^{-1}$. All measurements were recorded by the accumulation of 128 scans, and the vibrational energies are reported in wavenumber (cm^{-1}).

3.2.4 X-ray diffraction (XRD)

X-ray diffraction (XRD) patterns of the clay, hydrogel and their nanocomposites were obtained by (Shimadzu – XDR – 6000) diffractometer using $\text{Cu-K}\alpha$ radiation ($\lambda = 0.154\text{ nm}$) under a voltage of 30kV and current of 40 mA. All specimens were analyzed in continuous scan mode with 2θ ranging from 5° to 50° at a scanning rate of 1°min^{-1} . Additionally, the basal spacing or the distance of two adjacent nanoclay platelets was determined from the $d(001)$ reflection position, which is calculated by Bragg's equation ($n\lambda = 2d\sin\theta$).

3.2.5 Scanning electron microscopy (SEM)

Hydrogel and nanocomposites morphologies were observed using a ZEISS EVO LS15 electronic microscope operating at an accelerating voltage of 10 kV. First, the samples were swollen, until the equilibrium stage (48h) at $25^\circ\pm 1^\circ\text{C}$, in two different media: distilled water and solution from the filtrate of the water+cement mixture. After this step, they were frozen in liquid nitrogen and freeze-dried at -55°C for 24 h in a lyophilizer (model Enterprise II Terroni). Finally, the fractured nitrogen samples were gold-sputtered before SEM observation.

3.2.6 Swelling degree (SD) in distilled water or solution from the filtrate of the water+cement mixture

The hydrophilic properties of nanocomposites hydrogels were determined by measuring their swelling degree (SD) in two different swelling media: distilled water or water + Portland cement solution. Both determinations were measured at room temperature ($25^\circ\pm 1^\circ\text{C}$) by gravimetric analysis on an analytical balance (Shimadzu model AUY-220).

After purified in the dialysis process for 7 days, the samples were cut into circles of 22 mm diameter and dried in an oven at $40\pm 1^\circ\text{C}$ for 48 h. Then, they were placed into a vessel

containing 20 mL of each swelling medium. Noteworthy that the swelling measurements were performed in triplicate for each hydrogel-type analyzed.

For each predetermined time interval (measurements every 1 hour up to 8 hours, then at 24h, 32h, 48, and 72 hours), the samples were withdrawn from swelling media, and the excess of the water surface was gently removed with soft paper. Then, their weights were measured using an analytical balance (Shimadzu AUY-220-I). Immediately, the samples were again placed on the vessel. Finally, SD was calculated by using Equation 3.1:

$$SD = \frac{M_t}{M_d} \quad (\text{g H}_2\text{O or solution per g hydrogel}) \quad \text{Equation 3.1}$$

where M_t and M_d are the swollen mass at time t and the dried hydrogel, respectively. The measures were performed in triplicate ($n = 3$), and the error bars in the graph corresponding to the standard deviation.

3.2.7 Kinetic parameters

Kinect parameters were obtained through swelling degree measures as the function of time (F versus t) in different solutions. For each F versus t curve, the diffusion exponent (n) and diffusion constant (k) were calculated using Peppas Equation 3.2 [13].

$$\frac{M_t}{M_{eq}} = kt^n \quad \text{Equation 3.2}$$

where M_{eq} is the hydrogel mass at equilibrium time, t is the time, k is a diffusion constant (dependent on hydrogel type and swelling medium), and n is known as diffusion exponent that supplies the kind of water absorption mechanism.

Equation 3.2 was applied from the initial stage until 60% of the curve. Thus, the kinetic parameters involved in the mechanism of diffusion of water towards hydrogel were determined by the slope and linear coefficients of the $\ln(M_t/M_{eq})$ versus $\ln(t)$ curve, respectively.

3.2.8 Statistical analysis

The experimental results of the swelling degree in equilibrium and kinect parameters were available by analysis of variance (ANOVA) from Tukey test, with a 5% significance level, using SISVAR[®] software.

3.3 RESULTS AND DISCUSSION

3.3.1 Fourier transform infrared spectroscopy (FTIR)

FTIR spectra of the hybrid nanocomposites composed of PAAm, CMC, and Cloisite- Na^+ swollen in distilled water or solution from the filtrate of the water+cement mixture are presented in Figure 3.2 ((a) and (b)), and their characteristic spectroscopic bands are described in Table 3.1.

Table 3.1 - Main FTIR spectroscopic assignments PAAm/MBAAm/CMC + Cloisite Na^+ FTIR (distilled water or solution from the filtrate of the water+cement mixture as swelling medium)

| PAAm/MBAAm/CMC + Cloisite Na^+ (distilled water as swelling medium) | | | PAAm/MBAAm/CMC + Cloisite Na^+ (Filtrated water+cement mixture as swelling medium) | | |
|--|---|--------------|---|--------------------------------------|--------------|
| Peak (cm^{-1}) | Assignment | Ref. | Peak (cm^{-1}) | Assignment | Ref. |
| 3635 | O-H structural and O-H water interlayer stretchings | [14-16] | 3430 | O-H stretching | [28-30] |
| 3420 | O-H stretching | [14, 16, 17] | 3190 | N-H stretching | [18, 19, 31] |
| 3190 | N-H stretching | [18, 19] | 2920 | CH_2 stretching | [14, 15, 20] |
| 2926 | C-H stretching | [14, 15, 20] | 1665 | C=O stretching | [16, 17, 21] |
| 1665 | C = O stretching | [14, 17, 21] | 1630 | O-H bending | [30, 32, 33] |
| 1642 | O-H vibration | [22, 23] | 1560 | COO^- vibration | [25, 31] |
| 1456 | C-N stretching | [14, 24] | 1456 | C-N stretching | [14, 31] |
| 1420 | COO^- stretching | [16, 25] | 1120 | Si-O-Si vibrations | [20, 24] |
| 1120 | Si-O-Si vibration | [16, 17, 24] | 1184 | Si-O-Si stretching | [14] |
| 1042 | Si-O-Si vibration (tetrahedra layer) | [21-23] | 1042 | Si-O-Si vibration (tetrahedra layer) | [21-23] |
| 913 | Al-OH bending | [22, 26] | 875 | CO_3^{2-} bending | [33, 34] |
| 526 | Si-O-Si vibration Si-O-Al bending | [14, 20] | 620 | SO_4^{2-} bending | [35, 36] |
| 462 | Si-O-Al bending | [20, 26, 27] | 518 | Si-O-Al bending | [14, 20] |
| | | | 462 | Si-O-Al bending | [20, 26, 27] |

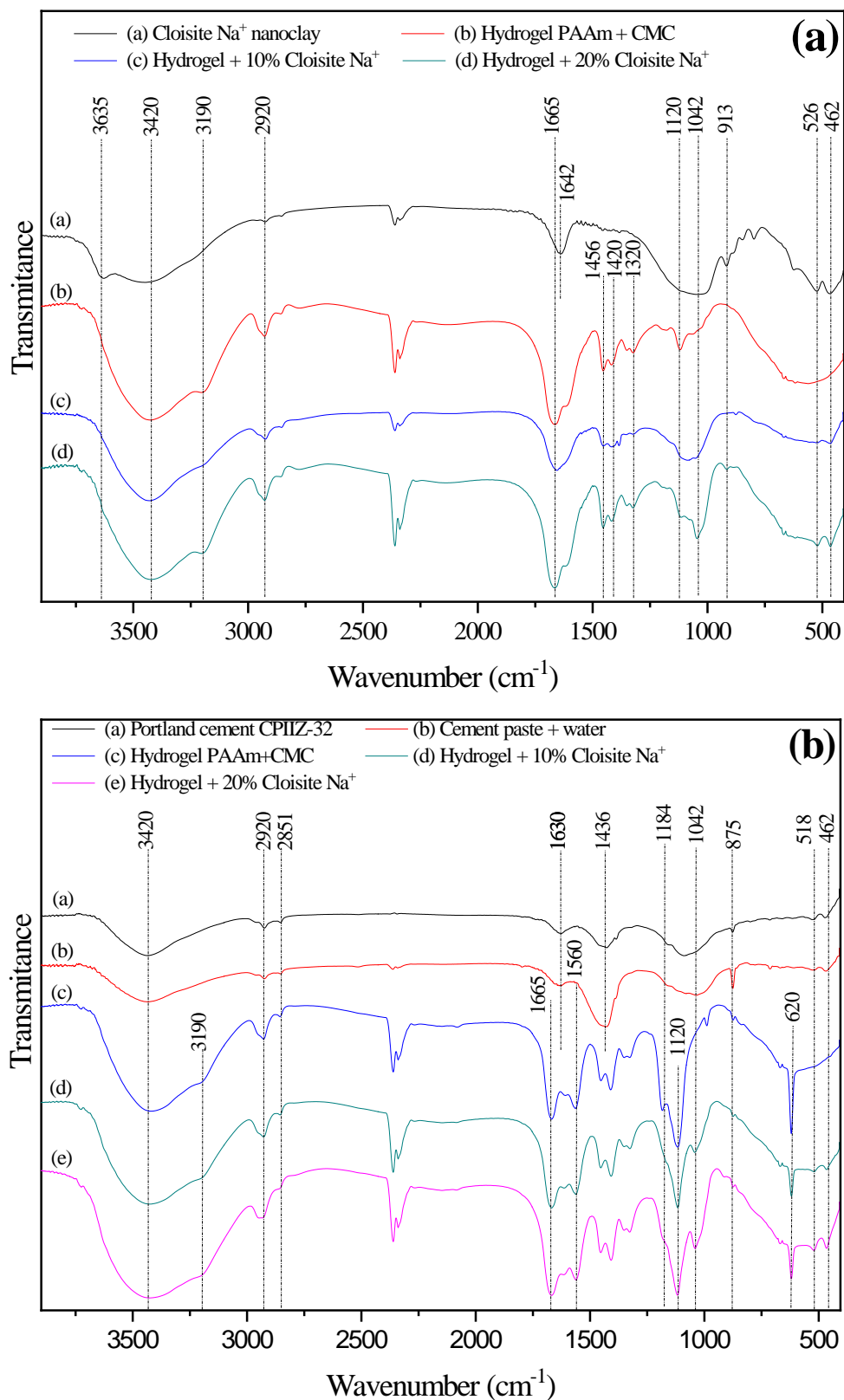


Figure 3.2 - FTIR spectra of PAAm/ MBAAm/ CMC + Cloisite Na⁺ swollen in (a) distilled water, and (b) solution from the filtrate of the water+cement mixture.

Nanoclay Cloisite Na⁺ presented a band at 3635 cm⁻¹ [14-16] and 3420 cm⁻¹ [14, 16, 17] related to the spectroscopic stretchings of bound water and the associated hydroxyl groups, respectively, which indicates that Cloisite Na⁺ is rich in -OH between oct- and tetrahedral sheets [15].

FTIR spectrum of the pure hydrogel is similar to that of hybrid nanocomposite hydrogel, which shows a broad peak at 3420 cm⁻¹ for its hydrogen-bonded -OH group [14, 16, 17]. Stretching vibration absorption peaks of -N-H and -CH_x after polymerization of AAm monomer appeared around 3190 cm⁻¹ [18, 19] and 2926 cm⁻¹ [14, 15, 20], respectively.

Peaks related to the -C-N of the secondary amide coming from AAm [37] or MBAAm appear near to 1456 cm⁻¹ [14, 24], and stretchings of -COO⁻ of this same group were assigned to 1665 cm⁻¹ [14, 17, 21] and 1420 cm⁻¹ [16, 25] regions, thus, evidencing the presence of the crosslinking agent, monomer, and polysaccharide in the hydrogel matrix.

Moreover, the FTIR hybrid nanocomposite hydrogels containing Cloisite Na⁺ show a spectroscopic peak at 1120 cm⁻¹ [16, 17, 24], 1042 cm⁻¹ [21-23], 913 cm⁻¹ [22, 26] 526 cm⁻¹ [14, 20] and 426 cm⁻¹ [20, 26, 27], that correspond to Si-O-Si vibrations of tetrahedral layer, Al-OH bending, Si-O-Al bending, respectively. Notably, all these bands refer to the characteristic absorption peaks of Cloisite Na⁺ [37], confirming their presence is involved in the hydrogel polymerization process. Despite the presence of characteristic Cloisite Na⁺ peaks, no evidence of clay-matrix chemical bonding was observed, i.e., the nanoclay can be physically anchored to the polymer matrix.

From Figure 3.1 (b), it was possible to confirm that FTIR of nanocomposite hydrogels swollen in solution from the filtrate of the water+cement mixture are very similar, except at 1630 cm⁻¹ [30, 32, 33] due to the bending vibration of -OH referent to water-free or water in gypsum (present in the cement), and at 1560 cm⁻¹ [25, 31] attributed the presence of -COO⁻ group in carboxylate anion. A shift of the COO⁻ band from 1420 to 1560 cm⁻¹ was observed, which can be attributed to the combination with calcium ions, corroborating that presented by Fernandes et al. [27], present in the swelling medium. New absorption peaks at 875 cm⁻¹ and 620 cm⁻¹, corresponding to a bending vibration of -CO₃²⁻ [33, 34] and bending vibration of -SO₄²⁻ [35, 36], respectively, were also observed.

Remarkably, the appearance of the -CO₃²⁻ and -SO₄²⁻ signals in the FTIR spectra is probably related to the development of the carbonatation process [37] and the presence of the hydration products of cement - as ettringite, that can be visualized in SEM images (see Section 3.3.3). It indicates that the hydrogel swelling in solution from the filtrate of the

water+cement mixture medium can form a cement hydration product in the superficial and internal hydrogel walls, but without modifying its foliated aspect, characteristic of hydrogels.

Furthermore, FTIR spectra showed absorption peaks at 518 cm^{-1} [14, 20] and 462 cm^{-1} [20, 26, 27], that correspond to Si-O-Si vibrations, Si-O-Al bending, respectively, and that it is present both in the cement composition and in the nanoclay used in the synthesis of hybrid hydrogels.

3.3.2 X-ray diffraction (XRD)

XRD patterns of Cloisite Na⁺ nanoclay, Portland cement paste, and the hybrid hydrogels are shown in Figure 3.3 (a and b).

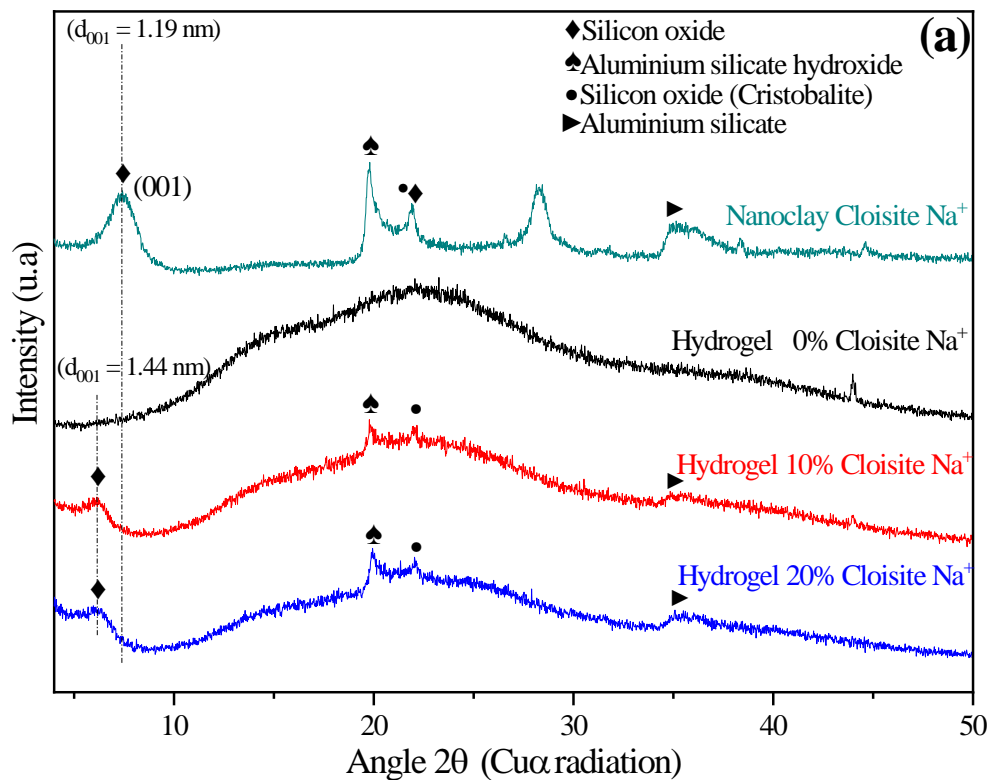


Figure 3.3a - X-ray diffraction for PAAm/ MBAAm/ CMC + Cloisite Na⁺ swollen in distilled water.

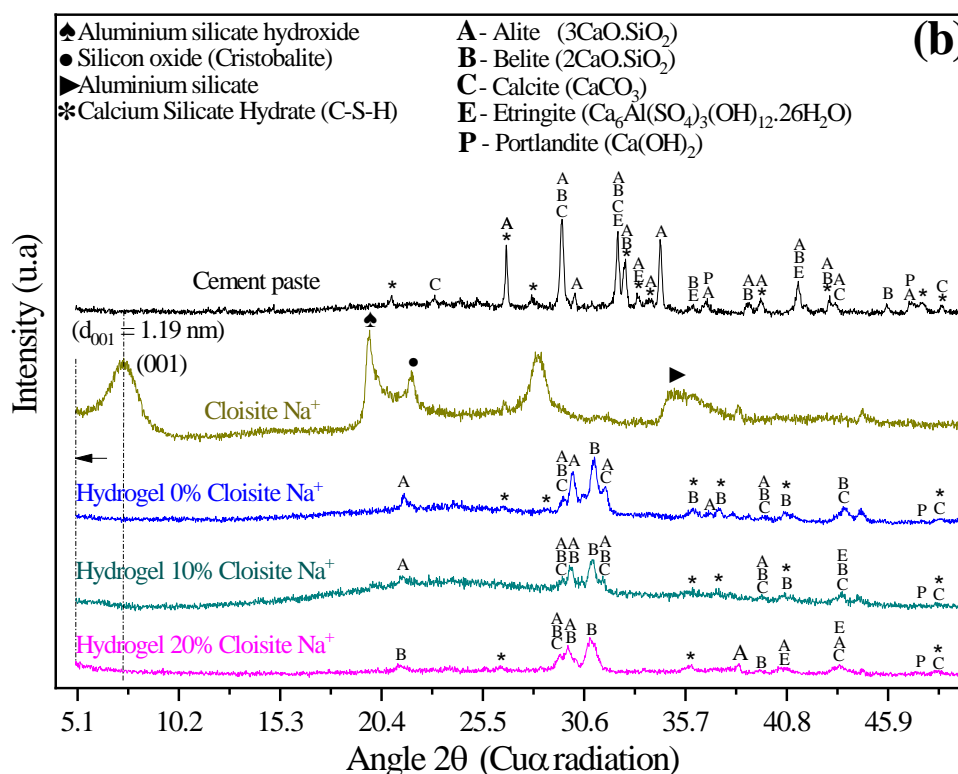


Figure 3.3b - X-ray diffraction for PAAm/ MBAAm/ CMC + Cloisite- Na^+ swollen in solution from the filtrate of the water+cement mixture

XRD analysis of the Cloisite Na^+ nanoclay (Figure 3.3a) displayed a reflection at $2\theta = 7.36^\circ$ assigned to the (001) crystalline plane or d_{001} interlayer basal spacing of 1.19 nm, agreeing with other authors [16, 38]. Besides, the reflections at $2\theta = 19.8^\circ$, 21.9° , and 28.3° could also be observed, corresponding to aluminum silicate hydroxide, silicon oxide, and aluminum silicate hydroxide [39], respectively.

XRD patterns of hydrogel pure (PAAm and CMC) and hybrid nanocomposite hydrogels (PAAm/ CMC and Cloisite Na^+) confirmed that these matrices are predominantly amorphous expected due to their chains have high crosslinking density. However, it is possible to observe from hybrid hydrogels XRD that the characteristic nanoclay peak ($2\theta = 7.36^\circ$) shifted to the small angle of the $2\theta = 6.28^\circ$, causing an increase in basal spacing ($d_{001} = 1.44$ nm). This increase indicated the intercalation of nanoclay Cloisite Na^+ in the polymer matrix, as mentioned by other authors [20].

The main reason for nanoclay intercalation was reported by Wang and Wang [40], which indicated that CMC molecules were successfully intercalated into the spacing of clay layers, reducing their crystal structure. He et al. [37] also related that the interaction between AAm monomer and montmorillonite during the polymerization process could form a gel mesh structure that occasioned the increase in the basal spacing.

It is reported that the arrangement of clay layers results in a broad XRD pattern, broadening of d_{001} peak observed in modified montmorillonite reflected a lower degree of ordering for montmorillonite layers compared with natural clay. Therefore, the interlayer structure of montmorillonite is damaged, and the weakening of the hydrogen bonding reduced its crystallinity [37].

However, when swelling in solution from the filtrate of the water+cement mixture (Figure 3.3b), the nanocomposites change their behaviors. The diffractograms indicated the amorphous character of the hydrogel in nanocomposites was discrete with the increase of the Cloisite Na^+ in the polymeric matrix. From XDR analysis of the hybrid hydrogels solution from the filtrate of the water+cement mixture, it was no observed the basal spacing of the nanoclay peak was ($2\theta = 7.36^\circ$; $d_{001} = 1.19$ nm) in the polymeric matrices. Probably the nanoclay platelets are exfoliated in the hydrogel chains because this peak shifted to small angles under $2\theta = 4^\circ$.

The diffractograms of hybrid hydrogels also revealed new crystallized phases attributed to cement hydration products such as alite ($3\text{CaO} \cdot \text{SiO}_2$), belite ($2\text{CaO} \cdot \text{SiO}_2$), calcite (CaCO_3), ettringite ($\text{Ca}_6\text{Al}(\text{SO}_4)_3(\text{OH})_{12} \cdot 26\text{H}_2\text{O}$), and portlandite ($\text{Ca}(\text{OH})_2$), which are also present in the cement paste diffractogram. Notably, the presence of these crystallized phases is consistent with the SEM (as discussed in the next Section) and FTIR results that allow visualizing these products impregnated on the surface of the hydrogel walls and the identification of the $-\text{CO}_3^{2-}$ and $-\text{SO}_4^{2-}$ groups.

3.3.3 Scanning electron microscopy (SEM)

The correlation between the physical and morphological properties of the different hydrogels was also investigated. Three-dimensional network porous structures were studied and analyzed using the SEM technique. SEM micrographs of the internal structure of hydrogels swelled in distilled water are presented in Figure 3.4 (a, b, and c). They are formed by the porous uniformly distributed structure of a sponge, similarly, as already mentioned in the literature [41, 42]. Thus, their water uptake and its retention rate depend on hydrogel porosity and mean pore size. Hence, one of the most important properties, which should be considered, is hydrogel microstructure morphologies [17].

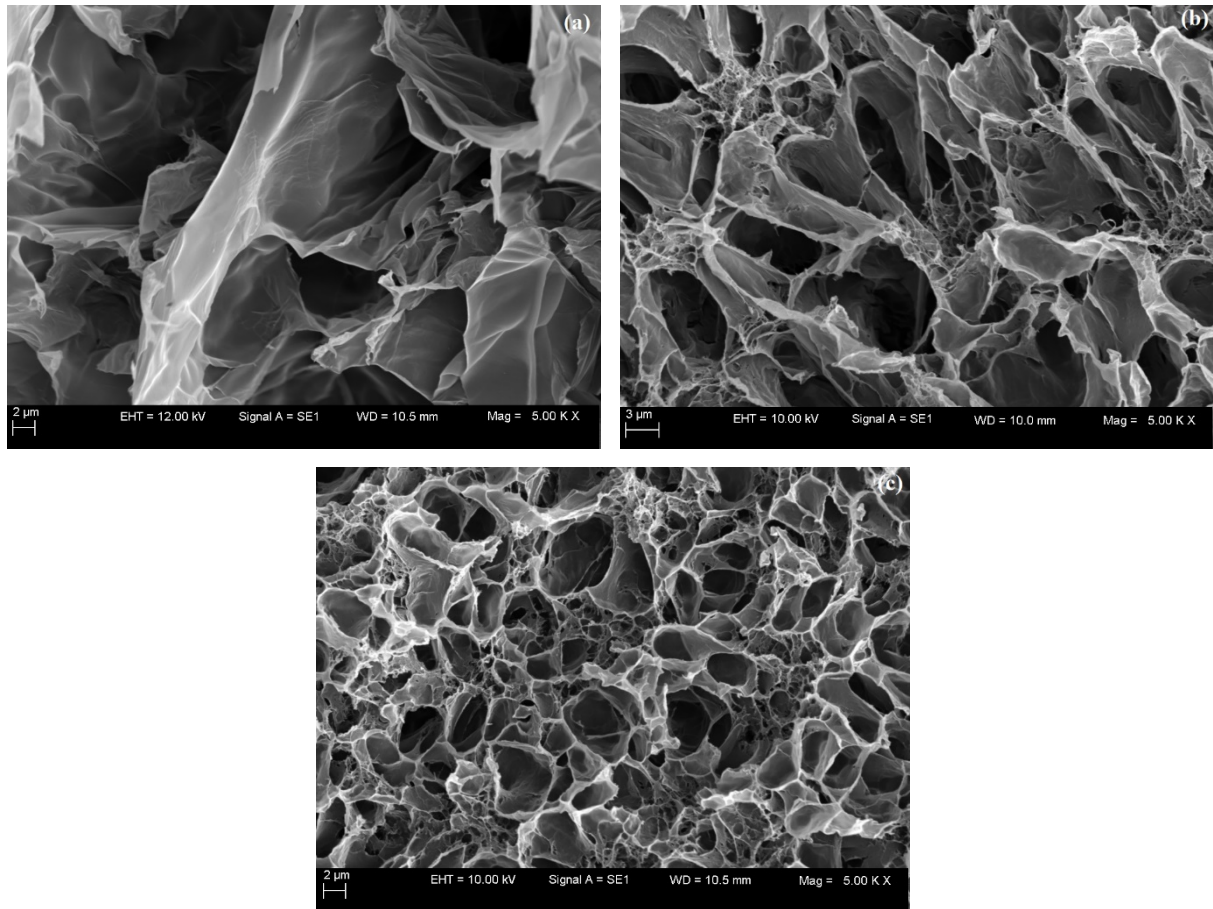


Figure 3.4 - SEM micrographs (5000x magnification) of hydrogel swelled in distilled water: (a) PAAm+CMC, (b) PAAm+CMC+10% Cloisite Na⁺, (c) PAAm+CMC+20% Cloisite Na⁺.

The open spaces (pores) among the polymer network decreased, and the number of pores increased when the nanoclay concentration used in the hydrogel preparation increased, corroborating with Cojocariu et al. [10]. Here, SEM images confirming a solid correlation between morphology and water-uptake capacity. Hydrogels with large pores (Figure 3.4a) interact more significantly with water molecules, resulting in considerable water uptake. In contrast, as shown in Figure 3.4c, Cloisite Na⁺-based nanocomposites have a tighter structure with smaller pore sizes. In this way, the area of the pores in contact with water molecules is small, which contributes to decreasing water-uptake capacity [43], corroborating with the swelling degree results.

However, when the hydrogels are swelling solution from the filtrate of the water+cement mixture, their morphological properties present some changes, as can be seen in Figures 3.5 (a, b, c, d, e, and f).

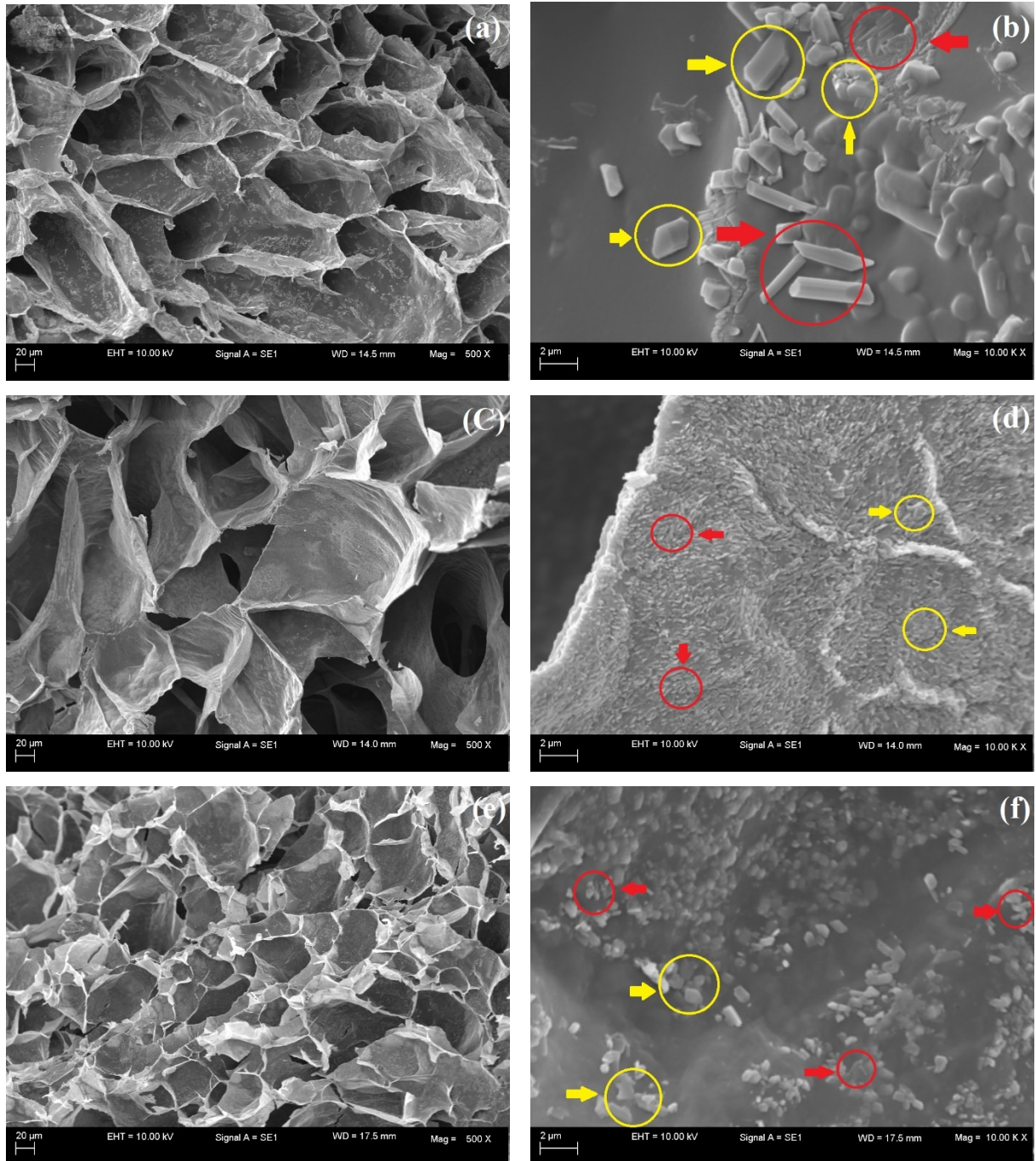


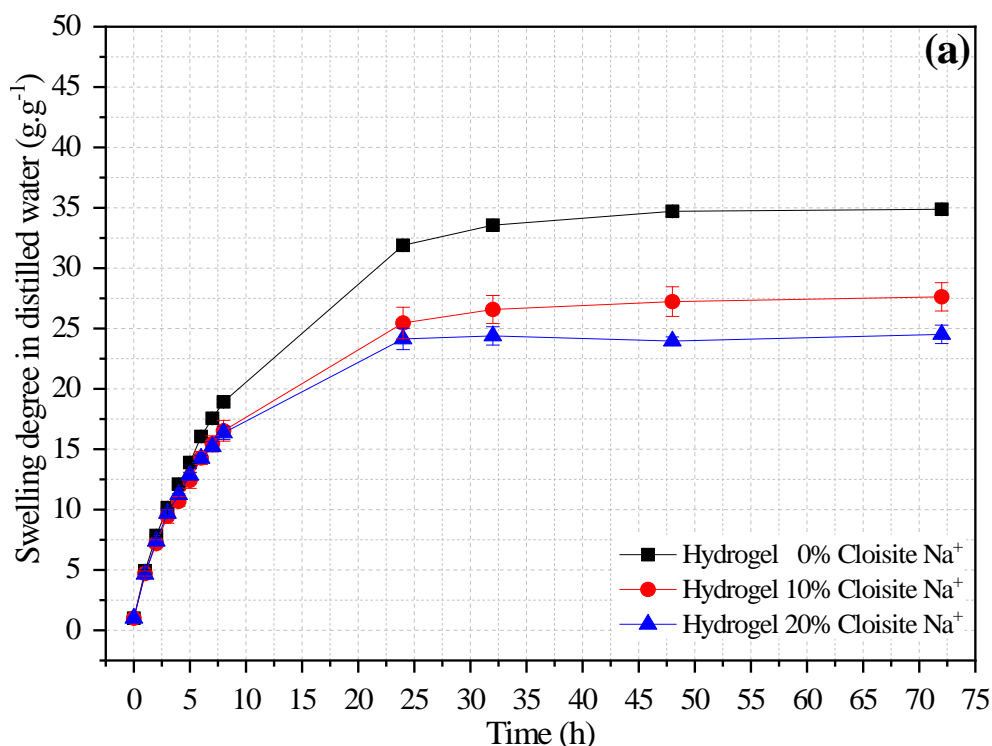
Figure 3.5 - SEM micrographs (500x and 10000x magnification) of hydrogel swelled solution from the filtrate of the water+cement mixture: (a-b) PAAM+CMC, (c-d) PAAM+CMC+10% Cloisite Na⁺, (e-f) PAAM+CMC+20% Cloisite Na⁺.

The porous structure of hydrogels remains, and they are showing an increase in the number of smaller pores as the nanoclay concentration increases. It causes a reduction in its water absorption capacity, similar to the hydrogels swelled in distilled water. On the contrary, it is possible to observe cement hydration products on the hydrogel surfaces in Figures 3.5 (b, d, and f). Note the presence of ettringite ($\text{Ca}_6\text{Al}(\text{SO}_4)_3(\text{OH})_{12}\cdot 26\text{H}_2\text{O}$) characterized by needle

shape (represented by the red circle in SEM), as well as the presence of portlandite ($\text{Ca}(\text{OH})_2$) with its hexagonal shape crystals [44] (represented by the yellow circle in SEM). Remarkably, these cement hydration products are impregnated in the hydrogel walls, as discussed in the IR spectra and X-ray diffractograms.

3.3.4 Swelling degree (SD)

Swelling degree (SD) analysis of hybrid hydrogels is necessary once the controlled water release over time depends on this property and can contribute to a more effective internal curing procedure of cementitious materials [45] due to the continuous cement [6] hydration inside of these materials. The absorption behaviors of hydrogels in distilled water and the solution from the filtrate of the water+cement mixture are shown in Figures 3.6 (a and b), respectively.



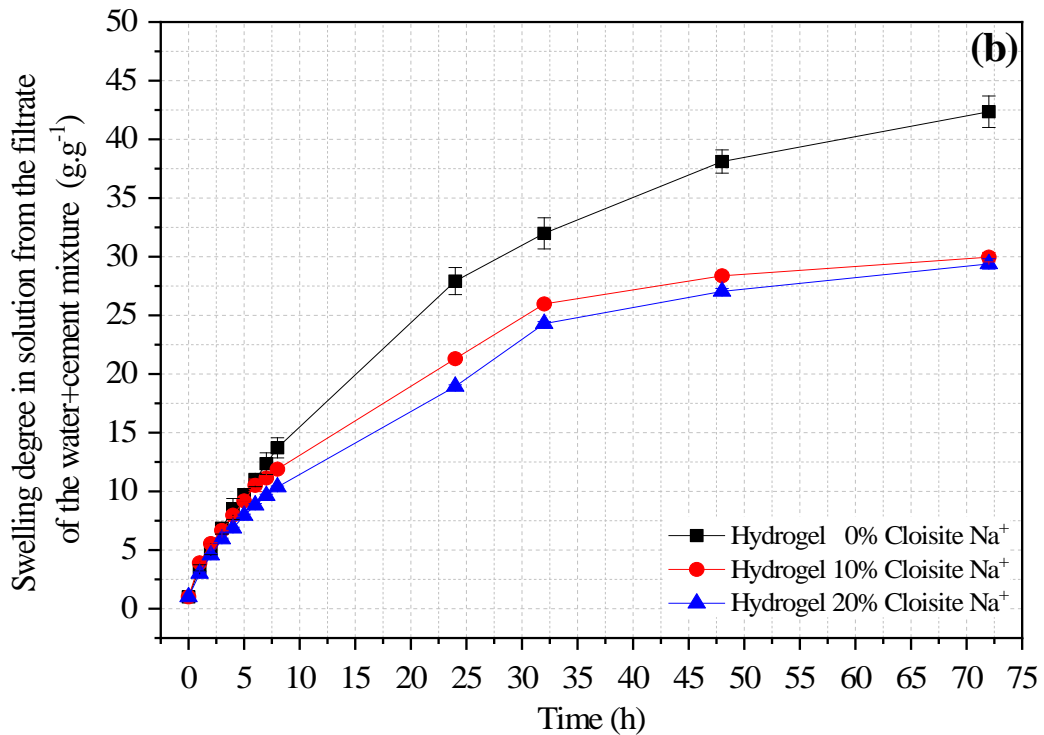


Figure 3.6 - Swelling curves as a function of time for hydrogels with different Cloisite Na⁺ concentrations in (a) distilled water and (b) solution from the filtrate of the water+cement mixture.

There are evident differences in the behavior of nanocomposite hydrogels in these two different environments. It is seen from Figure 3.6a that all hydrogels showed water absorption in the range of 24–32 (g.g⁻¹) in distilled water. Also, the Cloisite Na⁺ interferes directly in this hydrophilic property because the higher its concentration, the lower hydrogels swelling degree, corroborating with reported by Aalaie et al. [46]. The author verified that the equilibrium degree of swelling of the nanocomposites decreases with the increase of montmorillonite content because the free hydrophilic groups of the nanocomposite reduce with the Na⁺ increases, decreasing the difference in the osmotic pressure between the matrix and the swelling medium and, consequently a retraction of the hydrogels with Cloisite Na⁺ [46].

In the first eight hours of testing, it was possible to observe an accelerated water absorption, independently of the concentration of nanoclay, reaching the equilibrium conditions after 48 hours. Similar behavior was also observed by Yenzawa et al. [47]. The results showed that the PAAm+CMC hydrogel had $SD_{\text{equilibrium}}$ equal to 34.71 ± 1.92 g.g⁻¹. For hybrid hydrogels with 10% and 20% Cloisite Na⁺ concentration, the average $SD_{\text{equilibrium}}$ were 27.23 ± 1.30 g.g⁻¹ and 24.39 ± 0.88 g.g⁻¹ respectively.

The relationship between SD_{eq} and the amount of Cloisite Na^+ in the nanocomposites was shown in Figure 3.7.

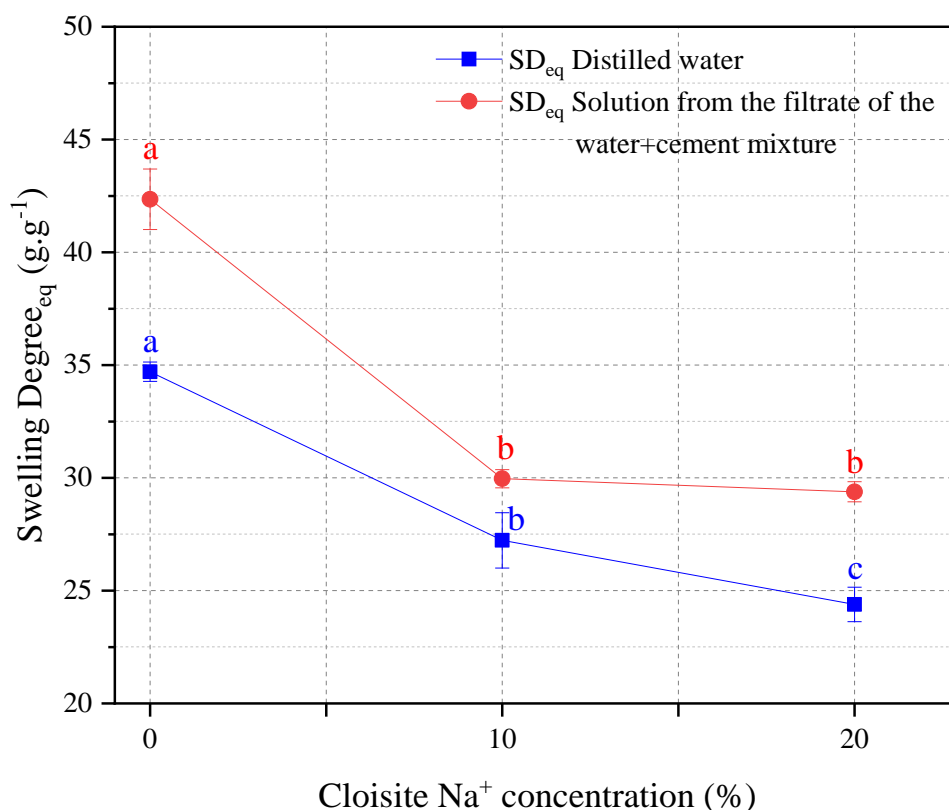


Figure 3.7 - Effect of the amount of Cloisite Na^+ on the equilibrium swelling degree. *Average with their respective standard deviation values, followed by equal letters, do not differ statistically from each other following the Tukey test with a 95% confidence level.

The reduction of SD_{eq} for hybrid hydrogels (10 and 20% Cloisite Na^+) was 21.55% and 29.73%, respectively, when compared with PAAm+CMC hydrogel. This behavior can be attributed to the presence of nanoclay as a physical crosslinker in the polymeric matrix, which can cause a reduction in the expansion capacity of the chain and the water storage capacity in its pores [10, 43]. These behaviors also can be attributed to their molecular structure and morphology [48] that could be analyzed from SEM images.

Comparatively to the results presented in Figures 3.6 (a and b), the behavior of hydrogels in solution from the filtrate of the water+cement mixture revealed different features from that in distilled water. Because the behavior of sorption and desorption kinetics was altered due to factors such as pH and the presence of ions in the solution [49].

In the first eight hours of testing, it was possible to observe an accelerated water absorption, independently of the concentration of nanoclay, similar to the results presented from hydrogels swelled in the distilled water medium. However, the hydrogels in the solution

from the filtrate of the water+cement mixture need more time to complete their equilibrium state. At 72 hours, the water absorption process continued with minor variations, so the results showed that the $SD_{\text{equilibrium}}$ of PAAm+CMC hydrogel was $42.35 \pm 1.34 \text{ g.g}^{-1}$, and the values for hybrid hydrogels with 10% and 20% Cloisite Na^+ concentration were $29.96 \pm 0.41 \text{ g.g}^{-1}$ and $29.38 \pm 0.44 \text{ g.g}^{-1}$, respectively. Compared to the hydrogels swollen in distilled water, the nanocomposites, when placed in solution from the filtrate of the water+cement mixture, presented an increase of around 28, 18, and 22 % at the same nanoclay concentrations.

From Figure 3.7, it was observed that values of SD_{eq} of all types of hydrogels were higher than the reference values in distilled water. One of the possible causes is the alkalinity of the solution from the filtrate of the water+cement mixture ($\text{pH} = 13.1$). The physical properties of hydrogels are affected by this change in pH, and the presence of acidic ($-\text{COOH}$) or basic (OH^-) groups can accept or release protons. In addition, at high pH values, the alkaline groups are deprotonated, and the acid groups are ionized. Therefore, electrostatic interactions are weak and lead to a more open structure with a large capacity for swelling [49].

Another possible cause is related to the solvation process. The bivalent cation Ca^{2+} is typical in a cement solution, and it can change the absorption behavior of hydrogel samples [50]. Solvation is a function of the ions present in the solution from the filtrate of the water+cement mixture, Ca^{2+} cations can group water molecules and enter into the structure of the hydrogel, and to increase the swelling degree as observed in the results because these cations can interact and bind with carboxylate groups from different AAm chains in the polymer.

However, Ca^{2+} can form additional physical crosslinks that restrain the movement of AAm chains, which provoke a reduction of the hydrogel swelling capacity [51] due to the migration of ions from the pore solution into the hydrogels. Indeed, a screening effect reduces the electrostatic repulsion in the polymeric networks of the hydrogels [51-53].

The swelling of hydrogels is a complex phenomenon because the solution from the filtrate of the water+cement mixture consists of multi-species, and the concentration of ions varies with cement type, dosage, among other aspects. In this way, it is necessary to analyze this phenomenon to understand better the effect of this polymer in the cementitious matrix.

3.3.5 Kinetic parameters

The mechanism of water absorption is associated with the diffusional exponent (n) and the diffusion speed of the solvent (k) [27]. The mechanism can occur in four different ways: where $n < 0.45$, the mechanism occurs by *Fickian* diffusion; when $n = 0.89$, the diffusion occurs by case II-transport; in other words, this mechanism is governed by polymer swelling (chains relaxation); for $0.45 < n < 0.89$, the diffusion mechanism is classified as anomalous transport (non-*Fickian* diffusion), that is, the combination of the two previous; and when $n > 0.89$ corresponds to super case II-transport [13, 54-56]. Changes in kinetic parameters as a function of Cloisite Na⁺ concentration are shown in Table 3.2.

Table 3.2 - Values of k and n obtained for different concentrations of Cloisite Na⁺ in the hydrogels swelled in distilled water and solution from the filtrate of the water+cement mixture media.

| Cloisite Na ⁺ concentration (% w/w) | Distilled Water | | | | Solution from the filtrate of the water+cement mixture | | | |
|--|--|--------------------|---------------------------|----------------|---|--------------------|---------------------------|----------------|
| | SD _{eq} (g.g ⁻¹) | n | k (h ⁻¹) | R ² | SD _{eq} (g.g ⁻¹) | n | k (h ⁻¹) | R ² |
| 0 | 34.707 ^a | 0.598 ^a | 0.154 ^a | 0.990 | 42.351 ^a | 0.637 ^a | 0.098 ^a | 0.998 |
| 10 | 27.229 ^b | 0.546 ^a | 0.197 ^a | 0.983 | 29.962 ^b | 0.542 ^a | 0.142 ^b | 0.996 |
| 20 | 24.389 ^c | 0.548 ^a | 0.198 ^a | 0.969 | 27.436 ^b | 0.582 ^a | 0.112 ^{a,b} | 0.999 |

*Average with their respective standard deviation values, followed by equal letters, do not differ statistically from each other following the Tukey test with a 95% confidence level.

All nanocomposites in the distilled water medium presented values of n above 0.45 and below the control matrix. Thus, the water absorption mechanism of all hydrogels has anomalous behavior when the diffusion times and relaxation rates of the chains are comparable. In this case, both the sorption and transport of molecules are affected by the presence of pre-existing microcavities in the polymeric matrix [55]. However, the increase in the Cloisite Na⁺ concentration in the nanocomposite matrices modifies the water absorption, tending to *Fickian* transport, where the diffusion rate is much slower than the relaxation time of the polymer chain. This relaxation time is the time it takes for the chain to settle, that is, to come into balance with the presence of the solute or solvent.

The presence of nanoclay in the polymer matrix increased the values of the constant diffusion k . The authors believe that the oxygen bound to the silicon of the nanoclay platelets may simultaneously interact with the CMC chain groups and with distilled water, accelerating the water absorption process [47]. However, it is intended that even accelerating the velocity

of water absorption, the nanoclay also acts as a crosslinking agent, contributing to the decrease in total water absorbed by the matrix. These results corroborated with SD results, whereas these nanocomposites were those with less water absorption capability.

Contrary analyzes of the k kinetic parameters of hydrogels in solution from the filtrate of the water+cement mixture allowed to observe a decrease in the velocity of water absorption compared to results obtained from swelling degree in distilled water. For this same swelling media, diffusion coefficient (n) values confirmed that the swelling mechanisms of all hydrogels have a non *Fickian* or anomalous behavior, similar to the swelled in distilled water. Notably, the increase of Cloisite Na⁺ in the polymeric matrices not caused changes in these parameters.

Thus, these results corroborated that increases in the swelling degrees in solution from the filtrate of the water+cement mixture were related to the solvation process caused by the presence of ions in cementitious solution.

3.4 CONCLUSIONS

This study analyzed the physical, chemical, and morphological properties of hybrid hydrogels containing different concentrations of Cloisite Na⁺ nanoclay, having two different swelling media, i.e., distilled water or solution from the filtrate of the water+cement mixture. The findings from this study are listed as follows:

- PAAm, CMC, and Cloisite Na⁺ nanoclay nanocomposite hydrogel were successfully synthesized via free-radical polymerization using different amounts of Cloisite Na⁺. SEM and FTIR techniques confirmed that the nanoclay was incorporated into the hydrogel matrix.
- SEM images showed that the concentration of nanoclay increases the crosslinking density of the polymer chains. As a result, it was possible to observe some hydration products of cement on the surface of hydrogels. It was also verified in the FTIR that indicated CO₃²⁻ and SO₄²⁻ groups related to carbonatation and ettringite formation.
- XRD patterns indicated that the amorphous character of the hydrogel in the nanocomposites was discrete. However, it is possible to observe crystalline peaks attributed to cement hydration products when they swelled the cementitious solution. In addition, it was no observed the basal spacing of the nanoclay peak ($2\theta = 7.36^\circ$; $d_{001} = 1.19$ nm) in the nanocomposite matrices, indicating that its platelets are probably

exfoliated in the hydrogel chains when these hydrogels are swelled in solution from the filtrate of the water+cement mixture.

- The presence of Cloisite Na⁺ interferes directly with the absorption mechanism in both swelling media. Thus, comparing the hydrogels swollen in distilled water, the nanocomposites, when placed in water and cement solution, presented an increase of around 22, 10, and 20 % in the degree of swelling of the hydrogel containing 0, 10, and 20% (wt/wt) Cloisite Na⁺ concentrations, respectively.
- The diffusion coefficient (n) values confirmed that the swelling mechanisms of the hybrid nanocomposites tend to anomalous behavior when the diffusion times and relaxation rates of the chains are comparable. In this case, pre-existing microcavities in the polymeric matrix affect both the sorption and transport of molecules.

Thus, the application of hybrid nanocomposites becomes an alternative for cementitious materials to attenuate problems related to retraction, and therefore guarantee the improvement of its properties, whether in a fresh or hardened state.

3.5 REFERENCES

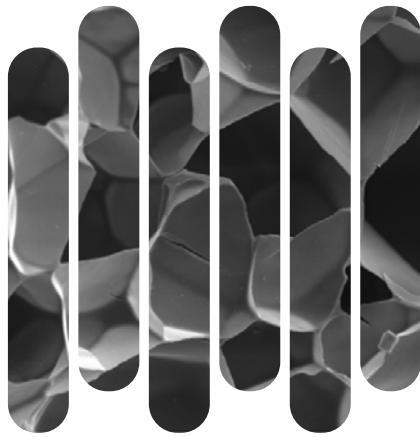
- [1] D. M. Nascimento, Y. L. Nunes, M. C. Figueirêdo, H.M. de Azeredo, F. A. Aouada, F. A., J. P. Feitosa, A. Dufresne, Nanocellulose nanocomposite hydrogels: technological and environmental issues. *Green Chem.*, 20 (2018), 2428-2448.
- [2] D. Snoeck, L. Pel, N. De Belie, N., The water kinetics of superabsorbent polymers during cement hydration and internal curing visualized and studied by NMR. *Sci. Rep.* 7 (2017), 1-14.
- [3] F. Wang, J. Yang, S. Hu, X. Li, Cheng, H., Influence of superabsorbent polymers on the surrounding cement paste. *Cem. Concr. Res.*, 81 (2016), 112–121.
- [4] X. Chen, S. Wu, J. Zhou, J., Influence of porosity on compressive and tensile strength of cement mortar. *Constr. Build. Mater.*, 40 (2013), 869-874.
- [5] S. H. Kang, S. G. Hong, J. Moon, The effect of superabsorbent polymer on various scale of pore structure in ultra-high performance concrete. *Constr. Build. Mater.*, 172 (2018), 29-40.
- [6] J. C. D. Santos, M. M. Tashima, M. R. D. Moura, F. A. Aouada, Obtainment of hybrid composites based on hydrogel and Portland cement. *Quim. Nova*, 39 (2016), 124-129.
- [7] M. Irani, H. Ismail, Z. Ahmad, Preparation and properties of linear low-density polyethylene-g-poly (acrylic acid)/organo-montmorillonite superabsorbent hydrogel composites. *Polym. Test.* 32 (2013), 502-512.
- [8] S. Liang, L. Liu, Q. Huang, K. L. Yam, Unique rheological behavior of chitosan modified nanoclay at highly hydrated state. *J. Phys. Chem. B.*, 113 (2009), 5823–5828.

- [9] S. S. Ray, M. Bousmina, Biodegradable polymers and their layered silicate nanocomposites. In *greening the 21st-century materials world Progress. J. Mater. Sci.*, 50 (2005), 962–1079.
- [10] A. Cojocariu, L. Profire, M. Aflori, C. Vasile, C., In vitro drug release from chitosan/Cloisite 15A hydrogels. *Appl. Clay Sci.*, 57 (2012), 1–9.
- [11] D. W. S. Nascimento, M. R. de Moura, L. H. C. Mattoso, F. A. Aouada, Hybrid Biodegradable Hydrogels Obtained from Nanoclay and Carboxymethylcellulose Polysaccharide: Hydrophilic, Kinetic, Spectroscopic and Morphological Properties. *J. Nanosci. Nanotechnol.*, 17 (2017), 821–827.
- [12] M. G. Hernández, J. J. Anaya, M. A. G. Izquierdo, L. G. Ullate, Application of micromechanics to the characterization of mortar by ultrasound. *Ultrasonics*, 40 (2002), 217–221.
- [13] P. L. Ritger, N. A. Peppas, A simple equation for description of solute release II. Fickian and anomalous release from swellable devices. *J. Control. Release*. 5 (1987), 37–42.
- [14] S. Ganguly, S. Mondal, P. Das, P. Bhawal, P. P. Maity, S. Ghosh, N. C. Das, Design of psyllium-g-poly (acrylic acid-co-sodium acrylate)/cloisite 10A semi-IPN nanocomposite hydrogel and its mechanical, rheological and controlled drug release behaviour. *Int. J. Biol. Macromol.*, 111 (2018), 983–998.
- [15] B. Tanc, N. Orakdogan, Charged groups synergically enhanced elasticity and tunable swelling/shrinking of poly (dialkylaminoethyl methacrylate)/layered silicate nanocomposite cryogels. *Polymer*, 178 (2019), 121627.
- [16] W. Wang, J. Wang, Y. Zhao, H. Bai, M. Huang, T. Zhang, S. Song, High-performance two-dimensional montmorillonite supported-poly(acrylamide-co-acrylic acid) hydrogel for dye removal. *Environ. Pollut.*, 257 (2019), 113574.
- [17] Y. Bao, J. Ma, N. Li, Synthesis and swelling behaviors of sodium carboxymethyl cellulose-g-poly (AA-co-AM-co-AMPS)/MMT superabsorbent hydrogel. *Carbohydr. Polym.*, 84 (2011), 76–82.
- [18] Z. Zhao, H. Chen, H. Zhang, L. Ma, Z. Wang, Polyacrylamide-phytic acid-polydopamine conducting porous hydrogel for rapid detection and removal of copper (II) ions. *Biosens. Bioelectron.*, 91 (2017), 306–312.
- [19] M. M. Ghobashy, M. A. Elhady, pH-sensitive wax emulsion copolymerization with acrylamide hydrogel using gamma irradiation for dye removal. *Radiat. Phys. Chem.*, 134 (2017), 47–55.
- [20] D. Romanzini, V. Piroli, A. Frache, A. J. Zattera, S. C. Amico, Sodium montmorillonite modified with methacryloxy and vinylsilanes: influence of silylation on the morphology of clay/unsaturated polyester nanocomposites. *Appl. Clay Sci.*, 114 (2015), 550–557.
- [21] M. Yadav, S. Ahmad, Montmorillonite/graphene oxide/chitosan composite: Synthesis, characterization and properties. *Int. J. Biol. Macromol.*, 79 (2015), 923–933.
- [22] S. Kar, B. Kundu, R. L. Reis, R. Sarkar, P. Nandy, R. Basu, S. Das, Curcumin ameliorates the targeted delivery of methotrexate intercalated montmorillonite clay to cancer cells. *Eur. J. Pharm. Sci.*, 135 (2019), 91–102.

- [23] M. Shabaniyan, M. Hajibeygi, K. Hedayati, M. Khaleghi, H. A. Khonakdar, New ternary PLA/organoclay-hydrogel nanocomposites: Design, preparation and study on thermal, combustion and mechanical properties. *Mater. Des.*, 110 (2016), 811-820.
- [24] Y. Mansoori, S. V. Atghia, M. R. Zamanloo, G. Imanzadeh, M. Sirousazar, Polymer-clay nanocomposites: Free-radical grafting of polyacrylamide into organophilic montmorillonite. *Eur. Polym. J.*, 46 (2010), 1844-1853.
- [25] S. Nesrinne, A. Djamel, Synthesis, characterization and rheological behavior of pH-sensitive poly (acrylamide-co-acrylic acid) hydrogels. *Arab. J. Chem.* 10 (2017), 539-547.
- [26] J. Madejová, J., FTIR techniques in clay mineral studies. *Vib. Spectrosc.*, 31 (2013), 1-10.
- [27] R. S. Fernandes, F. N. Tanaka, M. R. de Moura, F. A. Aouada, Development of alginate/starch-based hydrogels crosslinked with different ions: Hydrophilic, kinetic and spectroscopic properties. *Mater. Today Commun.* 21, 1 (2019), 100636.
- [28] M. A. Sikandar, W. Ahmad, M. H. Khan, F. Ali, M. Waseem, M., Effect of water resistant SiO₂ coated SrAl₂O₄: Eu²⁺ Dy³⁺ persistent luminescence phosphor on the properties of Portland cement pastes. *Constr. Build. Mater.*, 228 (2019), 116823.
- [29] J. Liu, N. Farzadnia, C. Shi, X. Ma, Shrinkage and strength development of UHSC incorporating a hybrid system of SAP and SRA. *Cem. Concr. Compos.*, 97 (2019), 175-189.
- [30] J. Sun, H. Shi, B. Qian, Z. Xu, W. Li, X. Shen, Effects of synthetic CSH/PCE nanocomposites on early cement hydration. *Constr. Build. Mater.*, 140 (2017), 282-292.
- [31] P. Zhong, M. Wyrzykowski, N. Toropovs, L. Li, J. Liu, P. Lura, Internal curing with superabsorbent polymers of different chemical structures. *Cem. Concr. Res.*, 123 (2019), 105789.
- [32] P. Feng, H. Chang, X. Liu, S. Ye, X. Shu, Q. Ran, The significance of dispersion of nano-SiO₂ on early age hydration of cement pastes. *Mater. Des.*, 186 (2020), 108320.
- [33] B. Lu, C. Shi, J. Zhang, J. Wang, Effects of carbonated hardened cement paste powder on hydration and microstructure of Portland cement. *Constr. Build. Mater.*, 186 (2018), 699-708.
- [34] D. O. Santos, Durabilidade de pastas de cimento contendo a rede polimérica Epoxy-Etilenodiamina: avaliações em ambientes aquosos quimicamente agressivos. Doctoral thesis, Federal University of Sergipe, Brazil, 2017.
- [35] C. R. F. Junior, M. R. de Moura, F. A. Aouada, Synthesis and characterization of intercalated nanocomposites based on poly(methacrylic acid) hydrogel and nanoclay Cloisite-Na⁺ for possible application in agriculture. *J. Nanosci. Nanotechnol.* 17 (2017), 5878-5883.
- [36] M. Y. Ashfaq, M. A. Al-Ghouti, D. A. Da'na, H. Qiblawey, N. Zouari, Investigating the effect of temperature on calcium sulfate scaling of reverse osmosis membranes using FTIR, SEM-EDX and multivariate analysis *Sci. Total Environ.*, 703 (2020), 134726.
- [37] F. He, Q. Zhou, L. Wang, G. Yu, J. Li, Y. Feng, Fabrication of a sustained release delivery system for pesticides using interpenetrating polyacrylamide/alginate/montmorillonite nanocomposite hydrogels. *Appl. Clay Sci.*, 183 (2019), 105347.

- [38] P. T. Bertuoli, D. Piazza, L. C. Scienza, A. J. Zattera, Preparation and characterization of montmorillonite modified with 3-aminopropyltriethoxysilane. *Appl. Clay Sci.* 87 (2014), 46–51.
- [39] W. P. Gonçalves, J. Silva, J. Gomes, R. R. Menezes, G. A. Neves, H. C. Ferreira, L. N. L. Santana, Avaliação da influência de diferentes tratamentos térmicos sobre as transformações de fases esmectitas. *Cerâmica*, 60 (2014), 316-322.
- [40] M. M. Wang, L. Wang, Synthesis and characterization of carboxymethyl cellulose/organic montmorillonite nanocomposites and its adsorption behavior for Congo Red dye. *Water Sci. Eng.* 6 (2013), 272-282.
- [41] C. R. F. Junior, F. N. Tanaka, A. Bortolin, M. R. de Moura, F. A. Aouada, Thermal and morphological characterization of highly porous nanocomposites for possible application in potassium-controlled release. *J. Therm. Anal. Calorim.* 131 (2018), 2205-2212.
- [42] V. V. Panic, Z. P. Madarevic, T. Volkov-Husovic, S. J. Velickovic, Poly(methacrylic acid) based hydrogels as sorbents for removal of cationic dye basic yellow 28: Kinetics, equilibrium study and image analysis. *Chem Eng J.* 217 (2013), 192-204.
- [43] F. A. Aouada, B. S. Chiou, W. J. Orts, L. H. C. Mattoso, Physicochemical and morphological properties of poly(acrylamide) and methylcellulose hydrogels: Effects of monomer, crosslinker and polysaccharide compositions. *Polym. Eng. Sci.*, 49 (2009), 2467–2474
- [44] P. Stutzman, Scanning electron microscopy imaging of hydraulic cement microstructure. *Cem. Concr. Comp.*, 26 (2004), 957–966.
- [45] C. Schroefl, V. Mechtcherine, P. Vontobel, J. Hovind, E. Lehmann, E., Sorption kinetics of superabsorbent polymers (SAPs) in fresh Portland cement-based pastes visualized and quantified by neutron radiography and correlated to the progress of cement hydration. *Cem. Concr. Res.*, 75 (2015), 1–13.
- [46] J. Aalaie, E. Vasheghani-Farahani, A. Rahmatpour, M. A. Semsarzadeh, Effect of montmorillonite on gelation and swelling behavior of sulfonated polyacrylamide nanocomposite hydrogels in electrolyte solutions. *Eur. Polym. J.*, 44 (2008), 2024–2031.
- [47] U. G. Yonezawa, M. R. de Moura, F. A. Aouada, Hybrid bionanocomposites formed from polysaccharide hydrogels and nanoclay II: incorporation in substrate to seedling improving. *Cult. Agron.* 26 (2017), 82-94
- [48] K. Farzanian, K. Pimenta Teixeira, I. Perdigão Rocha, L. De Sa Carneiro, A. Ghahremaninezhad, The mechanical strength, degree of hydration, and electrical resistivity of cement pastes modified with superabsorbent polymers. *Constr. Build. Mater.*, 109 (2016), 156–165.
- [49] A. M. Slavutsky, M. A. Bertuzzi, Formulation and characterization of hydrogel based on pectin and brea gum. *Int. J. Biol. Macromol.*, 123 (2019), 784-791.
- [50] C. Schröfl, V. Mechtcherine, M. Gorges, Relation between the molecular structure and the efficiency of superabsorbent polymers (SAP) as concrete admixture to mitigate autogenous shrinkage. *Cem. Concr. Res.*, 42 (2012), 865–873.

- [51] H. X. D. Lee, H. S. Wong, N. R. Buenfeld, Effect of alkalinity and calcium concentration of pore solution on the swelling and ionic exchange of superabsorbent polymers in cement paste. *Cem. Concr. Comp.*, 88 (2018), 150–164.
- [52] A. Bajpai, A. Giri, Water sorption behavior of highly swelling (carboxy methylcellulose-g-polyacrylamide) hydrogels and release of potassium nitrate as agrochemical. *Carbohydr. Polym.*, 53 (2003), 271–279.
- [53] J. A. Garcia, M. R. de Moura, F. A. Aouada, Efeito do ph, espécie e concentração iônica na absorção de água de hidrogéis bionanocompósitos constituídos de CMC/PAAM/LAPONITA RDS. *Quim. Nova*, 42 (2019), 831-837.
- [54] S. Ibrahim, G. A. M. Nawwar, M. Sultan, Development of bio-based polymeric hydrogel: Green, sustainable and low-cost plant fertilizer packaging material. *J. Environ. Chem. Eng.* 4 (2016), 203-210.
- [55] B. A. Aderibigbe, K. Varaprasad, E. R. Sadiku, S. S. Ray, X. Y. Mbianda, M. C. Fotsing, S. C., Agwuncha, Kinetic release studies of nitrogen-containing bisphosphonate from gum acacia crosslinked hydrogels. *Int. J. Biol. Macromol.*, 73 (2015), 115–123.
- [56] R. París, I. Quijada-Garrido, Swelling and hydrolytic degradation behavior of pH-responsive hydrogels of poly[(N-isopropylacrylamide)-co-(methacrylic acid)] crosslinked by biodegradable polycaprolactone chains. *Polym. Int.*, 58 (2009), 362–367.



CHAPTER 4

FRESH PROPERTIES OF MORTARS

“Fresh properties of cement-mortars with hybrid nanocomposite addition based in Cloisite Na⁺ hydrogels”

4.1 OVERVIEW

Cement composites are one of the most widely produced materials in civil construction [1-3] due to their versatility, low cost, excellent mechanical performance, and durability during their useful life [4-6]. The importance of this material can be verified in the function of its global annual production around 35 to 53 billion tons, which is the second material, most used after water [3]. Thus, cement-mortars must be studied because they are responsible for several functions to ensure a good surface finish when applied as a coating or to ensure a uniform tension distribution to accommodate the associated deformations to thermal expansions and shrinkage [7] when used in masonry confection.

For mortars to adequately perform their functions throughout their useful life, they must have satisfactory behavior in their fresh state properties. These often depend directly on dosage studies and the water amount present in the mixture [8, 9].

Water, in this context, is an essential component for cement materials because it influences hardened state properties them [10], mainly to the questions concerning their microstructure and mechanical properties. Therefore, cement-materials technology challenges controlling water [11] to ensure cement particle hydration more effectively. One way to achieve this control over water is by developing and applying new types of admixtures, which can assist in substantially improve the characteristics of these materials in their fresh and hardened state [11]. Thus, due to some advantages, these admixtures are becoming widespread and indispensable components to produce almost all types of mortars and concretes, especially the high-performance [2]. Thus, because their addition does not change the mix proportions i.e., the water/cement (w/c) rate can be maintained or even reduced to improve the resistance and durability, preserving the material fluidity [12].

Several researches focus on the new chemistry additives field, mainly to ensure higher water availability to internal curing procedures [13-15] in cement-materials with a w/c ratio lower. These internal curing agents highlight the absorbent polymers as hydrogels that are interesting alternatives to gradual control of cement particle hydration due to their ability to absorb water and release it [16, 17] later into the hydrating cementitious matrix.

Hydrogels are hydrophilic polymeric materials with a three-dimensional crosslinked chain obtained through various polymerization processes. When in contact with water, they swell and increase their volume compared to the initial volume [18, 19]. They can be classified following their physical state, their crosslinking process of chemistry or physical [20], or following their raw materials based on natural polymers, semi-synthetics, or

synthetics [21]. Several studies are targeted and extensively analyzed using synthetic and commercial superabsorbent polymers (SAP) [22-26] as an internal curing agent to cement materials. These are based on polyacrylates, poly(acrylic acid), polyacrylamide, and polymetacrylamide. Superabsorbent polymers are used in civil construction field researches because they present a longer useful life, good mechanical resistance, and higher water absorption capacity [20, 27].

On the other hand, new hydrogels have been studied to obtain an absorbent polymer with similar properties to the SAP. These are the hybrid nanocomposite based on the hydrogel with Cloisite Na⁺ nanoclay incorporated with good mechanical properties [28] similar to synthetic polymers, presenting the advantage to have a biodegradable composition polysaccharide as carboxymethylcellulose [29-31].

Hydrogels, in addition to being applied as internal curing agents [32] they also are utilizing to improve the freeze resistance [33, 34] crack-sealing [35] and to reduce the shrinkage process during the hardening phase [36].

Remarkably, the applications of these polymers can happen in two manners, that is, in their dry or presoaked state, and both application options change rheological and physical aspects of mortars in their fresh state [37]. Moreover, it can also impact the hardened state of these mortars.

The application of dry hydrogels directly in the mix can remove an amount of kneading water in the function of their absorption and release kinect, reducing the w/c ratio of the mortar [38, 39, 40]. Thus, the amount of water removed in the fresh state depends on the physicochemical properties as swelling degree and chemical composition of these polymers. Another factor that impacts the absorption water is the swelling medium because the hydrophilic groups of hydrogels or SAP can have behaviors altered depending on the concentration of Ca²⁺, Na⁺, K⁺, OH⁻ e SO₄²⁻ ions, disperses in dosage water [16, 41].

The application of dry hydrogels to fresh mortars causes an increase in their yield stress and plastic viscosity [38] and provides a reduction in slump flow. However, these aspects are often corrected using superplasticizers [42] or an extra water portion [43] corresponding to the swelling degree of the polymer.

When the hydrogels or the SAP are used in their presoaked states also causes a change in the rheological properties of the mixture since part of the dosing water is found inside the polymer. However, the presoaked hydrogel is a potential option to introduce water into the curing process without the need to add a larger volume of water during the mortar mix [44].

In this context, the total w/c ratio reduces, decreasing the material's workability in its fresh state [42]. Nevertheless, the water-controlled release ensures internal humidity for the curing procedures, thus avoiding retraction at early ages [32] and ensuring more effective hydration of cement particles [45].

However, the effect of applying hybrid nanocomposites presoaked in the properties of cement-mortars with w/c ratio lower needs a wide investigation to elucidate how the incorporation of these hydrogels can affect their properties in the fresh state. Therefore, the present study aimed to evaluate the features of cementitious mortars in their fresh state when presoaked hybrid nanocomposite hydrogels were added. The changes in the consistency index, density, air content, water retention, and exudation rate were investigated in detail to make the production of cementitious materials feasible using more innovative internal curing agents. Thus, to obtain an advance in the technology of cementitious materials from getting mortars with characteristics comparable to the properties of mortars cured by traditional methods already known.

4.2 EXPERIMENTAL

4.2.1 Hydrogel synthesis and mortar preparation

All materials and details about hybrid nanocomposite hydrogel synthesis and mortar preparation have been previously presented in sections 2.1-2.3, Chapter 2.

4.2.2 Density in the fresh state

Density in the fresh state of mortar is also known as specific mass and varies with air content and specific weights of the constituent materials, mainly the aggregates. Thus, to complement the rheological properties of cement materials, three specimens were used to determine the density, following the NBR 13278 [46] recommendations.

After the mortar preparations, three cylindrical molds (diameter = 100 mm and height = 128 mm) were filled ($35 \pm 2^\circ\text{C}$ and relative humidity $\sim 55\%$), and the samples were mechanically vibrated (vibrated table SOLOTEST[®], Brazil) to eliminate incorporated air bubbles during the mechanical mix. After, the specimen masses were recorded using a semi-analytical balance (Shimadzu BL-3200H), and the values of fresh densities were calculated using Equation 4.1.

$$d = \frac{M_{ci} - M_{vi}}{V_{ri}} \quad \text{Equation 4.1}$$

where d = density in the fresh state (g.cm^{-3}), M_{ci} = mass of cylindrical mold (g) containing the mortar “ i ”; M_c = mass of empty cylindrical mold (g), and V_c = volume of cylindrical mold (cm^3).

The final value of densities in the fresh state for different mortars corresponds to the average value obtained from the three samples masses tested.

4.2.3 Air content

Air content ($A - (\%)$) was determined according to NBR 13278 [46], following the same procedure used in section 4.2.2, Equation 4.2.

$$A (\%) = 100 * \left(1 - \frac{d}{d_t}\right) \quad \text{Equation 4.2}$$

where d = density in the fresh state (g.cm^{-3}), d_t =theoretical density mass of the mortar (g.cm^{-3}). The theoretical density mass of mortar (d_t) is obtained by using Equation 4.3, considering the mass density of each mortar component material.

$$d_t = \frac{(m_{hydrogel} + m_{water} + m_{cement} + m_{sand})}{\left(\frac{m_{hydrogel}}{\gamma_{hydrogel}}\right) + \left(\frac{m_{water}}{\gamma_{water}}\right) + \left(\frac{m_{cement}}{\gamma_{cement}}\right) + \left(\frac{m_{sand}}{\gamma_{sand}}\right)} \quad \text{Equation 4.3}$$

where $m_{hydrogel}$, m_{water} , m_{cement} , and m_{sand} are hydrogel, water, cement, and sand masses (g), respectively; $\gamma_{hydrogel}$, γ_{water} , γ_{cement} , and γ_{sand} correspond to specific densities of the hydrogel, water, cement, and sand (g.cm^{-3}), respectively.

The $A (\%)$ values of each mortar presented in the results are the average value obtained from the three samples testing.

4.2.4 Water retention

Water retention capacity in fresh mortars is significant because available the water inside the mix increase. As a result, it can improve cement hydration and obtain a mechanical

strength gain. Thus, water retention analysis in hybrid mortars is realized because the hydrogels can act as water retentor agents. This study followed EN 1015-8 [47] recommendations, testing six samples of each fresh mortar.

After mortar preparation ($35 \pm 2^\circ\text{C}$ and relative humidity $\sim 55\%$), a fraction was collected, and it was casting inside the cylindrical mold (m_1) with a diameter of 100 mm and a height of 25 mm. The excess mortar was then removed from the top of the mold, and the mortar + mold set mass (m_3) was recorded using a semi-analytical balance (Shimadzu BL-3200H).

Subsequently, gauze and filter papers (m_{2i}) - weighed previously in a dry state - are placed on the set so that on a flat surface and in an inverted position, a load of 2 kg is placed on the set for 5 minutes. Finally, the filter paper was removed and again weighed (m_{4i}). Thus, the water retention is determined following Equation 4.4.

$$WRV_i = 100 - W_{4i} \quad \text{Equation 4.4}$$

where WRV_i = water retention of mortar sample "i" (%); W_{4i} = relative water loss by mortar "i" (%), calculated by using Equation 4.5.

$$W_{4i} = \frac{(m_{4i} - m_{2i})}{(m_{5i} - W_{1i})} * 100\% \quad \text{Equation 4.5}$$

where m_{5i} = amount of paste "i" inside the mold (g), calculated by using Equation 4.6, and W_{1i} = total water contained in paste "i" (g), calculated by using Equation 4.7.

$$m_{5i} = m_{3i} - m_{1i} \quad \text{Equation 4.6}$$

where m_{3i} = mold mass containing paste "i" (g); m_{1i} = mass of the mold associated with paste "i" (g).

$$W_{1i} = \frac{m_{water\ "i"}}{m_{mortar\ "i"}} \quad \text{Equation 4.7}$$

where $m_{water\ "i"}$ = total water mass used to produce the mortar "i" (g); $m_{mortar\ "i"}$ = total mortar mass "i" (g); com $i = 1, 2, 3, \dots, n$.

4.2.5 Consistency index

The determination of the consistency index was based on the ASTM C1437 [48]. This technique permitted the analysis of the influence of the nanocomposite hydrogels on the fresh

properties of the hybrid mortars. This testing was performed immediately after the hybrid-mortars mixing. The addition of the fresh mortar into the trunk-conical mold on a flow table (CONTECO[®], Brazil) occurs in three layers. The first layer was densified with 15 strokes randomly distributed in the mass. The second and third layers were densified with 10 and 5 strokes, respectively. The excess mortar was removed, and the mold was vertically removed. Finally, 30 strokes were applied to the flow table for 30 s. Thus, three measures of the diameter of the mortar on the table were obtained. The consistency index average was calculated by the three diameters obtained from its scattering.

4.2.6 Exudation test

One of several manners to study the water retention behavior of hydrogels is through the exudation rate. In this way, using this specific technique can help in dosage studies with hydrogels and prevent segregation in fresh cement mortars.

This methodology was based on RILEM MR-6 [49]. The samples were only prepared by manual compaction (i.e., without using a vibration table). Initially, 5 beakers of 500 mL were used to store the fresh mortars. By using a graduated pipette, the accumulated water on the paste surface was removed after 15, 30, 60, 180, and 240 minutes. After each extraction, the water volume was then measured. The exudation rate was calculated by the ratio between exudate water by the surface area of each beaker.

4.2.7 Statistical analysis

The experimental results for each treatment sets were available by analysis of variance (ANOVA) from the Tukey test, with a 5% significance level, using SISVAR[®] software.

4.3 RESULTS AND DISCUSSION

4.3.1 Density in the fresh state

The mortar density in the fresh state is an important parameter because it directly influences productivity and well-being aspects to who works with it. In this sense, as lighter is the mortar more workable, it will be too long, which reduces its application's effort, resulting in higher productivity [50]. The effects of hydrogels in density in the fresh state for mortars

produced with different Cloisite Na⁺ nanoclay concentrations and w/c = 0.40 are shown in Figure 4.1.

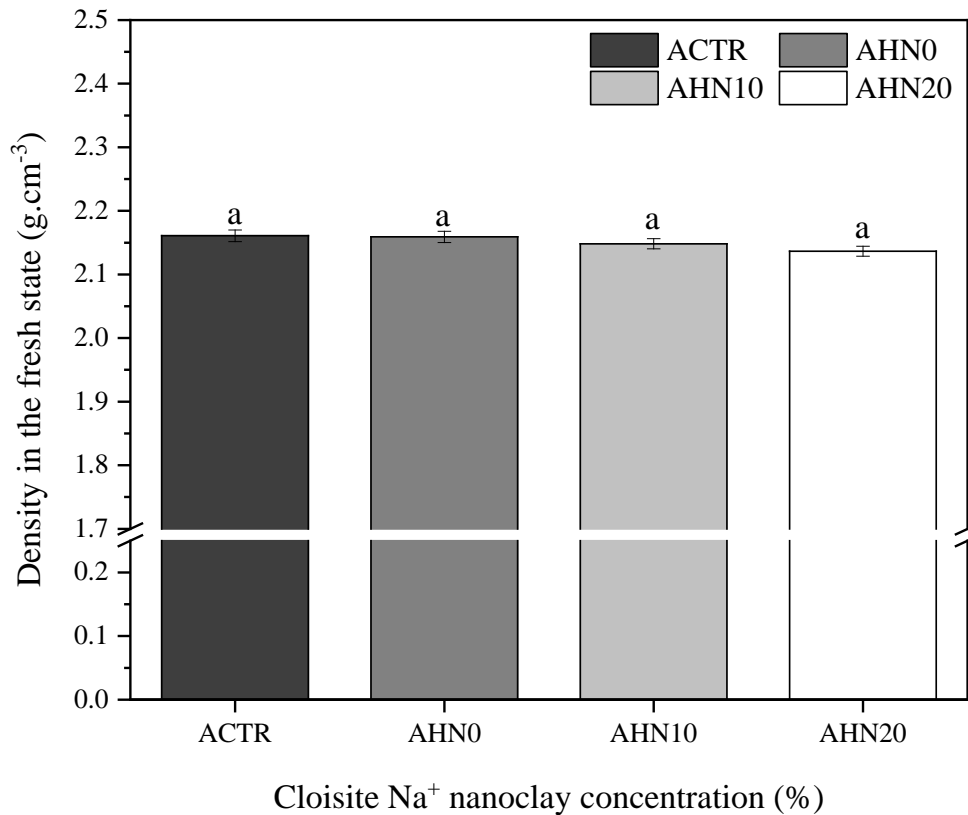


Figure 4.1 – Density in the fresh state for mortars produced with different Cloisite Na⁺ nanoclay hydrogels and water/cement of 0.40. *Average with their respective standard deviation values followed by equal letters do not differ statistically from each other, following the Tukey test with a 95% confidence level.

The average value of density in the fresh state of all hydrogel mortars was $\sim 2.15 \pm 0.01$ g.cm⁻³. It did not present significant statistical variation compared with the control mortar, whose average value was 2.16 ± 0.01 g.cm⁻³. From the settlement and coating mortar classification proposed by standard NBR 13281 [51], the mixes can be classified as “D6 class” because they all presented densities higher than 2 g.cm⁻³.

On the other hand, some authors report in their studies a reduction in concretes produced with commercial synthetic superabsorbent polymers base in polyacrylates and polyacrylic acid studied by Azarajifari et al. [43] Kang et al. [52], respectively. Many authors attribute this behavior to the air incorporated increases caused by the hydrogel presence in the mixes [38, 53, 54].

The results also corroborating with results obtained by Cunha et al. [55], whose average value of mortar (w/c ratio = 0.40) densities in the fresh state produced with 0.2-0.3%

de SAP (poly(acrylic acid)-polyacrylamide) was 2.24 g.cm^{-3} , and with values for mortars with SAP (acrylamide/acrylic acid copolymer) (0.2% w/wt cement) produced by Esteves et al. [56], around 2.25 g.cm^{-3} .

Other authors presented similar results. For instance, Mechtcherine et al. [32] found a density of 2.33 g.cm^{-3} for reference mortar (w/c ratio of 0.30) and 2.31 g.cm^{-3} for the mortar with 0.3% of poly(acrylic acid) SAP.

4.3.2 Air content

An important factor related to the fresh state properties of the cementitious materials is the air content in the mix. This occurs because during the cement-materials preparation, the mechanical stirring permits that the air is naturally mixed into the water so that it is subsequently eliminated during the mortar launch and densification process [57]. Thus, Figure 4.2 presents the relation between the density in the fresh state and air content variation for mortars produced with hydrogels with different Cloisite Na^+ nanoclay concentrations.

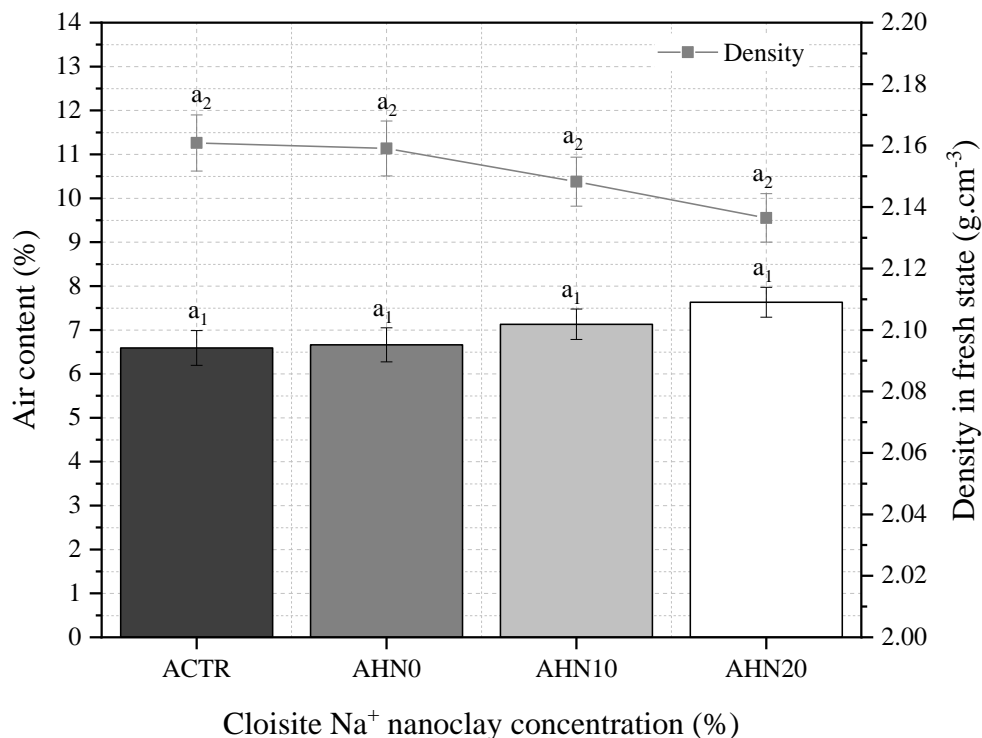


Figure 4.2 – Relation between density in the fresh state and air content (%) for mortars produced with different Cloisite Na^+ nanoclay hydrogels. *Average with their respective standard deviation values followed by equal letters do not differ statistically from each other, following the Tukey test with a 95% confidence level.

Although the results did not present statistical variation among themselves, it is possible to verify a tendency in the air content property, i.e., increasing the nanoclay quantity

in the cementitious matrices. Notably, all mortars demonstrated a minor air content % recommended by the ASTM C270-19a [58], whose maximum values for this parameter are 18%. The results are interesting because, first of all, the air content could improve freeze-thaw resistance discussed widely by several authors [39, 54, 59, 60].

The increased air content property is more pronounced to AHN10 and AHN20 mortars, whose increases were approximately 8.2% and 15.8%, respectively, compared to the ACTR mortar reference. This behavior can be related to the reinforcement effect of the cloisite-Na⁺ nanoclay [61, 62], resulting in a more stable hydrogel during the mechanical stirring, preventing it from being reduced to small particles and consequently disintegrating in the mixtures.

Laustsen et al. [63] used polyacrylamide-poly(acrylic acid) SAP to produce concretes. They concluded that the air content increase in the fresh state is associated with water inside SAP particles can be weakly connected. Thus, during the cement hydration, water from SAP will be released, filling the spaces in cement-material created by chemical shrinkage, spaces that would otherwise be empty pores. In this sense, the water-filled SAP particles are partly or fully drained during the hydration, creating SAP voids [63]. The authors affirm that swollen SAP particles generate a stable void system since they have a reduced tendency to segregate and coalesce.

Dudziak et al. [64] also verify that the use of poly(acrylic acid) SAP exhibited some improvement in air content and density in the fresh state of pastes and mortars. As also expected, Mechtcherine et al. [32], applying poly(acrylic acid) SAP in mortars formed from cement, silica fume, and sand, observed that polymer pronounced modify the mass consistency, and the air content of the fresh mortar increased around 2.3% concerning the reference mix.

Cunha et al. [55] obtained a result similar to this type of mortar and SAP. The authors attributed the expressive increase of air content to the presence of air bubbles left in the matrix during the release process of the curing water, which can also affect the development of the mechanical properties.

Suarez [65] discussed that higher SAP content added smaller will be the density in the fresh state of the mortars produced with cement, silica fume, and sand. The dosage with SAP (0.2% content) showed a density reduction due to the higher air content occasioned by the SAP particles and curing water in the mix. The air content increases from 1.6% to reference mortar (w/c ratio = 0.40) to 2.9% to mortar with 0.2% of SAP.

Thus, the results obtained corroborating with the discussion presented by other researchers, indicating that nanocomposite hydrogels directly modify the fresh properties of cement materials and confirming that air content and density in the fresh state are inversely proportional.

4.3.3 Water retention

Water retention is a property associated with the capacity of fresh mortar to maintain its workability when subject to solicitations that occasioned kneading water losses either by evaporation or water absorption by the settlement substrate [50]. The importance of this property is mainly in its application aspects, influencing the adherence and productivity of those who apply it. Figure 4.3 shows the water retention for reference mortars and nanocomposite hybrid-mortars, varying the Cloisite Na⁺ nanoclay concentration in its polymeric matrix.

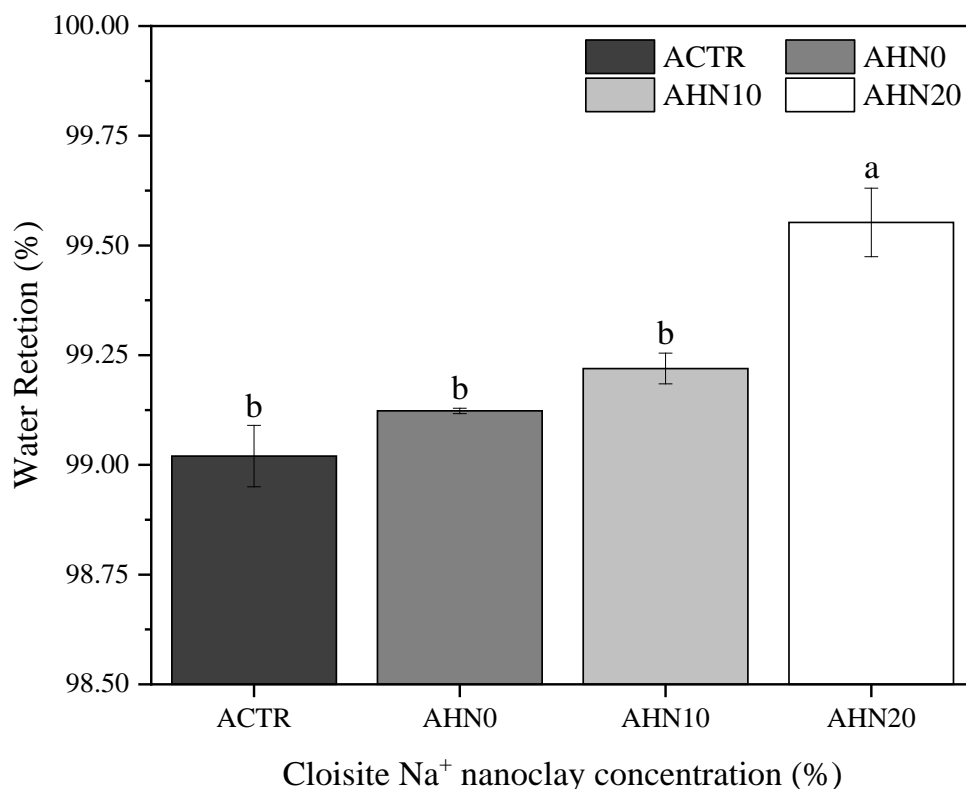


Figure 4.3 – Comparative of the water retention for mortars containing nanocomposites prepared from different Cloisite Na⁺ nanoclay amounts and water/cement of 0.40. *Average with their respective standard deviation values followed by equal letters do not differ statistically from each other, following the Tukey test with a 95% confidence level.

In general, the results presented a slight variation (but statistically significant) among them, with an overall average value of 99% in water retention for all mortars. Satisfactorily,

these results are according to ASTM C270-19a [58], where the minimum retention is 75% and the recommendations of NBR 13278 [46] that permits to classify these mortars as “Class E” because they have water retention values between 95 and 100%.

As mentioned, the application of hydrogels with Cloisite Na⁺ nanoclay in these mortars increased this index, being more evident for AHN20 mortar, i.e., highest nanoclay concentration in its polymeric structure. The hydrogels without and with 10% nanoclay in their compositions did not cause significant statistical effects for mortars compared with the reference sample ACTR. These small variations were 0.1% and 0.2% for AHN0 and AHN10 mortars produced with 0.5% (wt/wt cement) hydrogel, respectively. However, AHN20 mortar increased 0.5% concerning ACTR mortar, revealing that the nanoclay acts as an important agent in water retention by the polymer. This occurs because the polymeric structure of hydrogel modifies its morphology, acting, as already discussed, as a physical crosslinker and changing the absorption and release water kinetics [66, 67].

This behavior can be related to the water parcel of dosage of hydrogel-mortars presoaked to reduce the availability of free water in the mix. In contrast, this amount of water is stored, a priori, within the polymer particles [1]. Thus, an internal water reservoir is created into the fresh cement material, acting as a curing agent by gradually releasing absorbed water during the hydration process [68]. This trend was also observed by Tenório Filho et al. [69], who affirm that synthetic SAP hydrogels absorb and retain a certain amount of the water (depending on their absorption capacity) after water reservoir acting, keeping its level of internal relative humidity high for a considerable time. Indeed, Jensen et al. [70] noted that water retention in SAP also reduces free water content and w/b ratio due to its capacity of absorption or retention part of the mixed water upon dosage in concrete.

Water retention of these mortars due to the hydrogel dosage directly affects the workability. Thus, the consistency index decreases according to the future discussion presented in section 4.3.4. Although this direct reduction and modification in the rheological properties of the cement materials are related by several authors [17, 39], the water retention can be interesting because it allows that internal humidity is maintained [54]. This gain may prevent cracks due to plastic shrinkage [71] and improve the hydration of cement particles.

4.3.4 Consistency index

The consistency index is a parameter defined in function of the purpose of application of the cementitious material. This material does not present any segregation process for each

mixing, transportation, placing, and surface finishing process, and a homogeneous mixture can be obtained [57, 72]. Thus, this index measures the workability, which is considered one of the most important properties of cement-based materials, and a key, site-specific factor considered in mortar design [73]. The changes in consistency index for mortars produced with different water/cement ratios (w/c) and mortars with different hydrogel and nanoclay concentrations with w/c of 0.40 are shown in Figures 4.4 (a and b), respectively.

In general, the results demonstrated that the consistency indexes depend directly on the quantity of available water used in mortar preparation [37]. Figure 4.4a showed this condition for mortar without hydrogels, where the higher the w/c ratio, the higher the free water quantity in the mix, and consequently, better mortar workability. The consistency index increased about 61% when realized a comparison between the w/c ratios of 0.50 and 0.35. Therefore, this evidenced that this expressive increase can be attributed to the friction reduction between the mixed solid particles caused by the rise in water content [74].

Contrary, although these cement-material types improve their workability, it is known that the strength compressive can inversely vary with the water/cement ratio [7]. Thus, the mortar's final water/binder ratio is the most critical factor determining the hardened mechanical properties [75]. Therefore, this is an important parameter to be evaluated mainly in cementitious materials that require excellent mechanical performance.

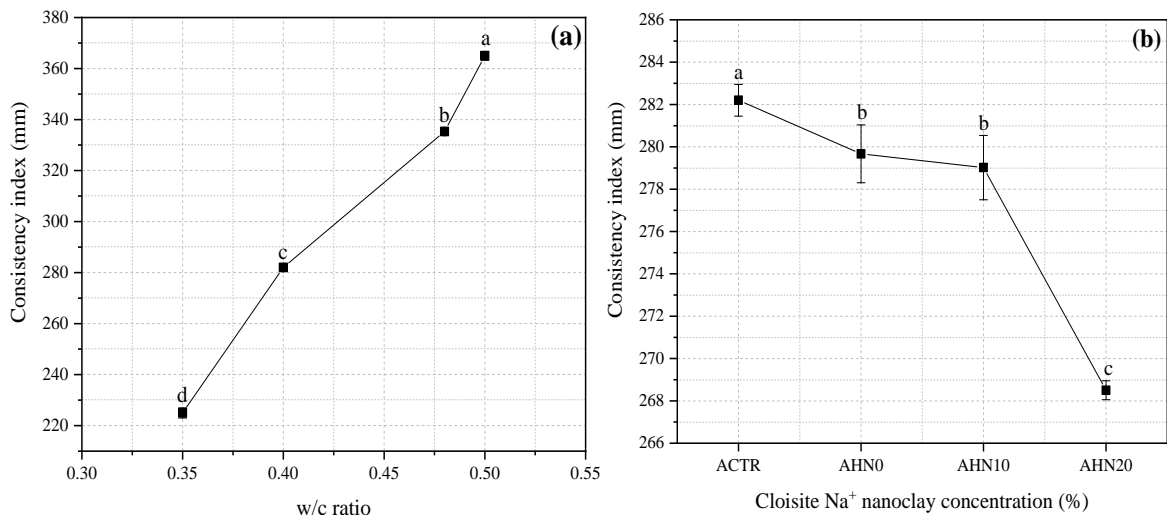


Figure 4.4 – Comparative of the consistency index for mortars with different water/cement ratios (a); different Cloisite Na⁺ nanoclay hydrogels and water/cement of 0.40 (b). *Average with their respective standard deviation values, followed by equal letters, do not differ statistically from each other, following the Tukey test with a 95%* confidence level.

Figure 4.4b presents the changes in the consistency index caused by Cloisite Na⁺ nanoclay concentration variation present in the hydrogel. All mortars were produced with a

w/c ratio of 0.40. Due to this condition, a hydrogel dosage of 0.50% demonstrates a satisfactory mechanical performance and workability conforming to previous studies realized by our research group [76,77]. Furthermore, it was possible to note that all mortars with hydrogel had good workability, although its consistency index had been reduced with the concentration Cloisite Na⁺ increase.

The decreases in the slump flow regarding the control were 0.9%, 1.1%, and 4.9% for AHN0, AHN10, and AHN20 mortars. The reduction in free water in the fresh mixture will inevitably affect the workability of material cementitious [78]. In contrast, an effective w/c ratio is lower than those proposed by the initial dosage because part of free water remained in the absorbent polymer matrix.

Gupta et al. [44] observed that the flow is significantly reduced even at higher SAP (sodium polyacrylate-based commercial) dosage as the amount of pre-absorbed water in SAP increases. Two main reasons are probably related: i) the reduction in free water content in the fresh mix due to absorption of water by SAP; ii) the swollen SAP particles, which act as soft aggregates. The results presented by these authors showed that 0.3% SAP-mortars reduced around 17% the values of slump when compared with reference mortar produced with cement, sand, and water (1: 2.75 w/c ratio = 0.45).

Similarly, Dang et al. [42] demonstrated that synthetic SAP based on sodium polyacrylate (Hebei Xiguang Chemical Technology Co. Ltd.), presoaked with deduction of mix internal curing water, also had a significant influence in the slump of concretes. They verified that concretes produced with 0.3% of SAP in their composition present a reduction of about 31% in their consistency index compared with reference samples, following the same trend to the obtained results. Yang et al. [79] also observed that cement-mortars with 0.4% of synthetic SAP (polyacrylic acid), concerning the cement mass, reduced its slump flow, attributing it to the thickening effect caused to SAP in the mixture due to the free water absorption by these polymers.

Senff et al. [17] showed that the presence of dry synthetic SAP (Evonik[®]) reduces the mortar workability, and this decrease is attributed to ionic nature and the interconnect chain structure of SAP particles that improve the chemical affinity with the water kneading molecules, increasing the level of absorption of these polymers. Consequently, the relative quantity of free water available in the mix decreased, being necessary to adjust the w/c ratio to maintain the workability to a more extended period.

Another relevant aspect to be discussed about the results obtained (Figure 4.4b) is that besides hybrid nanocomposites to have evident potential as hidroretentor agents, as also described by Paiva et al. [38], the Cloisite Na⁺ nanoclay presence directly influences the absorption and release kinect of the hydrogel over time, impacting on the fluidity of cement-material in their fresh state.

This occurs because the nanoclay, besides acting as a reinforcing agent, can improve some physical properties of polymers [29, 80, 81] and increase the hydrophilic properties of these nanocomposites [82]. Thus, the effect obtained by adding the nanoclay is to reduce the swelling degree since the clay intercalated into the polymeric chains can act as a crosslinking agent for these polymer networks and, consequently, a slower water release over time [61], reducing the workability when applied in cement-materials.

4.3.5 Exudation index

Exudation in cement materials is a type of segregation in which part of the mixing water tends to migrate to the surface of the mortar early age produced. It is caused by the inability of the mixture solid constituents to retain all the mixing water when they settle towards the bottom [74]. Exudation is not necessarily harmful, and the effective w /c ratio can be decreased, with a consequent increase in resistance, if the exudation is not disturbed. In this context, hydrogels can contribute to the water retention stage at more recent ages and prevent this type of phenomenon. From Figure 4.5, it is possible to analyze the behavior of mortars without and with hybrid nanocomposites about changes in the exudation rate of this type of cementitious material caused by the water retention, as already discussed in section 4.3.3.

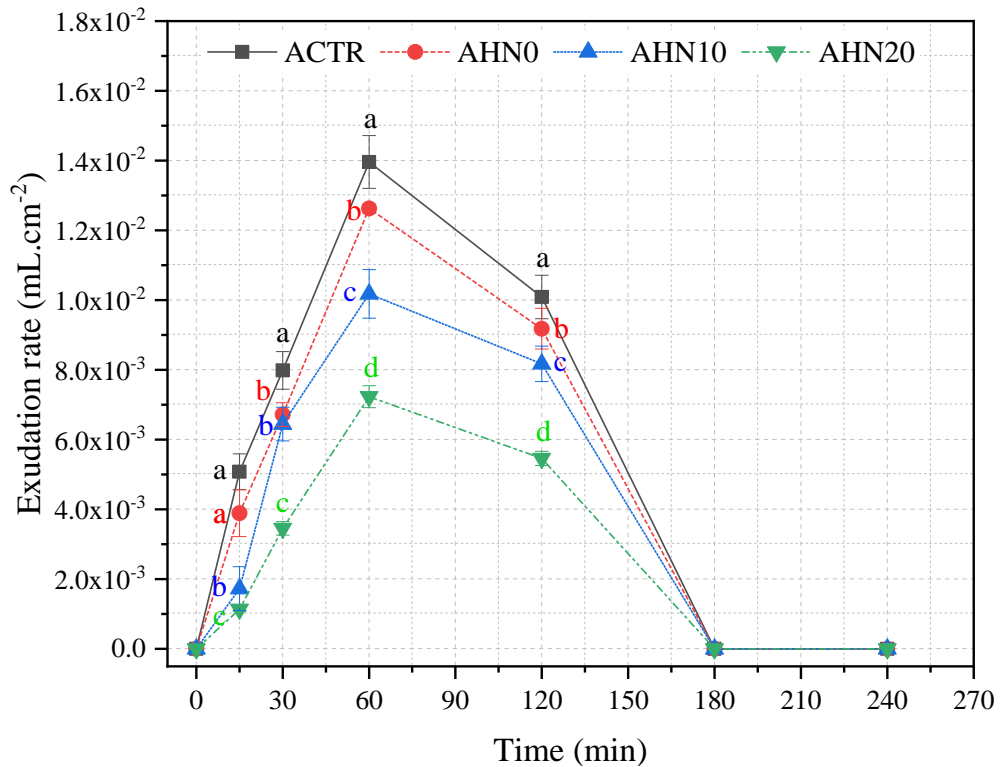


Figure 4.5 – Exudation index as the function of time for cement-mortars with different Cloisite Na⁺ nanoclay hydrogels and water/cement of 0.40. *Average with their respective standard deviation values, followed by equal letters, do not differ statistically from each other following the Tukey test with a 95% confidence level.

In general, results pointed that all mortars with hydrogel in their composition presented an exudation index reduction, indicating that the hydrogels act as water retains agents [20, 37, 83]. From the graphical representation (Figure 4.5), it is possible to observe a sharp growth in the exudation rate in the first 60 minutes, where it reaches its maximum value. After this time, exudation rates decreased in the function of initial and end-setting time of cement Portland used.

The maximum values of these decreases observed near 60 min were 9.5%, 27.1%, and 41.3% to AHN0, AHN10, and ANH20 mortars, respectively, about the reference ACTR mortar, and permit to relate them with the previous results already discussed. The Cloisite Na⁺ nanoclay concentration causes higher water retention, a reduction in the consistency index, and, consequently, a decrease in exudation rate, according to Table 4.1.

Table 4.1 - Average value and standard deviation to physical properties in the fresh state to different mortars

| Mortar | Consistency index (mm) | Water Retention (%) | Density in fresh state (g/cm ³) | Exudation index (mL/cm ²) |
|--------|----------------------------|---------------------------|---|---------------------------------------|
| ACTR | 282.20 ± 0.75 ^a | 99.02 ± 0.07 ^b | 2.16 ± 0.01 ^a | 0.0140 ± 0.0007 ^a |
| AHN0 | 279.02 ± 1.52 ^b | 99.12 ± 0.01 ^b | 2.16 ± 0.01 ^a | 0.0130 ± 0.0001 ^b |
| AHN10 | 279.67 ± 1.36 ^b | 99.22 ± 0.04 ^b | 2.15 ± 0.01 ^a | 0.0100 ± 0.0006 ^c |
| AHN20 | 268.50 ± 0.45 ^c | 99.55 ± 0.08 ^a | 2.14 ± 0.01 ^a | 0.0070 ± 0.0003 ^d |

Average with their respective standard deviation values, followed by equal letters, do not differ statistically from each other following the Tukey test with a 95% confidence level.

Yan et al. [60] justify this decrease in free water in the cement matrix, caused by hydrogels as a common phenomenon of “competitive absorption” between SAP and cement-based materials during mixing, which notably influences the workability and rheology of these mixtures.

These behaviors are related to factors previously discussed, mainly the free water decreases in the mixture because part of the kneading water is found inside the polymer [3], and the nanoclay concentration directly influences the kinetics of release of this. Sarbapalli et al. [1] concluded that the SAP add provides a specific improvement in the water retention property of the studied mortars. They found that an increased dosage of SAP (based on acrylamide/acrylate) causes a more significant reduction in the rate of water loss due to the water retention capacity by the polymer.

Therefore, using hydrogels in the mortar as a moisturizing agent, avoiding excessive exudation rates, can contribute to preventing problems such as weakening of paste-aggregate adhesion, reducing permeability, and preventing the formation of a porous surface layer, weak and with little durability [57].

4.4 CONCLUSIONS

This study investigated the effect of hydrogels as water retains agents on the fresh properties of mortars. The findings from this study are listed as follows:

- The average density value in the fresh state of all hydrogel-mortars presents significative statistical variation compared with the control mortar, whose average value was 2.16±0.01 g.cm⁻³.
- The increased air content property is more pronounced for AHN10 and AHN20 mortars, increasing 8.2% and 15.8%, respectively. This behavior can be related to the

nanoclay concentration increases in the polymer matrix because the cloisite- Na^+ nanoclay can act as a reinforcement agent, resulting in a more stable hydrogel during the mechanical stirring, preventing it from being reduced to small particles and consequently disintegrates in the mixtures.

- In general, the results presented a slight variation among them, with a general average value of 99% in water retention to all mortars. This behavior can be related to the water parcel of dosage of hydrogel-mortars presoaked to reduce the availability of free water in the mix because this amount of water is stored, a priori, within the polymer particles.
- The decreases in the slump flow were 0.9%, 1.1%, and 4.9% for AHN0, AHN10, and AHN20 mortars, respectively, compared with the ACTR mortar. The reduction in free water of the fresh mixture will inevitably affect the workability of material cementitious. In addition, the effective w/c ratio is lower than that proposed by the initial dosage because part of free water is stored in the absorbent polymer matrix.

Remarkably, hybrid nanocomposites based in Cloisite Na^+ nanoclay and hydrogel directly influence cement materials' fresh properties. The results permitted us to conclude that the presence of this polymer in the cementitious matrix provoked an increase in water retention and a decrease in the exudation index, acting as an internal curing agent. Despite consistency index reduction and becoming more difficult the mortar application, this behavior can improve mechanical strength.

However, hybrid hydrogel application is a potential material to the construction field because it can bring innovation more biodegradable. That control better an important factor to cement-materials that is the water.

4.5 REFERENCES

- [1] D. Sarbapalli, Y. Dhabalia, K. Sarkar, B. Bhattacharjee Application of SAP and PEG as curing agents for ordinary cement-based systems: impact on the early age properties of paste and mortar with water-to-cement ratio of 0.4 and above, *Eur. J. Environ. Civ. Eng.* 21, 10 (2017), 1237-1252.
- [2] F. Sanchez, K. Sobolev, Nanotechnology in concrete—a review. *Constr. Build. Mater.*, 24, 11 (2010), 2060-2071.
- [3] A. Mignon, D. Snoeck, P. Dubruel, S. Van Vlierberghe, N. De Belie, Crack mitigation in concrete: superabsorbent polymers as key to success? *Mater.* 10, 3 (2017), 237-262.

- [4] A. Pourjavadi, S. M. Fakoorpoor, A. Khaloo, P. Hosseini, Improving the performance of cement-based composites containing superabsorbent polymers by utilization of nano-SiO₂ particles. *Mater. Des.* 42 (2012), 94-101.
- [5] L. De Meyst, E. Mannekens, M. Araújo, D. Snoeck, K. Van Tittelboom, S. Van Vlierberghe, N. De Belie, Parameter Study of Superabsorbent Polymers (SAPs) for Use in Durable Concrete Structures. *Mater.* 12, 9 (2019), 1-15.
- [6] K. Van Tittelboom, N. De Belie, Self-Healing in Cementitious Materials—A Review. *Mater.* 6, 6 (2013), 2182–2217.
- [7] V. G. Haach, G. Vasconcelos, P. B. Lourenço, Influence of aggregates grading and water/cement ratio in workability and hardened properties of mortars. *Constr. Build. Mater.* 25, 6 (2011), 2980–2987.
- [8] J. M. Casali, F. D. Melo, V. C. Serpa, A. L. Oliveira, A. M. Betioli, L. M. L. Calçada, Influence of cement type and water content on the fresh state properties of ready mix mortar. *Ambient. Constr.* 18, 2 (2018), 33–52.
- [9] A. K. H. Kwan, W. W. S. Fung, Roles of water film thickness and SP dosage in rheology and cohesiveness of mortar. *Cem. Concr. Comp.* 34, 2 (2012), 121–130.
- [10] G. Espinoza-Hijazin, Á. Paul, M. Lopez, Concrete Containing Natural Pozzolans: New Challenges for Internal Curing. *J. Mater. Civil Eng.* 24, 8 (2012), 981–988.
- [11] V. Mechtcherine, Use of superabsorbent polymers (SAP) as concrete additive, *RILEM Technical Letters*, 10 (2016), 81-87.
- [12] L. G. Li, A. K. H. Kwan, Effects of superplasticizer type on packing density, water film thickness, and flowability of cementitious paste. *Constr. Build. Mater.* 86 (2015), 113–119.
- [13] R. R. Al-Omari, M. Y. Fattah, A. M. Kallawi, Stress transfer from pile group in saturated and unsaturated soil using theoretical and experimental approaches. In: *MATEC Web Conf.*, 120 (2017), 1-12.
- [14] K. Venkateswarlu, S. V. Deo, M. Murmu, M. Overview of effects of internal curing agents on low water to binder concretes. *Mater. Today-Proc.* (2020).
- [15] A. S. El-Dieb, Self-curing concrete: Water retention, hydration, and moisture transport. *Constr. Build. Mater.* 21, 6 (2007), 1282-1287.
- [16] C. Schroefl, V. Mechtcherine, P. Vontobel, J. Hovind, E. Lehmann, Sorption kinetics of superabsorbent polymers (SAPs) in fresh Portland cement-based pastes visualized and quantified by neutron radiography and correlated to the progress of cement hydration. *Cem. Concr. Res.* 75, 8 (2015), 1-13.
- [17] L. Senff, R. C. E. Modolo, G. Ascensão, D. Hotza, V. M. Ferreira, J. A. Labrincha, Development of mortars containing superabsorbent polymer. *Constr. Build. Mater.* 95, 21 (2015), 575-584.
- [18] F. A. Aouada, M. R. D. Moura, P. R. Fernandes, A. F. Rubira, E. C. Muniz, Caracterização mecânica e estrutural de um dispositivo PDLC baseado em hidrogéis de PAAm e cristal líquido liotrópico LP/DeOH/H₂O. *Quím. Nova*, 37, 8 (2014), 1302-1307.

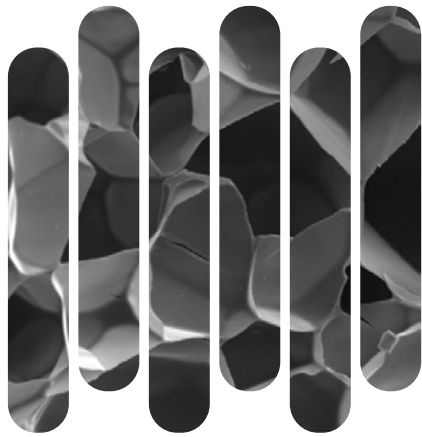
- [19] R. da Silva Fernandes, M. R. de Moura, G. M. Glenn, F. A. Aouada, Thermal, microstructural, and spectroscopic analysis of Ca²⁺ alginate/clay nanocomposite hydrogel beads. *J. Mol. Liq.* 265, 16 (2018), 327-336.
- [20] K. Varaprasad, G. M. Raghavendra, T. Jayaramudu, M. M. Yallapu, R. Sadiku, A mini review on hydrogels classification and recent developments in miscellaneous applications. *Mater. Sci. Eng. C.* 79, 11 (2017), 958-971.
- [21] D. Pasqui, M. de Cagna, R. Barbucci, Polysaccharide-based hydrogels: the key role of water in affecting mechanical properties. *Polymers*, 4, 3 (2012), 1517-1534.
- [22] H. X. D. Lee, H. S. Wong, N. R. Buenfeld, Potential of superabsorbent polymer for self-sealing cracks in concrete. *Adv. Appl. Ceram.* 109, 5 (2010), 296-302.
- [23] C. Schröfl, D. Snoeck, V. Mechtcherine, A review of characterization methods for superabsorbent polymer (SAP) samples to be used in cement-based construction materials: Report of the RILEM TC 260-RSC. *Mater. Struct.* 50, 4 (2017), 197-216.
- [24] M. Hu, J. Guo, J. Du, Z. Liu, P. Li, X. Ren, Y. Feng, Development of Ca²⁺-based, ion-responsive superabsorbent hydrogel for cement applications: Self-healing and compressive strength. *J. Colloid Interface Sci.* 538, 6 (2019). 397-403.
- [25] P. F. Reis, F. Evangelista Jr, E. F. Silva, Profile of internal relative humidity and depth of drying in cementitious materials containing superabsorbent polymer and nano-silica particles. *Constr. Build. Mater.* 237, 9 (2020), 1-9.
- [26] G. M. Raghavendra, T. Jayaramudu, K. Varaprasad, G. S. M. Reddy, K. M. Raju, Antibacterial nanocomposite hydrogels for superior biomedical applications: a facile eco-friendly approach. *RSC Adv.* 5, 19 (2015), 14351-14358.
- [27] I. M. Garnica-Palafox, F. M. Sánchez-Arévalo, Influence of natural and synthetic crosslinking reagents on the structural and mechanical properties of chitosan-based hybrid hydrogels. *Carbohydr. Polym.* 151, 17 (2016), 1073-1081.
- [28] W. Wang, J. Wang, Y. Zhao, H. Bai, M. Huang, T. Zhang, S. Song, S. High-performance two-dimensional montmorillonite supported-poly (acrylamide-co-acrylic acid) hydrogel for dye removal. *Environ. Pollut.* 257, 2 (2020), 1-12.
- [29] S. Liang, L. Liu, Q. Huang, K. L. Yam, Unique rheological behavior of chitosan-modified nanoclay at highly hydrated state. *J. Phys. Chem. B*, 113, 17 (2009), 5823-5828.
- [30] S. S. Ray, M. Bousmina, A. Maazouz, Morphology, and properties of organoclay modified polycarbonate/poly (methyl methacrylate) blend. *Polym. Eng. Sci.*, 46, 8 (2006), 1121-1129.
- [31] C. N. Cheaburu-Yilmaz, R. P. Dumitriu, M. T. Nistor, C. Lupusoru, M. I. Popa, L. Profire, C. Silvestre, C. Vasile, Biocompatible and biodegradable chitosan/clay nanocomposites as new carriers for theophylline-controlled release. *J. Pharm. Res. Int.* 6, 4 (2015), 228-254.
- [32] V. Mechtcherine, M. Gorges, C. Schroefl, A. Assmann, W. Brameshuber, A. B. Ribeiro... S. I. Igarashi, Effect of internal curing by using superabsorbent polymers (SAP) on autogenous shrinkage and other properties of a high-performance fine-grained concrete: results of a RILEM round-robin test. *Mater. Struct.* 47, 3 (2014), 541-562.

- [33] V. Mechtcherine, C. Schroefl, M. Wyrzykowski, M. Gorges, P. Lura, D. Cusson, ... S. I. Igarashi, Effect of superabsorbent polymers (SAP) on the freeze-thaw resistance of concrete: results of a RILEM interlaboratory study. *Mater. Struct.* 50, 14 (2017), 1-19.
- [34] S. Mönnig, P. Lura, Superabsorbent polymers—an additive to increase freeze-thaw resistance of high strength concrete. In: Grosse CU (ed) *Advances in construction materials in 2007*. Springer, Heidelberg, 351–358, 2007.
- [35] D. Snoeck, N. de Belie, Autogenous healing in strain-hardening cementitious materials with and without superabsorbent polymers: an 8-year study. *Front. Mater.* 6, 48 (2019), 1-12.
- [36] O. M. Jensen, P. F. Hansen, Water-entrained cement-based materials: II. Experimental observations. *Cem. Concr. Res.* 32, 6 (2002), 973-978.
- [37] V. Mechtcherine, E. Secrieru, C. Schröfl, Effect of superabsorbent polymers (SAPs) on rheological properties of fresh cement-based mortars—Development of yield stress and plastic viscosity over time. *Cem. Concr. Res.* 67, 1 (2015), 52-65.
- [38] H. Paiva, L. P. Esteves, P. B. Cachim, V. M. Ferreira, Rheology, and hardened properties of single-coat render mortars with different types of water retaining agents. *Constr. Build. Mater.* 23, 2 (2009), 1141-1146.
- [39] J. Liu, K. H. Khayat, C. Shi, Effect of superabsorbent polymer characteristics on rheology of ultra-high performance concrete. *Cem. Concr. Compos.* 112, 8 (2020), 1-11.
- [40] E. Gruyaert, B. Debbaut, D. Snoeck, P. Díaz, A. Arizo, E. Tziviloglou... N. de Belie, Self-healing mortar with pH-sensitive superabsorbent polymers: testing of the sealing efficiency by water flow tests. *Smart Mater. Struct.* 25, 8 (2016), 084007.
- [41] P. Zhong, M. Wyrzykowski, N. Toropovs, L. Li, J. Liu, P. Lura, Internal curing with superabsorbent polymers of different chemical structures. *Cem. Concr. Res.* 123, 9 (2019), 1-11.
- [42] J. Dang, J. Zhao, Z. Du, Effect of superabsorbent polymer on the properties of concrete. *Polymers*, 9, 12 (2017), 1-17.
- [43] H. AzariJafari, A. Kazemian, M. Rahimi, A. Yahia, Effects of presoaked super absorbent polymers on fresh and hardened properties of self-consolidating lightweight concrete. *Constr. Build. Mater.* 113, 13 (2016), 215-220.
- [44] S. Gupta, Effect of presoaked superabsorbent polymer on strength and permeability of cement mortar. *Mag. Concr. Res.* 70, 9 (2018), 473-486.
- [45] O. M. Jensen, Use of superabsorbent polymers in concrete. In: *Concrete international*, 35, 1, 48-52, 2013.
- [46] Associação Brasileira de Normas Técnicas (ABNT), *Argamassa para assentamento e revestimento de paredes e tetos: determinação da densidade de massa e do teor de ar incorporado*. NBR 13278, Rio de Janeiro, RJ, 2005.
- [47] European Committee for Standardization, EN 1015-8. *Methods of test for mortar for masonry - Part 8: Determination of water retentivity of fresh mortar*. European Committee for Standardization (CEN), 1999.
- [48] American Society for Testing and Materials (ASTM), C1437-15, *Standard test method for flow of hydraulic cement mortar*. West Conshohocken: PA, (2013).

- [49] RILEM – International Union of Testing and Research Laboratories for Materials and Structures. MR-6. Tendency of water to separate from mortars (bleeding). France, 1982.
- [50] H. Carasek, Argamassas. In: *Materiais de Construção Civil e princípios de ciência e engenharia de materiais*. Ed. G. C. Isaia, 2.ed. Ibracon, São Paulo, 893-944, 2010.
- [51] Associação Brasileira de Normas Técnicas (ABNT), , Argamassa industrializada para assentamento de paredes e revestimentos de paredes e tetos-Especificação e métodos de ensaios. NBR 13281, Rio de Janeiro, RJ, 2005.
- [52] S. H. Kang, S. G. Hong, J. Moon, Absorption kinetics of superabsorbent polymers (SAP) in various cement-based solutions. *Cem. Concr. Res.* 97, 7 (2017), 73-83.
- [53] R. D. Toledo Filho, E. F. Silva, A. N. Lopes, V. Mechtcherine, L. Dudziak, L. Effect of superabsorbent polymers on the workability of concrete and mortar. In *Application of Super Absorbent Polymers (SAP)*. IN: *Concrete Construction*, Springer, Dordrecht, 39-50, 2012.
- [54] H. S. WONG, Concrete with superabsorbent polymer. In: *Eco-Efficient Repair and Rehabilitation of Concrete Infrastructures*. Woodhead Publishing, 467-499, 2018.
- [55] T. A. Cunha, P. Francinete, M. A. Manzano, L. A. Aidar, J. G. Borges, E. F. Silva, Determination of time zero in high strength concrete containing superabsorbent polymer and nano-silica. *J. Build. Path. Rehab.* 1, 1 (2016), 1-18.
- [56] L. P. Esteves, H. Paiva, V. M. Ferreira, P. Cachim, Effect of curing conditions on the mechanical properties of mortars with superabsorbent polymers. *Materiales de Construcción*, 60, 298 (2010), 61-72.
- [57] L. A. F. Bauer, *Materiais de construção 1: Novos materiais para construção civil*. LTC, Rio de Janeiro, RJ, Brazil, 2000.
- [58] American Society for Testing and Materials (ASTM), C270-19a. Standard specification for mortar for unit masonry. West Conshohocken: PA, 2013.
- [59] H. W. Reinhardt, A. Assmann, Enhanced durability of concrete by superabsorbent polymers. In: *International symposium brittle matrix composites*. Woodhead Publishing Warsaw, 2009, 291-300.
- [60] Y. Tan, H. Chen, Z. Wang, C. Xue, R. He, Performances of Cement Mortar Incorporating Superabsorbent Polymer (SAP) Using Different Dosing Methods. *Materials*, 12, 10 (2019), 1-13.
- [61] D.W. Nascimento, M. R. de Moura, L. H. Mattoso, F. A. Aouada, Hybrid biodegradable hydrogels obtained from nanoclay and carboxymethylcellulose polysaccharide: hydrophilic, kinetic, spectroscopic and morphological properties. *J. Nanosci. Nanotechnol.* 17, 1 (2017), 821-827.
- [62] M. Irani, H. Ismail, Z. Ahmad, Preparation and properties of linear low-density polyethylene-g-poly (acrylic acid)/organo-montmorillonite superabsorbent hydrogel composites. *Polym. Test.* 32, 3 (2013), 502-512.
- [63] S. Laustsen, M. T. Hasholt, O. M. Jensen, Void structure of concrete with superabsorbent polymers and its relation to frost resistance of concrete. *Materials and Structures*, 48, 1-2 (2015), 357-368.

- [64] L. Dudziak, V. Mechtcherine, V. Enhancing early-age resistance to cracking in high-strength cement based materials by means of internal curing using super absorbent polymers. In: RILEM Proc. PRO. 2010. p. 129-139.
- [65] M. L. G. SUAREZ, Polímeros superabsorventes (PSA) como agente de cura interna para prevenir fissuração em concreto de alta resistência. Dissertation Master degree, Universidade de Brasília, Brasília, 2015.
- [66] C. R. F. Junior, M. R. de Moura, F. A. Aouada, Synthesis and Characterization of Intercalated Nanocomposites Based on Poly (methacrylic acid) Hydrogel and Nanoclay Cloisite-Na⁺ for Possible Application in Agriculture. *J. Nanosci. Nanotechnol.* 17, 8 (2017), 5878–5883.
- [67] R. Ianchis, C. Ninciuleanu, I. Gifu, E. Alexandrescu, R. Somoghi, A. Gabor, ... A. Roseanu, Novel Hydrogel-Advanced Modified Clay Nanocomposites as Possible Vehicles for Drug Delivery and Controlled Release. *Nanomaterials*, 7, 12 (2017), 443.
- [68] D. Shen, X. Wang, D. Cheng, J. Zhang, G. Jiang, G. Effect of internal curing with super absorbent polymers on autogenous shrinkage of concrete at early age. *Constr. Build. Mater.* 106, 6 (2016), 512-522.
- [69] J. R. Tenório Filho, E. Mannekens, K. Van Tittelboom, D. Snoeck, N. de Belie, Assessment of the potential of superabsorbent polymers as internal curing agents in concrete by means of optical fiber sensors. *Constr. Build. Mater.* 238, 9 (2020) 1-8.
- [70] O. M. Jensen, P. F. Hansen, P. F. Water-entrained cement-based materials. *Cem. Concr. Res.* 32, 6 (2002), 973–978.
- [71] X. Kong, Z. Zhang, Z. Lu, Effect of presoaked superabsorbent polymer on shrinkage of high-strength concrete. *Mater. Struct.* 48, 9 (2014), 2741–2758.
- [72] D. Snoeck, D. Schaubroeck, P. Dubruel, N. de Belie, Effect of high amounts of superabsorbent polymers and additional water on the workability, microstructure and strength of mortars with a water-to-cement ratio of 0.50. *Constr. Build. Mater.* 72, 24 (2014), 148–157.
- [73] I. Justo-Reinoso, A. Caicedo-Ramirez, W. V. Srubar, M. T. Hernandez, Fine aggregate substitution with acidified granular activated carbon influences fresh-state and mechanical properties of ordinary Portland cement mortars. *Constr. Build. Mater.* 207, 14 (2019), 59–69.
- [74] F. A. Neville, J. J. Brooks, *Tecnologia do concreto*. Bookman, Porto Alegre, RS, Brazil, 2013.
- [75] R. Hendrickx, S. Roels, K. Van Balen, Measuring the water capacity and transfer properties of fresh mortar. *Cem. Concr. Res.* 40, 12 (2010), 1650–1655.
- [76] J. C. D. Santos, M. M. Tashima, M. R. de Moura, F. A. Aouada, Obtainment of hybrid composites based on hydrogel and Portland cement. *Química Nova*, 39, 1 (2016), 124-129.
- [77] S. L. Cilli, H. C. Silva, A. Watanuki Filho, M. R. D. M. Aouada, F. A. Aouada, Otimização de metodologia de obtenção de pastas cimentícias contendo hidrogéis. *J. Exp. Tech. Instrum.* 2, 1, (2019), 1-9.
- [78] X. Ma, Q. Yuan, J. Liu, C. Shi, Effect of water absorption of SAP on the rheological properties of cement-based materials with ultra-low w/b ratio. *Constr. Build. Mater.* 195, 2 (2019), 66–74.

- [79] J. Yang, F. Wang, Influence of assumed absorption capacity of superabsorbent polymers on the microstructure and performance of cement mortars. *Constr. Build. Mater.* 204, 11 (2019), 468–478.
- [80] S. S. Ray, M. Bousmina, Poly (butylene succinate-co-adipate)/montmorillonite nanocomposites: effect of organic modifier miscibility on structure, properties, and viscoelasticity. *Polymer*, 46, 26 (2005), 12430-12439.
- [81] A. Cojocariu, L. Profire, M. Aflori, C. Vasile, In vitro drug release from chitosan/Cloisite 15A hydrogels. *Appl. Clay Sci.* 57, (2012), 1–9.
- [82] M. Jawaid, M., A. el K. Qaiss, R. Bouhfid, Nanoclay Reinforced Polymer Composites. *Engineering Materials*. (2016).
- [83] D. Snoeck, L. Pel, N. de Belie, The water kinetics of superabsorbent polymers during cement hydration and internal curing visualized and studied by NMR. *Sci. Rep.* 7, 1 (2017), 1-14.



CHAPTER 5

HARDENED PROPERTIES OF MORTARS - Part 1

“Mechanical properties of cementitious mortars internally cured with hybrid nanocomposites based on hydrogel and nanoclay.”

5.1 OVERVIEW

Water is an important compound to cement-materials production because, from cement particles, hydration is possible to obtain hydration products that are responsible for gain mechanical strength over time [1]. However, the hydration process is responsible for the better performance of hardened state properties of cementitious materials, such as stiffness, densification, and stability of the cementitious matrix [2]. Sometimes, procedures are required to achieve these properties, more effective curing, i.e., to maintain the moisture content in the fresh mix [3].

In this way, recent researches [3,4] have been developed and demonstrated very promising the application of the hydrogels in cement matrices. Understanding the behavior of hydrogels in cementitious materials is necessary for the optimum design of internal curing [5].

Hydrogels as absorbent polymers can assist in the gradual hydration supplying water inside the samples, i.e., maintaining its internal humidity [6]. Moreover, the application of these polymers modifies the porosity of the cementitious microstructure, and consequently, the mechanical properties, like compressive strength and modulus of elasticity of cementitious materials, as reported by several researchers [7-9].

In this study, a hybrid nanocomposite hydrogel based on polyacrylamide, carboxymethylcellulose (CMC), and different Cloisite Na⁺ nanoclay concentrations (%wt/ wt of acrylamide and CMC) as a mortar internal curing agent was prepared. The effects on hardened state properties such as bulk density, flexural strength, tensile, compressive strength, and elastic modulus were determined and discussed, also aiming to understand the interactions between inorganic and organic materials, which may help in the control and adjust of these properties. Thus, it is expected that the addition of the hydrogel nanocomposites will bring advances and improvements in the properties of the mortars. In the future, they can be used as an additive in civil construction.

5.2 EXPERIMENTAL

5.2.1 Hydrogel synthesis and mortar preparation

All materials and details about hybrid nanocomposite hydrogel synthesis and mortar preparation have been presented in sections 2.1-2.3, Chapter 2.

For the mechanical properties characterization, the samples were demolded after 24 hours of preparation. Then, the samples were conditioned, according to the NBR 9479

standard [10], in a humid chamber (relative humidity > 98% and temperature of $35 \pm 2^\circ\text{C}$) until the respective age. The final average value was obtained by the arithmetic mean of the results obtained for each type of mortar tested.

5.2.2 Bulk density

The determination of the bulk density was performed according to ASTM C642 [11] and NBR 13280 [12], obtaining 12 cylindrical (50 x 100 mm) samples of each mortar produced.

The values were determined before each compressive strength test at 7, 14, 28, 56, and 91 days. Note, all samples remained in a humid chamber, where they were completely saturated at the test time. For each age, the mass (m in g) of the samples was recorded on a semi-analytical balance (Shimadzu BL-3200H), and the volume (v in cm^3) was calculated according to their dimensions (diameter x height) and measured with the aid of a pachymeter (Mitutoyo 150mm) at three different points on the specimen. Thus, the bulk density (D in $\text{g}\cdot\text{cm}^{-3}$) was calculated by using Equation 5.1.

$$D = m/v \quad \text{Equation 5.1}$$

5.2.3 Flexural strength

The flexural strength tests were realized at 7, 14, and 28 days age following recommendations of ASTM C348-19 [13]. The prismatic specimens (40 x 40 x 160 mm) were molded by tamping in two layers and demolded after 24 hours. For each age, twelve samples were maintained in curing conditions (climate room with relative humidity > 95% and temperature of $35 \pm 2^\circ\text{C}$) until reaching the test age and performed in an EMIC Universal machine with a 200-ton load limit operating with a loading rate of 0.25 ± 0.05 MPa/s.

5.2.4 Tensile strength

For the determination of tensile strength, a diametral compressive force along the length of a cylindrical mortar specimen was applied within a prescribed range until failure occurs. All procedures were based on ASTM C496/C496M-17 [14], and samples were tested at ages 7, 14, and 28d.

The samples were then performed in an EMIC Universal machine with a 200-ton load limit. Six cylindrical ($\varnothing = 5$ cm and height = 10 cm) samples were tested for each age, and the tensile strength was calculated using Equation 5.2.

$$T = 2P / \pi ld \quad \text{Equation 5.2}$$

where T is the splitting tensile strength (MPa), P is the maximum applied load indicated by the testing machine (N), l and d are the length (m) and diameter of the specimens (m), respectively.

5.2.5 Compressive strength

The effectiveness of hydrogels as a reinforcing agent in cementitious composites was also analyzed from compressive strength measurements. For each mixture, twelve samples for each mortar were cast in cylindrical molds (50 x 100 mm), demolded after 24 hours, and maintained in the curing conditions until the compressive strength age (7, 14, 28, 56, and 91 days).

Compressive strength of control and polymeric mortars was performed in an EMIC Universal machine with a 200-ton load limit, maintaining the loading rate equal to 0.25 ± 0.05 MPa/s, following ASTM standard C-109/C109M-16 [15].

5.2.6 Dynamic elastic modulus

Dynamic elastic modulus was found by using prismatic molds (40 x 100 x 10 mm). The samples were removed from the mold after 24 hours. Six samples of each characteristic age were cast and stored under the same curing conditions, as described in the previous procedure, until 48 hours before the test. Immediately before the measures, these samples were dried in an oven (Quimis Q317M52, Brazil) at $40 \text{ }^\circ\text{C} \pm 1 \text{ }^\circ\text{C}$ for 48 hours.

Dynamic elastic modulus was obtained using a 100 V pulsator/receiver assembly system, 500 kHz transducer frequency, and digital storage oscilloscope (TDS 2022). Finally, the measures were realized in two different regions of the prismatic sample to obtain the mortar behavior throughout the specimen. All procedure was based on the ASTM C-597 [16], and it was determined at 7, and 28 days ages by applying the Equation 5.3.

$$E_d = v^2 * \rho * ((1 + \mu) * (1 - 2\mu) / (1 - \mu)) \quad \text{Equation 5.3}$$

where E_d is the dynamic elastic modulus (GPa), v is the ultrasonic velocity (m/s), ρ is the bulk density of mortars (kg/m^3) and μ = coefficient of poisson ($\mu = 0.20$).

5.2.7 Elastic modulus

The elastic modulus was determined for cylindrical molds (100 x 200 mm) with 7 and 28 days curing ages. Twelve samples, in each age, were cast and maintained in curing conditions (relative humidity > 95% and 25 °C) until the test age. This destructive test was carried out on an EMIC Universal machine with a 200-ton load limit and loading rate of 0.25 ± 0.05 MPa/s, following the ASTM C469M-14 standard [17]. The strain gauges were used directly on the samples to determine the strain data, and the elastic modulus was obtained by axial compression testing.

5.2.8 Volume of permeable voids spaces

Volumes of permeable voids spaces were tested following ASTM C642 [11] at 28 days of age. A total of six samples ($\emptyset = 3\text{cm}$ and height = 1.5 cm) for each mortar type were prepared, with three samples remaining under wet curing ($35^\circ\text{C} \pm 2^\circ\text{C}$ and 98% Relative Humidity), and other three samples under ambient curing ($35^\circ\text{C} \pm 2^\circ\text{C}$ and 55% Relative Humidity) conditions until 28 days.

At 28 d, the masses of the samples were determined on a semi-analytical balance (Shimadzu BL-3200H) and dried in an oven (Quimis Q317M52, Brazil) at 105 ± 5 °C for 72 hours. During this period, all masses were measured every 24 hours.

After 72 hours, the specimens were immersed in water ($25^\circ\text{C} \pm 2^\circ\text{C}$) for another 72 hours to determine the saturated mass after immersion, being again weighted every 24 hours. Subsequently, the previously immersed specimens were placed in a suitable receptacle, covered with water, and boiled for 5 hours. The samples were cooled by a natural loss of heat for 24 hours, then their saturated masses after boiling were determined (Shimadzu BL-3200H).

Finally, after immersion and boiling processes, all specimens had their apparent masses determined on a hydrostatic balance. Then, an estimate of the volume of permeable voids was determined by Equation 5.4.

$$\%Vol. \text{ permeable pore space (voids)} = [(g_2 - g_1)/g_2] * 100 \quad \text{Equation 5.4}$$

where g_1 = bulk density, dry, Mg/m^3 and g_2 = apparent density, Mg/m^3 . *(1 Mg/m^3 = 1 g/cm^3).

5.2.9 Statistical analysis

The experimental results for each treatment sets were available by analysis of variance (ANOVA) from the Tukey test, with a 5% significance level, using SISVAR[®] software.

5.3 RESULTS AND DISCUSSION

5.3.1 Bulk density

Figure 5.1 shows that the bulk density of the mortars was not influenced by either curing age or the presence of hydrogels or their nanocomposites. Similar results were presented by Esteves et al. [18] regarding a Portuguese Portland cement reinforced with a cross-linked acrylamide/acrylic acid copolymer.

The average bulk densities were $\sim 2.18 \pm 0.02 \text{ g.cm}^{-3}$. Only a discrete and not statistically significant decrease in this property was observed for the polymer-cement mortars compared to the control sample.

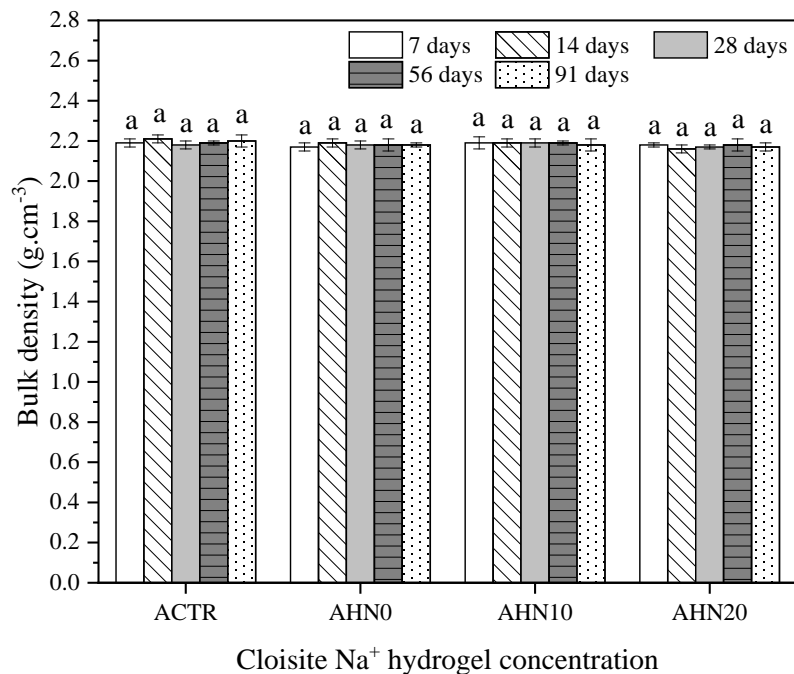


Figure 5.1 – Comparative of the evolution of bulk density over time for mortars control and mortars produced with 0, 10, and 20% Cloisite Na⁺ nanoclay hydrogels. *Average with their respective standard deviation values, followed by equal letters, do not differ statistically from each other following the Tukey test with a 95% confidence level.

This behavior suggested that the curing procedure used directly interfered with the effect of the hydrogels as internal curing agents because all samples were placed in a humid chamber (relative humidity of >95%) until the time of the test, indicating that the samples were fully saturated due to the high humidity rate. Thus, the hydrogels present in the microstructure of the cementitious material were probably fully or partially swollen, and water release did not occur or only occurred slower and partially. Another possible reason this index did not vary is the small amount of hydrogel (0.5% concerning the mass of cement) added to the mortar, which did not significantly interfere with the specific mass of the set.

Ideally, to verify the real effect of the hydrogels in the mortar, the samples would be exposed to low humidity conditions, thereby allowing the hydrogels to release water in a more controlled manner. Therefore, the continuous hydration of cement particles could be an efficient method for reducing shrinkage, as reported previously [19-21].

5.3.2 Flexural strength

The flexural strength of all cementitious mortars at 7, 14, and 28 d of aging can be visualized in Figure 5.2.

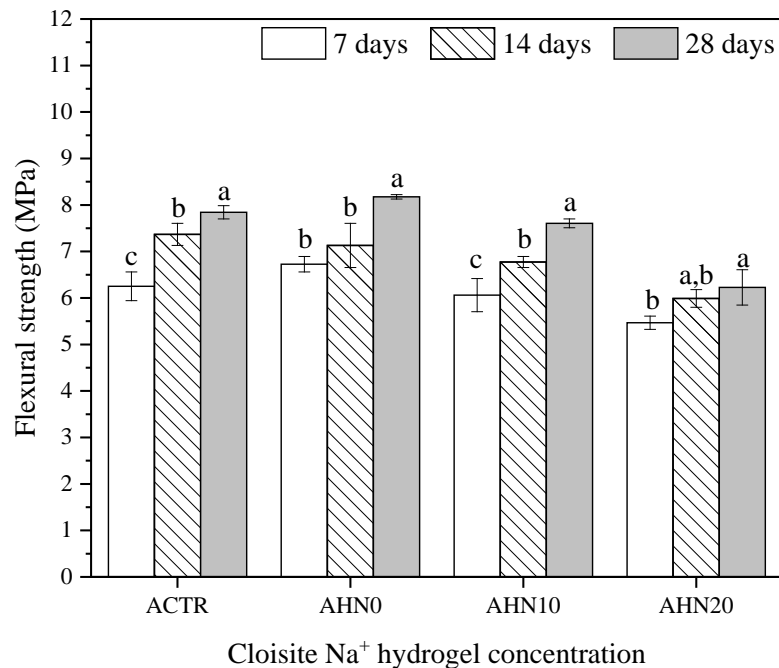


Figure 5.2 – Flexural strength of control and mortars produced with 0, 10, and 20% Cloisite Na⁺ nanoclay hydrogels at various ages. *Average with their respective standard deviation values, followed by equal letters or numbers, do not differ statistically from each other following the Tukey test with a 95% confidence level.

In general, all the mortars demonstrated similar behavior, i.e., their flexural strength increased over time. At 7 d, the flexural strengths of ACTR and AHN0 were statically similar, and their values were slightly superior to the AHN10 and AHN20 mortars, representing reductions of 3.10% and 12.58%, respectively, compared to the control sample. The behavior of the AHN0 mortar is possibly attributed to the faster release of water by the hydrogel, which indicates higher hydration at an early curing age. It also indicates that the Cloisite Na⁺ concentration in the hydrogel matrix modifies the water release [22].

At 14 d, the ACTR, AHN0, and AHN10 mortars presented similar average strength values of 7.36 ± 0.24 , 7.12 ± 0.48 , and 6.77 ± 0.12 MPa, respectively only the AHN20 mortar showed a significant reduction of 18.75% relative to the reference. Similarly, at 28 d, the flexural strengths of ACTR, AHN0, and AHN10 did not vary statistically, and the AHN20 mortar also presented a reduction of 20.54% relative to the reference.

Such reductions can be attributed to the presence of hydrogels acting as low mechanical resistance inclusions inside the mortars due to the previously established curing conditions (moisture curing in the humidity chamber). The high humidity in the curing process implies that the hydrogels remain swollen due to the saturated conditions of the environment.

At 28 d, it was possible to establish a relation between flexural strength and nanoclay concentration. The reductions in mortars produced with high nanoclay content hydrogels are related to longer water retention and release over time by the hydrogels [23]. Under the saturation conditions imposed by the wet curing process, polymers with higher Cloisite Na⁺ contents tend to remain swollen for longer, as small internal water reservoirs of low mechanical strength, in the cement matrix.

Similar results were also found by Farzarian et al. [5], where the addition of superabsorbent polymers decreased the strength of cement pastes. However, the authors applied synthetic hydrogels and attributed these reductions to the formation of macrovoids during water desorption by the hydrogels.

5.3.3 Tensile strength

The mechanical resistance of the mortars concerns the coating having a state of internal consolidation that can support simultaneous mechanical efforts, such as tensile, compression, and shear strain [24, 25].

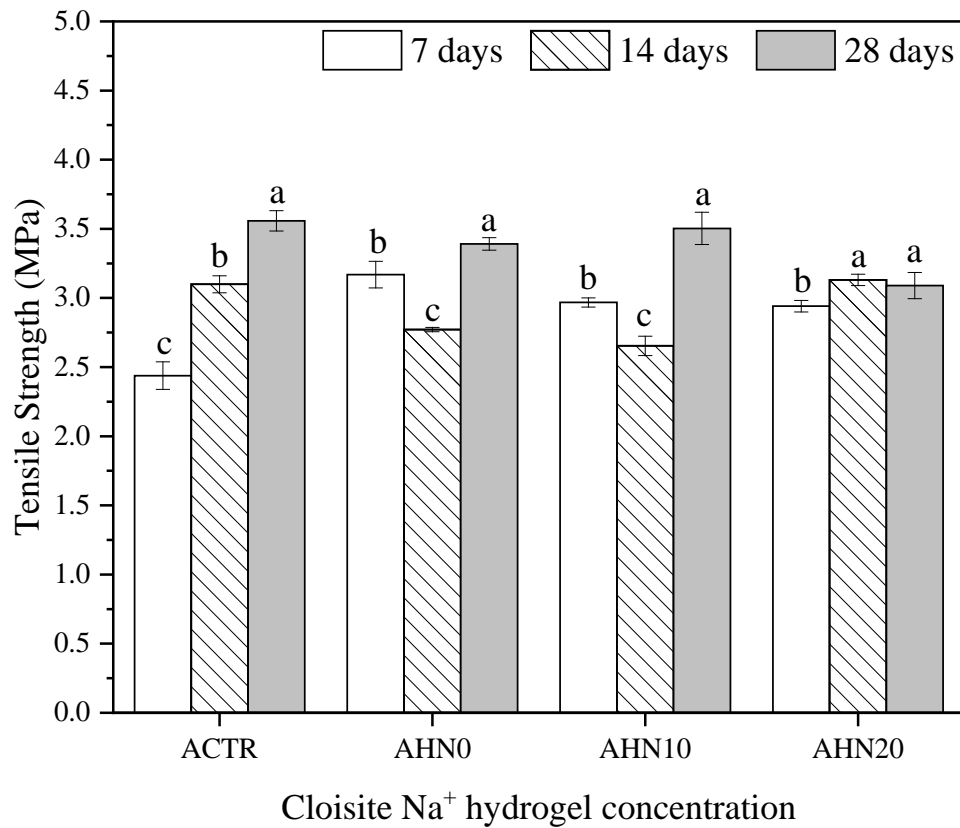


Figure 5.3 – Tensile strength mortars control and mortars produced with 0, 10, and 20% Cloisite Na⁺ nanoclay hydrogels at various ages. *Average with their respective standard deviation values, followed by equal letters or numbers, do not differ statistically from each other following the Tukey test with a 95% confidence level.

Figure 5.3 reveals that all the mortars increased their average values over time. After 7 d of aging, all the mortars with hydrogels had average values higher than the control samples. These increases were 29.9%, 21.7%, and 20.5% for AHN0, AHN10, and AHN20, respectively. However, with longer aging, the mortars with hydrogels showed more pronounced reductions at 28 d, with values of 4.51%, 1.14%, and 13.23% for AHN0, AHN10, and AHN20, respectively.

In agreement with the flexural strength results, the AHN20 mortar showed a more significant reduction over time, with values of ~2.95 MPa, very similar to those reported by Beushausen [26]. Similarly, it is possible that the curing conditions of the samples interfered directly in the behavior of the hydrogels in cementitious matrices. It is also noteworthy that the nanoclay concentration interferes in the behavior of the hydrogels as curing agents, as observed earlier.

The constancy of the average values observed for the AHN20 system over time is due to a slower water release inherent to this specific hydrogel. The hydration provided by this

composition is a guarantee of the availability of water needed to make the hydration reactions of the cement particles over time more effective. Thus, the microstructure of the mortar with hydrogels with high concentrations of nanoclay can become denser and have its tensile strength improved at later ages.

5.3.4 Compressive strength

The results of the compressive strength tests of the mortars are given in Figure 5. This mechanical property was increased for all the mortar systems over time, in agreement with earlier studies [5, 27]. This behavior can be related to the hydrogel contribution in the internal curing process.

At 7 d, the AHN0, AHN10, and AHN20 mortars presented decreases of 10.42%, 11.71%, and 14.69%, respectively, compared with the ACTR. These reductions can be attributed to two important factors: curing conditions and void formation, where the volumes of permeable pores, at 28 d, are higher in mortars with hydrogels.

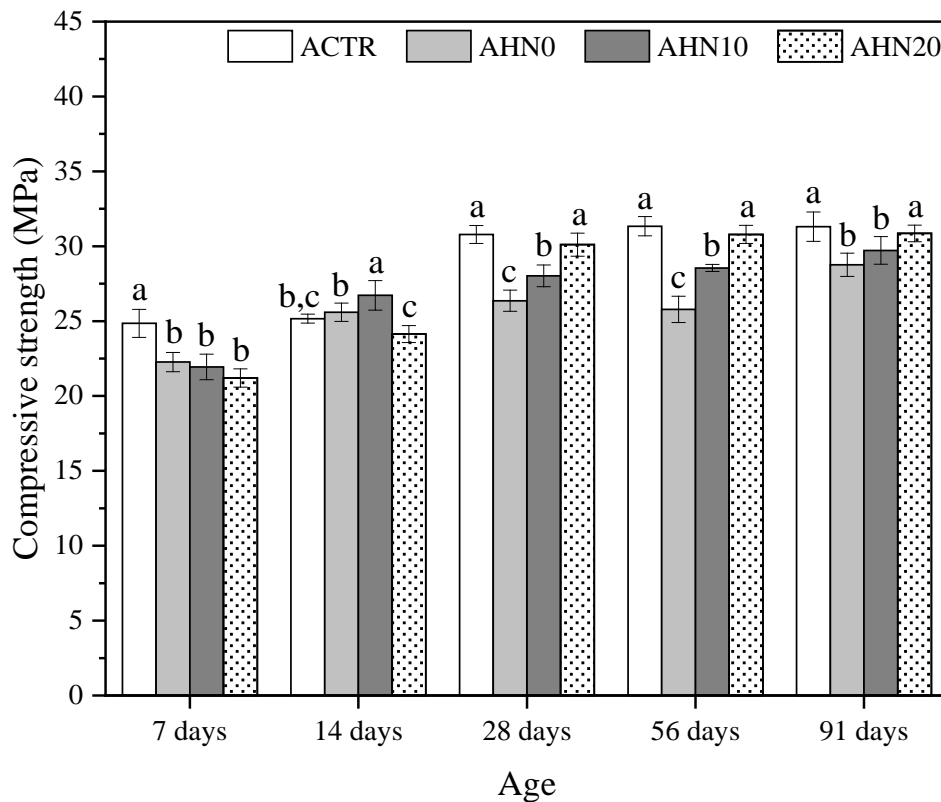


Figure 5.4 – Evolution of compressive strength over time for mortars produced with 0, 10, and 20% Cloisite Na⁺ nanoclay hydrogels. *Average with their respective standard deviation values, followed by equal letters, do not differ statistically from each other following the Tukey test with a 95% confidence level.

As the samples remained in wet curing (35 ± 2 °C and relative humidity of $>98\%$) until 24 h before their rupture, the hydrogels as absorbent polymers were totally or partially swollen with water inside the cement matrix, i.e., they may have released only a small amount of water. Thus, the hydrogels start to act as small water reservoirs [28] of low mechanical strength inside the mortars, causing a force scattering effect [19, 29] and consequently compromising their mechanical properties.

Similar behavior has been reported previously. Sun et al. [27] reported that the insertion of synthetic hydrogels weakened the mechanical properties of the mortars, especially during the early stages. Beushausen et al. [26] concluded that the addition of synthetic hydrogels resulted in a smaller strength mainly during the early ages, while Craeye et al. [30] confirmed that the use of hydrogels as internal curing agents also has some disadvantageous effects on the mechanical properties. However, the loss of strength seems to be partially recovered over time due to the water available for cement hydration given by the internal curing mechanisms [26]. At 28 d, the compressive strength improves as the nanoclay in the hydrogel increases; however, AHN0 and AHN10 show averages of 14.35% and 8.96% lower than the control.

In contrast, the AHN20 mortar presented values statically similar to the ACTR mortar, indicating that hydrogels with high nanoclay concentrations, regardless of the wet curing conditions, contributed to a decrease in the voids in the mortar, in agreement with the results presented in section 5.3.6. This highlights the positive actions of the polymer as a hydration agent in the cementitious matrix [31] and is also attributed to the mechanical reinforcing effect caused by the presence of nanoclay [24] in the polymer matrix.

Our results suggest that the controlled water release from hydrogels can contribute to controlling the chemical reactions initiated by the hydration of the components of Portland cement. Therefore, the main reactions are essentially the formation of calcium silicate hydrate (C-S-H), calcium aluminate hydrate, ettringite, calcium monosulfaluminate hydrate and calcium hydroxide from the hydration of calcium disilicate ($2\text{CaO}\cdot\text{SiO}_2$ or C_2S), calcium trisilicate ($3\text{CaO}\cdot\text{SiO}_2$ or C_3S), tricalcium aluminate ($3\text{CaO}\cdot\text{Al}_2\text{O}_3$ or C_3A) and tetracalcium aluminoferrite ($4\text{CaO}\cdot\text{Al}_2\text{O}_3\cdot\text{Fe}_2\text{O}_3$ or C_4AF) [32], as can be seen from the SEM images (Chapter 6).

Notably, at 91 d, the compressive strength increases continuously, and the differences in the resistance were reduced to 8.16% and 5.04% for the AHN0 and AHN10 mortars,

respectively, compared with the ACTR samples. The ACTR and AHN20 mortars showed the same mechanical behavior, with ~31 MPa.

These results indicated that the strength gain, at later ages, was more accentuated for the mortars with hydrogels with higher nanoclay concentrations because, as previously discussed, the water released by the hydrogel with 20% Cloisite Na⁺ occurs more slowly than the other types. Thus, water availability for a longer period may improve the hydration conditions of cementitious materials and consequently improve the compressive strength [33].

Notably, the results found for all mortars demonstrated that hydrogels directly influence the mechanical properties of the mortars tested. The AHN20 mortars, regardless of the type of curing applied, showed compressive strength similar to the ACTR mortars at later ages due to the presence of nanoclay at a concentration that allows a slow release of water over time its reinforcing effect on the polymer matrix.

5.3.5 Dynamic elastic modulus

The mechanical behavior of the cement mortars was also investigated using ultrasonic non-destructive testing [34]. The dynamic elastic modulus results presented in Figure 5.5 indicate that all the mortars prepared with hydrogels have a lower average value at 7 d than the ACTR mortar.

At 7 d, the reductions were 11.69%, 14.41%, and 20.83% for AHN0, AHN10, and AHN20, respectively. Despite presenting a reducing trend for the dynamic elastic modulus, with the increase of nanoclay in the hydrogels, the mortars with hydrogels did not present statistically significant differences between them. The pre-soaked hydrogels provide a reduction in ultrasonic velocity, which may also be related to the observed reduction in the compressive strength values for this age [34]. The dynamic modulus results agree with the compressive strength results since as the mechanical strengths reduced, this property also showed similar behavior.

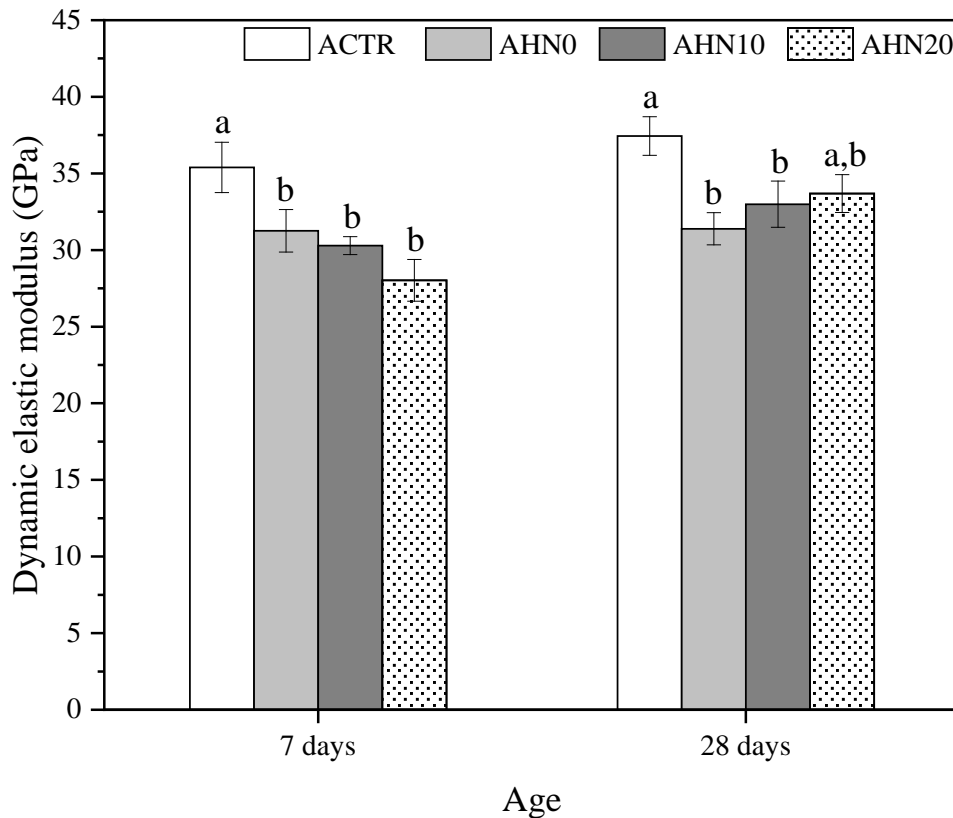


Figure 5.5 – Dynamic elastic modulus at 7 and 28 d obtained by ultrasonic velocity for mortars produced with 0, 10, and 20% Cloisite Na⁺ nanoclay hydrogels. *Average with their respective standard deviation values, followed by equal letters, do not differ statistically from each other following the Tukey test with a 95% confidence level.

At 28 d, the mortars with hydrogels also showed lower average values compared to the control. The reductions were 16.16% and 11.89% for AHN0 and AHN10, respectively, and they are smaller as the nanoclay concentration of the hydrogel increases. However, the result of the AHN20 mortar is statistically similar to the ACTR mortar. The average values of this matrix were 33.67 ± 1.24 GPa, showing that the presence of the nanocomposite increases its stiffness due to a possible improvement in matrix densification caused by a slower release process. This behavior is linked to the kinetics of water release by the polymer with a high amount of nanoclay, indicating that despite the lower swelling degree, this type of hydrogel [35] can release water for long periods in the internal curing process.

In addition, the Cloisite Na⁺ in the hydrogel may also act as a reinforcing agent for the microstructure of the mortar, mitigating the effects of porosity on the compressive strength and elastic modulus.

The discrete variation of the modulus represents a satisfactory condition because the polymer influences the chemical reactions initiated by the hydration of the Portland cement

components [32]. Thus, these products obtained due to hydration for a longer period can compensate for the porosity formed by the hydrogel after its complete water-release process, thereby making the matrix more compact with less shrinkage and consequently without microcracking seen in the SEM images.

5.3.6 Elastic modulus

A complementary method to analyze the mechanical properties of the mortars is through the elastic modulus (E-mod) determination at 7 and 28 d. Figure 5.6 shows the E-mod results for all mortars at the default ages.

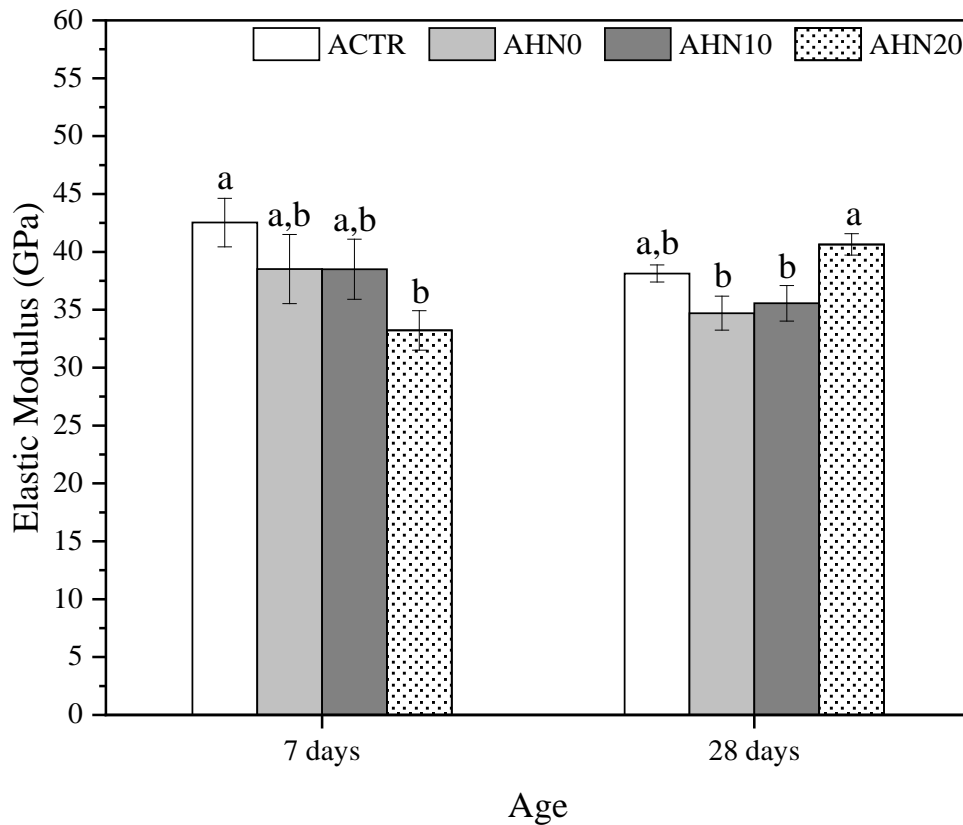


Figure 5.6 – Elastic modulus at 7 and 28 d for mortars produced with 0, 10, and 20% Cloisite Na⁺ nanoclay hydrogels. *Average with their respective standard deviation values, followed by equal letters, do not differ statistically from each other following the Tukey test with a 95% confidence level.

In general, the behavior of all the mortars was similar to the dynamic elastic modulus discussed previously, and they agree with the compression strength results. At 7 d, ACTR presented the highest E-mod, indicating that the hydrogel influences the elastic behavior of these matrices. The reductions observed were 8.81%, 8.85%, and 27.04% for AHN0, AHN10, and AHN20, respectively. However, the statistical analysis indicated that there are no

statistically significant differences between the ACTR, AHN0, and AHN10 mortars, while the values of AHN20 were statistically less than ACTR, in agreement with Beushausen et al. [26], who reported that the use of synthetic hydrogels remarkably reduces the modulus of elasticity of mortars.

This mechanical behavior is similar to the dynamic elastic modulus where the control samples presented higher values than those of AHN20, which had a reduction due to the water presence inside the hydrogel, since the release from the polymer is slower, and it can cause a loss in stiffness [26].

The increase in the rigidity of the mortars with hydrogel, quantified by the E-mod, can be observed at 28 d, where the AHN20 presented an average value of 40.64 ± 0.92 GPa, corresponding to an increase of 16.55% concerning ACTR due to the increase in the stress and the decrease in the strain presented by the mortar. These results also corroborate those for the compressive strength and dynamic elastic modulus. In contrast, the AHN20 was higher than other mortars (ACTR, AHN0, and AHN10) because they improve their densification occasioned by efficient hydration provided by the hydrogels with the highest nanoclay concentrations.

5.3.7 Volume of permeable pore space (voids)

The volumes of permeable pore spaces (voids) at 28 days using the results from this study are presented in Figures 5.7 (a and b), respectively. These results are important and complementary to understanding some of the mechanical behaviors observed previously. The desorption process by the hydrogel, over time, leads to the formation of voids in the microstructure and plays an important role in the mechanical properties [5].

Thus, each plot in Figures 5.7 (a and b) represents the mean result for each mortar at two different curing conditions. The results obtained were similar for the two curing conditions at 28 d, to which the samples were subjected before the test. Both the ACTR and AHN20 mortars presented a smaller pore volume, i.e., they did not present statistical differences between them. However, this behavior is more pronounced for samples placed in dry curing.

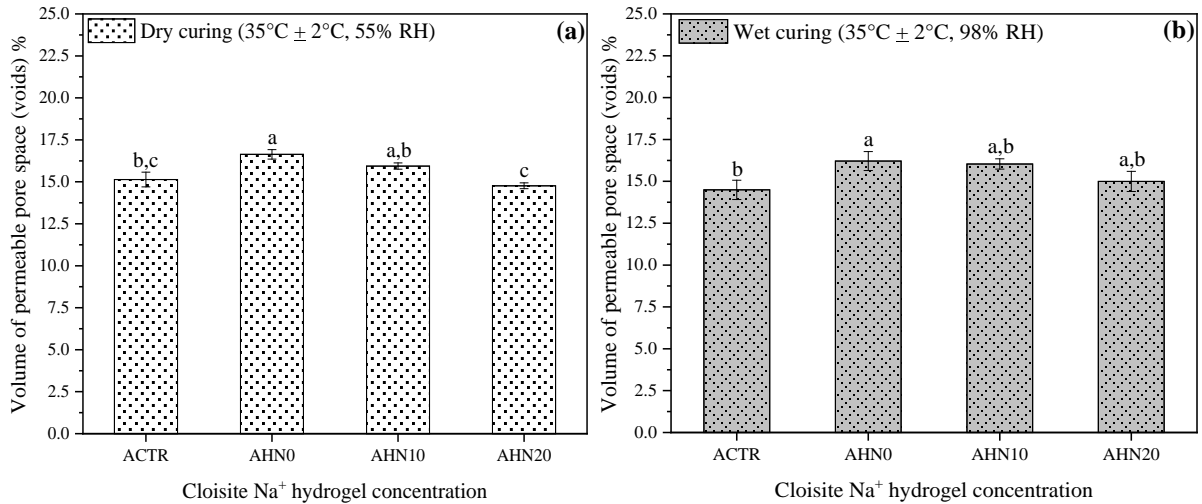


Figure 5.7 – Volume of permeable pore space (voids) at 28 d for mortars produced with 0, 10, and 20% Cloisite Na⁺ nanoclay hydrogels, in two different conditions: (a) dry and (b) wet curing. *Average with their respective standard deviation values, followed by equal letters do not differ statistically from each other following the Tukey test with a 95% confidence level.

For dry curing, AHN0 and AHN10 showed increases of 9.91% and 5.28%, respectively, relative to the control. Under wet curing conditions, for these same mortars, the increases were 11.87% and 10.67%, respectively. This indicates that the release of water is higher for the hydrogels with smaller amounts of nanoclay in their compositions, as reported previously [22, 23, 35].

Thus, AHN20 has slower kinetics of release inside the cementitious matrix, which possibly maintains the internal moisture for a longer period and consequently improves the hydration processes of the cement. Although the hydration products of the cement around the particles of the hydrogels can partially fill the voids occasioned by them, and thus small pores still can exist. The low resistance of the hydrogels introduces weak zones that decrease the mechanical performance of these mortars [27].

Moreover, even though they are still partially loaded with water inside the cement matrix, their high nanoclay concentration (20% wt/AAm + CMC wt) implies a more stable hydrogel structure, acting as a reinforcing agent and reducing the impact of porosity on the mechanical properties of the mortars.

The hydrogel presence impacted all the mechanical properties discussed in this study, and the results for the percentage of voids established this important relation between the mechanical properties and porosity. Nevertheless, this information is useful for designing new mortar composites since voids are sites of weakness that control the mechanical properties of these materials [36].

5.4 CONCLUSIONS

This study investigated the effect of hydrogels on the mechanical properties of mortars in their hardened state. The main findings are listed as follows:

- The bulk densities of the mortars do not change with the presence of hydrogel. The average values of bulk densities were $\sim 2.18 \pm 0.02 \text{ g.cm}^{-3}$. This indicated that the curing procedure used interfered directly with the effect of the hydrogel as an internal curing agent. This is because the hydrogels present in the microstructure of the cementitious material were probably fully swollen, and water release did not occur or occurred slower and partially. Another possible reason this index did not vary is the small amount of hydrogel (0.5% concerning the mass of cement) added to the mortar, which did not significantly interfere with the specific mass of the set.
- The hydrogel influences the mechanical behavior in all mortar systems studied. These reductions observed were attributed to control of the cementitious microstructure, which became more porous with the presence of hydrogels.
- Cloisite Na^+ acts as a reinforcing agent, and modifying its absorption and water release kinetics also contributed to improvements in the compressive strength at older ages. The increase of nanoclay in the hydrogel matrix permits a more controlled water release over time, possibly resulting in better internal hydration. Additionally, the AHN20 system presented improved mechanical behavior with longer aging.
- ACTR and AHN20 presented lower percentages of voids in their structures, and thus their mechanical properties were similar and better than AHN0 and AHN10. This leads to the conclusion that the low resistance of the hydrogels introduces weak zones that decrease the mechanical performance of these mortars.

Therefore, these hybrid nanocomposites are expected to bring new technology and improvements in the properties of cementitious material so that they can be applied in the future as efficient additives in the civil construction industry.

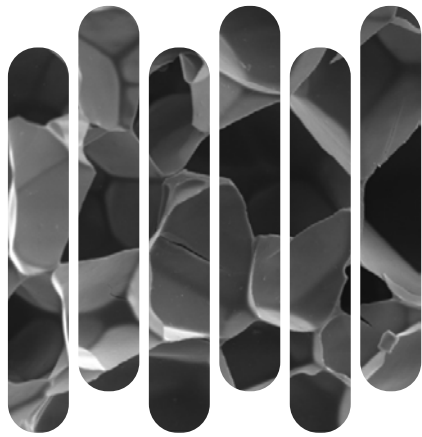
5.5 REFERENCES

- [1] P. K. Mehta; P. J. M. Monteiro, *Concreto: microestrutura, propriedades e materiais*, Sao Paulo: Ibracon, 2014.
- [2] F. C. R. Almeida, A. J. Klemm, Efficiency of internal curing by superabsorbent polymers (SAP) in PC-GGBS mortars, *Cem. Concr. Compos.* 88 (2018) 41–51.

- [3] X. Y. Liu, C. H. Huang, C. H. Zhuang, K. C. Hsu, C. H. Huang, An amphoteric hydrogel: Synthesis and application as an internal curing agent of concrete. *Journal of Applied Polymer Science*, 132 (2015), 1-9.
- [4] H. A. Abd El-Rehim, E. S. A. Hegazy, D. A. Dīaa, Radiation synthesis of eco-friendly water reducing sulfonated starch/acrylic acid hydrogel designed for cement industry. *Radiation Physics and Chemistry*, 85 (2013), 139-146
- [5] K. Farzanian, K. Pimenta Teixeira, I. Perdigão Rocha, L. de Sa Carneiro, A. Ghahremaninezhad, The mechanical strength, degree of hydration, and electrical resistivity of cement pastes modified with superabsorbent polymers, *Constr. Build. Mater.* 109 (2016) 156–165.
- [6] L. Montanari, P. Suraneni, W.J. Weiss, Accounting for Water Stored in Superabsorbent Polymers in Increasing the Degree of Hydration and Reducing the Shrinkage of Internally Cured Cementitious Mixtures, *Adv. Civ. Eng. Mat.*, 6 (2017) 583-599.
- [7] M. T. Hasholt, O.M. Jensen, K. Kovler, S. Zhutovsky, Can superabsorbent polymers mitigate autogenous shrinkage of internally cured concrete without compromising the strength?, *Constr. Build. Mater.* 31 (2012) 226–230.
- [8] X. Chen, S. Wu, J. Zhou. Influence of porosity on compressive and tensile strength of cement mortar. *Constr. Build. Mater.*, 40 (2013) 869-874.
- [9] S. H. Kang, S. G. Hong, J. Moon, J. The effect of superabsorbent polymer on various scale of pore structure in ultra-high performance concrete. *Constr. Build. Mater.*, 172 (2018) 29-40.
- [10] Associação Brasileira de Normas Técnicas (ABNT), Argamassa e concreto – Câmaras úmidas e tanques para cura de corpos de prova, NBR 9479:2006, Rio de Janeiro, RJ, 2016.
- [11] American Society for Testing and Materials (ASTM), C642M-13. Standard test method for density, absorption, and voids in hardened concrete. West Conshohocken: PA, 2013.
- [12] Associação Brasileira de Normas Técnicas (ABNT), Argamassa para assentamento e revestimento de paredes e tetos – Determinação da densidade de massa aparente no estado endurecido, NBR 13280:2005, Rio de Janeiro, RJ, 2016.
- [13] American Society for Testing and Materials (ASTM), C348–19. Standard test method for flexural strength of hydraulic–cement mortars. Annual book of ASTM standards. West Conshohocken: PA, 2017.
- [14] American Society for Testing and Materials (ASTM), C496/C496M-17. Standard Test Method for Splitting Tensile Strength of Cylindrical Concrete Specimens. West Conshohocken: PA, 2017.
- [15] American Society for Testing and Materials (ASTM), C642M-13. Standard test method for density, absorption, and voids in hardened concrete. West Conshohocken: PA, 2013.
- [16] American Society for Testing and Materials (ASTM), C597. Standard test method for pulse velocity through concrete. West Conshohocken: PA, 2016.

- [17] American Society for Testing and Materials (ASTM), C469M-14. Standard test method for static modulus of elasticity and Poisson's ratio of concrete in compression. West Conshohocken: PA, 2014.
- [18] L. P. Esteves, P. Cachim, V. M. Ferreira, Mechanical properties of cement mortars with superabsorbent polymers, *Adv. Constr. Mater.* 2007. (2007) 451–462.
- [19] O. M. Jensen, P. F. Hansen, Water-entrained cement-based materials, Principles and theoretical background. *Cem. Concr. Res.* 31 (2002) 647–654.
- [20] H. S. Sobral, “Propriedades do concreto fresco”, 1.ed., Associação Brasileira de Cimento Portland, São Paulo, Brasil, 2000.
- [21] S. Mönnig, P. Lura, P., In: *Advances in construction materials 2007*. Springer, Berlin, Heidelberg (2007) 351.
- [22] A. Bortolin, F. A. Aouada, L. H. Mattoso, C. Ribeiro, Nanocomposite PAAm/methyl cellulose/montmorillonite hydrogel: evidence of synergistic effects for the slow release of fertilizers, *J. Agric. Food Chem.*, 61, 31 (2013), 7431-7439.
- [23] D. W. S. Nascimento; M. R. de Moura; L. H. C. Mattoso; F. A. Aouada. Hybrid Biodegradable Hydrogels Obtained from Nanoclay and Carboxymethylcellulose Polysaccharide: Hydrophilic, Kinetic, Spectroscopic and Morphological Properties. *J. Nanosci. Nanotechnol.*, 17 (2017) 821–827.
- [24] H. Carasek. Argamassas. In: ISAIA, Geraldo Cechella. *Materiais de Construção Civil e Princípios de Ciência e Engenharia de Materiais*. 2. ed. IBRACON, Sao Paulo (2010) 893-941.
- [25] A. Pcziecsek, C. Effting, I. R. Gomes, A. Schackow, E. Henning. Análise estatística de propriedades mecânicas de argamassas com cinza volante e resíduo de borracha de pneus. *Journal Ibracon de Estruturas e Materiais*, 12 (2019) 790-811.
- [26] H. Beushausen, M. Gillmer, The use of superabsorbent polymers to reduce cracking of bonded mortar overlays, *Cem. Concr. Compos.* 52 (2014) 1–8.
- [27] B. Sun, H. Wu, W. Song, Z. Li, J. Yu, Design methodology and mechanical properties of Superabsorbent Polymer (SAP) cement-based materials, *Constr. Build. Mater.* 204 (2019) 440–449.
- [28] D. Snoeck, L. Pel, N. De Belie, The water kinetics of superabsorbent polymers during cement hydration and internal curing visualized and studied by NMR, *Sci. Rep.* 7 (2017) 1–14.
- [29] G. Lefever, E. Tsangouri, D. Snoeck, D. G. Aggelis, N. De Belie, D. Van Hemelrijck, Combined use of superabsorbent polymers and nanosilica for reduction of restrained shrinkage and strength compensation in cementitious mortars, *Constr. Build. Mater.* 251, 21 (2020), 118966.
- [30] B. Craeye, M. Geirnaert, G. D. Schutter. Super absorbing polymers as an internal curing agent for mitigation of early-age cracking of high-performance concrete bridge decks. *Constr. Build. Mater.*, 25 (2011) 1–13.

- [31] D. M. Nascimento, Y. L. Nunes, M. C. B. Figueirêdo, H. M. C. de Azeredo, F. A. Aouada, J. P. Feitosa, A. Dufresne. Nanocellulose nanocomposite hydrogels: technological and environmental issues. *Green Chem.*, 20 (2018) 2428-2448.
- [32] J. C. dos Santos, M. M. Tashima, M. R. de Moura, F. A. Aouada, Obtainment of Hybrid Composites Based on Hydrogel and Portland Cement, *Quim. Nova.* 39 (2016) 124–129.
- [33] J. Liu, N. Farzadnia, C. Shi, X. Ma, Shrinkage and strength development of UHSC incorporating a hybrid system of SAP and SRA, *Cem. Concr. Compos.* 97 (2019) 175–189.
- [34] V. S. Menezes; D. N. L. Ferronato; E. M. Santos; J. F. S. Feiteira. Estudo do comportamento da porosidade de pasta de cimento por ultrassom. In Congresso Brasileiro de Cerâmica, Volta Redonda, Rio de Janeiro, 60, 2016.
- [35] A. Cojocariu, L. Profire, M. Aflori, C. Vasile, C., In vitro drug release from chitosan/Cloisite 15A hydrogels. *Appl. Clay Sci.*, 57 (2012), 1–9.
- [36] Y. W. Mai, B. Cotterell, Porosity and mechanical properties of cement mortar. *Cem. Concr. Res.*, 15 (1985), 995-1002.



CHAPTER 6

HARDENED PROPERTIES OF MORTARS - Part 2

“Application of hybrid nanocomposites based on hydrogel and nanoclay as a technological potential for drying shrinkage reduction in cementitious mortars.”

6.1 OVERVIEW

Most cement-based materials consist of a binder matrix, with or without aggregates, and are considered as porous composites [1] with good durability and versatility [2], which contribute to their widespread usage and study in the field of construction technology [3,4].

However, because these materials are heterogeneous and multiphase [5], they have properties that are directly affected by the characteristics of each constituent material [2]. Therefore, research on chemical admixtures has been carried out, mainly regarding water control [6], because most of the chemical reactions of cement hardening occur in the presence of this component [7,8].

Water control is a method that ensures the more effective hydration of cement particles, which contributes to the development of a more uniform microstructure and pore structure [9,10], improving the mechanical properties and durability [11] cement-based materials.

This procedure is denominated as an "internal cure," and its function is not only to aid cement hydration but also to maintain high humidity inside the cement matrix [12]. It should also be emphasized that curing is an essential and recommended procedure for cementitious materials because, if correctly performed, it allows for potential gains in resistance and durability [13]. Examples of internal curing agents include materials such as lightweight-saturated aggregates [14] and absorbent polymers [6, 15].

On this basis, several studies on cementitious composites have been developed with the application of synthetic commercial superabsorbent polymers based on acrylamide, acrylic acid, sodium acrylate, and methyl acrylate in cementitious materials as internal curing agents [16-19]. The main characteristics of these polymers are the absorption and release of water over time [20], which effectively contribute to the maintenance of the internal moisture of the cementitious matrix, since traditional curing methods, such as wet and membrane curing, are considered external curing methods [10].

Thus, problems related to drying and shrinkage, such as the cracks [21], in cement materials with a low a/c ratio, can be minimized by applying these polymers to the mixture. Because they prevent the pores of the microstructure from remaining unsaturated, acting as an internal source of water to increase hydration and reduce drying effects [22].

In general, drying shrinkage occurs because the material suffers a decrease in internal relative humidity. Already water evaporation occurs from within the capillary network in the cementitious material exposed to air with lower relative humidity than that found in the

capillary pores [23], causing the appearance of cracks that can compromise the performance of the structure.

Therefore, the purpose is to obtain the hydrogels to neutralize the two mechanisms that cause the development of these volumetric deformations due to self-dissection, being them: i) decrease in the disjoining pressure between C-S-H gel particles; ii) decrease in the menisci radii of the pore water, which bespeaks an increase in tension both within the pore water and at its surface [6].

Thus, the purpose is to verify the effect of the hybrid nanocomposite on the behavior of properties of cementitious mortars, mainly in properties related to water absorption, loss of mass, shrinkage by drying, and microstructure. In short, the study of such composites makes it possible to evaluate the potential of semi-synthetic hydrogels as a technological innovation for the construction industry since the results are favorable to the improvement of the properties analyzed.

6.2 EXPERIMENTAL

6.2.1 Hydrogel synthesis and mortar preparation

All materials and details about hybrid nanocomposite hydrogel synthesis and mortar preparation have been presented in sections 2.1-2.3, Chapter 2.

6.2.2 Water absorption

The presence of nanocomposite hydrogels in the cementitious matrix can increase their porosity. The spaces filled with water are replaced by air at the end of the release water process by these polymers. Therefore, it was necessary to determine the water absorption by immersion, where the water is conducted and tends to occupy the permeable pores of a porous solid specimen. The test was performed following ASTM C1403-15 [24]. Four cylindrical samples ($\emptyset = 5$ cm and height = 10 cm) were produced. After the preparation and demolding of the samples, they remained in a humidity chamber (98% relative humidity and temperature of $35 \pm 2^\circ\text{C}$) until the test was performed.

The study was done at the ages of 7, 14, and 28 d to verify the water absorption over time. At these characteristic ages, the specimens were previously dried in an oven (Quimis Q317M52, Brazil) at $105 \pm 2^\circ\text{C}$ for 72 hours until achieved constant mass, i.e., when the

variation in mass measured is less than 0.5% of its initial mass. Thus, the dry mass (m_{dry}) could be measured on a semi-analytical balance (Shimadzu BL-3200H).

Subsequently, the samples were immersed in water at room temperature ($25 \pm 2^\circ\text{C}$ and relative humidity $\sim 55\%$) and kept for 72 hours in this immersed condition. Posteriorly, the saturated masses of the samples (m_{sat}) were measured (Shimadzu BL-3200H) each 24 hours to check the variation in mass throughout the test. Water absorption index was obtained by the ratio between the difference of the m_{sat} and m_{dry} by m_{dry} .

6.2.3 Capillarity coefficient

The capillarity coefficient of mortars aimed to analyze the effect of nanocomposite hydrogels on the velocity of water absorption and its durability throughout its useful life. The testing was performed according to the specifications of the European standard EN 1015-8 [25] and Brazilian standard NBR 15259:2005 [26]. A total of six prismatic samples (4 x 4 x 8 cm) were molded.

The samples after molding remained in wet curing (98% relative humidity and temperature of $35 \pm 2^\circ\text{C}$) until the age of the test. This was performed at 28 days, with 6 prismatic specimens with 40 x 40 x 80 mm dimensions for each mortar type. Initially, the samples were dried in an oven (Quimis Q317M52, Brazil) for 24 hours at $60 \pm 5^\circ\text{C}$ until a constancy of mass (semi-analytical balance Shimadzu BL-3200H).

After drying, the cross-sections of the samples were determined using a digital pachymeter to proceed with the process of waterproofing the side faces, except the bases, with beeswax. The application of the wax on the sides of the sample had the function of preventing water entrance.

Posteriorly, the samples were weighed (semi-analytical balance Shimadzu BL-3200H) individually and immersed, with the non-waterproofed bases in direct contact with a 10 mm water slide arranged in a container. All mass samples were measured at 10, 30, 60, 90, 180, 300, 480, and 1440 minutes. The determination of the capillary coefficient was calculated by the ratio between the difference between the saturated mass and the dry mass by the cross-section of the test body, and the capillary coefficient (C_i) was calculated by Equation 6.1.

$$C_i = \frac{(M_{90i} - M_{10i})}{A_i * (90^{1/2} - 10^{1/2})} \quad \text{Equation 6.1}$$

where M_{90i} (g) is the sample mass i at 90 minutes; M_{10i} (g) is the sample mass i at 10 minutes, and A_i is the transversal area of sample i in contact with water, expressed in dm^2 . The capillary coefficient of each mortar was calculated as the average of the 6 samples tested.

6.2.4 Weight loss

Weight loss of the samples evaluates the effect of the hydrogels on the velocity of mortar drying. Three prismatic samples (50x100x10 mm) of each type of mortar were used for the test. After 24 hours of mortar preparation, the samples were deformed and stored in a closed recipient to control humidity and temperature over time better. The temperature and relative humidity measurements inside the recipient and the sample masses were checked daily for 28 days (Shimadzu BL-3200H).

For this, a table-top Thermo hygrometer with internal and external sensor model TH-02 (Impac Ltda, Brazil) was used. These measurements were performed positioning the apparatus together with the samples, inside the closed recipient, for 5 min until complete stabilization. Thus, the weight loss of the samples was calculated by the difference in mass at time t and the initial mass.

6.2.5 Drying shrinkage

The determination of drying shrinkage followed NBR 15261 [27] and ASTM C596-18 [28] standards. For each type of mortar, 9 samples with 25 x 25 x 280 mm sizes were used and prepared following ASTM C490/C490M-17 [29].

For comparison, the analyses were performed under three different curing conditions, i.e., wet curing, controlled environment curing, and external curing. For each condition, 3 mortar samples were stored, remaining until the date of the measurements.

Wet curing was performed in a humidity chamber with a relative humidity of 98% and a temperature of $35 \pm 2^\circ\text{C}$. For controlled environment curing conditions, the samples remained in an oven (Quimis Q317M52, Brazil) with a relative humidity of ~55% and temperature of $35 \pm 2^\circ\text{C}$. Finally, external curing was performed in a room with a relative humidity of 46% and temperature of $30 \pm 2^\circ\text{C}$. For this condition, the samples were stored together with the weight loss test samples described in Section 6.2.4.

All samples' dimensional and mass variation measurements were performed at 1, 3, 5, 7, 10, 14, 21, and 28 days. For length variation measurement, an expandability/shrinkage

comparator with a digital clock (SOLOTEST[®], Brazil) with an accuracy of 0.001 mm was used, and the masses were measured using a semi-analytical balance (Shimadzu BL-3200H). The drying shrinkage ($D_{shrinkage}$ – mm/m) was obtained by the ratio between the difference between the initial measurement and the length measurement at the age i by the effective length of the samples, according to Equation 6.2.

$$D_{shrinkage} = (L_0 - L_i)/0.25 \quad \text{Equation 6.2}$$

where $D_{shrinkage}$ is the drying shrinkage (mm/m), L_0 (mm) is the measure of the initial sample length (mm), and L_i (mm) is the measure of the sample length at the age i .

The variation in mass was obtained by the difference in initial mass and mass at reading age by initial mass, according to Equation 6.3.

$$\text{Mass Variation (\%)} = [(m_0 - m_t)/m_0] * 100 \quad \text{Equation 6.3}$$

where m_0 (g) is the mass of the initial sample, and m_i (g) is the mass of the sample at the age i .

The drying shrinkage and mass variation values at the corresponding ages refer to the average value calculated by the three samples of each set.

6.2.6 Scanning electron microscopy (SEM) and Energy-Dispersive X-Ray (EDX) Spectroscopy

The microscopic analysis was conducted using the ACTR, AHN0, AHN10, and AHN20 mortars at 7 and 28 d age. The samples were a small piece of cementitious mortar removed from the central region of the mortar samples. They were dried for 48 h in an oven ($40 \pm 2^\circ\text{C}$). After, the surface was coated with a thin gold layer to avoid charging during SEM imaging. The micrographs of the analyzed samples were obtained using the ZEISS scanning electron microscope, model EVO/LS15, with an acceleration voltage of 20 kV.

The EDX technique was used to identify the chemical elements present in the mortars produced without and with nanocomposite hydrogels. For this, an Oxford Instruments X-ray dispersive energy spectroscope, Inca X-act model with 100 eV resolution, was used, in which it is coupled to the cited microscope.

6.2.7 Statistical analysis

The experimental results for each treatment sets were available by analysis of variance (ANOVA) from the Tukey test, with a 5% significance level, using SISVAR[®] software.

6.3 RESULTS AND DISCUSSION

6.3.1 Water absorption

The water absorption behavior of the mortars is one aspect to be evaluated in cement materials because this parameter directly influences their durability [30]. Furthermore, the water penetration in these matrices is an important physical process [31] because the high humidity levels can prejudice the building performance [32]. Figure 6.1 illustrates the effect of hydrogel application prepared from different Cloisite Na⁺ nanoclay in water absorption of the cementitious mortars.

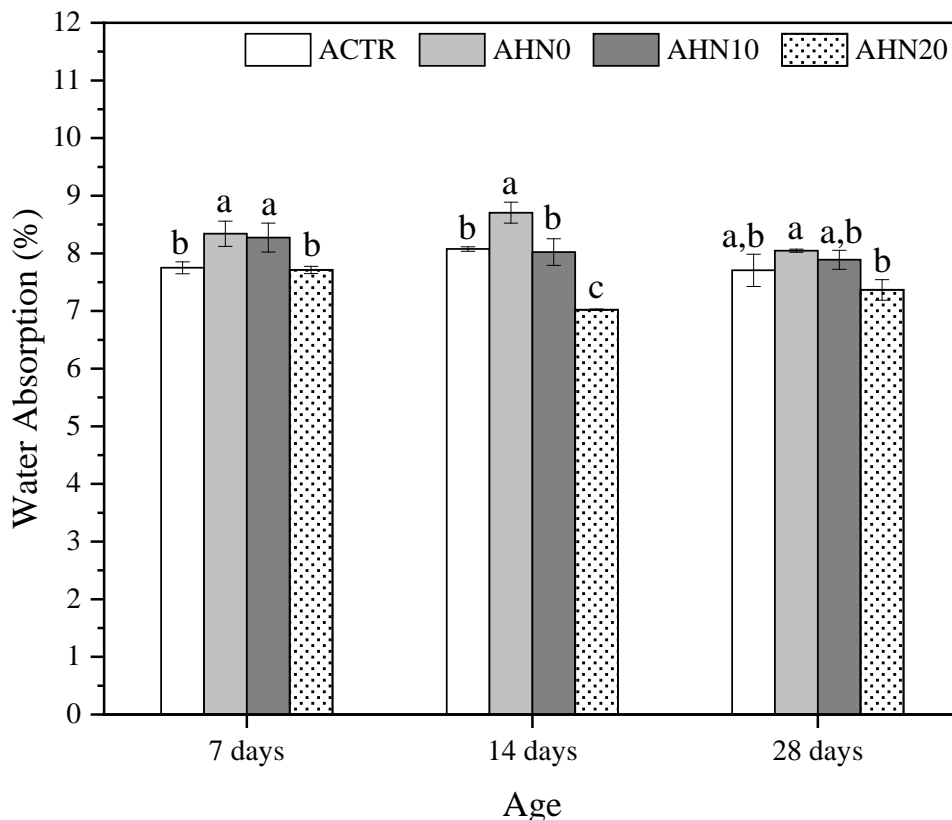


Figure 6.1 – Effect of hydrogels with different Cloisite Na⁺ concentrations in water absorption (%) of cement-mortars over time. *Average with their respective standard deviation values, followed by equal letters, do not differ statistically from each other following the Tukey test with a 95% confidence level.

At 7 d, AHN0 and AHN10 mortars presented average water absorption values of about 8.34% and 8.27%, respectively, while the ACTR and AHN20 mortars demonstrated a smaller

water absorption of 7.75% and 7.71%, respectively. The same behavior can be observed at 14 d except for AHN20 mortar, whose average value was 7.02 ± 0.01 %, indicating a reduction concerning other mortars.

The increasing trend in the water absorption of the AHN0 and AHN10 is related to the rehydration of hydrogel particles in the water medium, corroborating with the results shown by Sarbapalli et al. [19]. It is important to note that this behavior demonstrated that hydrogels had the same characteristics of swelling degree discussed in Chapter 3, and the increase of Cloisite Na⁺ concentration in polymer matrix decreases the absorption water by these hydrogels.

At 28 d, the results pointed that hydrogel with 20% of Cloisite Na⁺ was efficient, reducing around 4.41% of the water absorption compared to the control sample. These results corroborate with the results of the volume of permeable pores shown in chapter 5, where the % of voids in ACTR and AHN20 were lower than AHN0 and AHN10 mortars.

The relation between the Cloisite Na⁺ nanoclay concentration in the hydrogel matrix and the water absorption index is noteworthy. When the concentration increases, it is possible to analyze that the water absorption decreases in all ages. AHN20 absorption water is lower in later ages because the nanoclay acts as a physical crosslinker [49] in matrix polymer, increasing the crosslinking points, which restricted both the polymer chains and less water absorption. Thus, the water absorption index is directly interfered with by the swelling degree of the hydrogel, as reported in previous studies [33,34].

A factor to consider is the possibility that water released from the hydrogels results in continued hydration [35] of the cement matrix. For hydrogels with high nanoclay concentration, the continued hydration of the unhydrated cement grains can produce new calcium silicate hydrates (C-S-H), resulting in the sealing of small cracks [36]. This phenomenon makes the structure more compact [37], reflecting the mechanical properties seen previously.

Justs et al. [38] point in their studies that commercial superabsorbent polymers (SAP) increase the hydration degree at later ages due to the released additional water over time. It indicates a reduction of small capillary pores and consequently a reduction in water absorption, corroborating with similar behavior of AHN20 mortar.

Another important aspect of this behavior at later ages is that the hydrogels, when retaining part of the dosage water reducing the total w/c ratio that directly affects the total porosity and pore size distribution of hydrated cement paste. Therefore, the water reduction in

the system represents mixtures less porous and with the minor possibility of interconnection and, consequently, more difficult water entry [23].

The results confirmed that the nanocomposite hydrogels used to contribute as internal curing agents, as reported by several studies [12, 39], due to the controlled release preventing shrinkage and formation of cracks. In addition, considering that the vulnerability of this type of material depends on contact with water [40], the results obtained were satisfactory when nanocomposite hydrogels are added.

6.3.2 Capillarity coefficient

Water absorption through capillarity is a prominent transport mechanism [41] applied to describe cementitious material durability. In addition, the capillarity coefficient can often be used to understand pores structure formed in cement materials because their sorptivity allows performance analysis of these materials when exposed to adverse humidity conditions or aggressive substances transported through water [42].

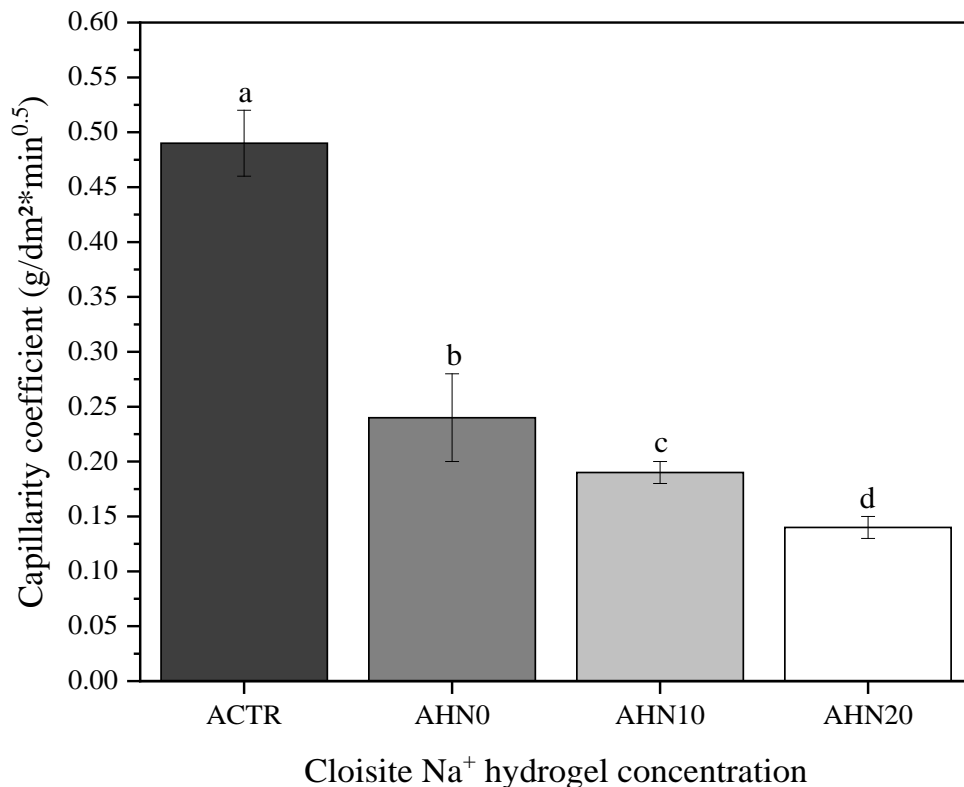


Figure 6.2 – Capillarity coefficient (g/dm²*min^{0.5}) of mortars at 28 days produced without or with different nanocomposites hydrogels. *Average with their respective standard deviation values, followed by equal letters, do not differ statistically from each other following the Tukey test with a 95% confidence level.

The results indicated that nanocomposite hydrogels used reduces the mortar capillarity coefficient extensively. Furthermore, the observed differences were statically significant, representing reductions of 51%, 61%, and 71% for AHN0, AHN10, and AHN20 mortars, respectively, compared to ACTR mortar. Notably, the capillary absorption behavior of these mortars was different from the water absorption results discussed previously at 28 d.

However, the decrease of capillarity is related to absorption water capacity by the hydrogels, i.e., Cloisite Na⁺ concentration in hydrogel matrix directly influences material capillarity due to factors because their presence altered the absorption and release kinetics of the hydrogel. Despite increasing the mechanical strength of the polymer, the nanoclay increase can make the crosslinking more rigid and their expansion more difficult, which results in less water absorption [34]. Thus, capillary rise for AHN20 mortars is impaired by the hydrogel with a lower swelling degree.

These reductions corroborate with the behavior of concretes with commercial SAP studied by Kong et al. [43]. In addition, the authors verified that enhanced hydration could leave to a capillary porosity reduction and refinement in the distribution of size pores, mainly in older ages.

Hydration products obtained through additional cement reactions can be useful to fill and refine these capillary pores [44]. Thus, the capillary porosity reduction results from better internal curing proceedings or a result of the decrease in the effective a/c ratio due to the retention of part of the water by the polymer [43]. Also, the hydrogel particles can provide the absorbed water during the drier periods to the non-hydrated grains of cement to the formation of new calcium silicate hydrated and promote the calcium carbonate precipitation [45].

The capillaries volume in cement-material hydrated depends on the water amount mixed with cement at the start of the hydration and the cement hydration degree [46] because their microstructure tends to be refined when the absorbent polymer is added. Indeed, the water distribution in cementitious materials optimizes the hydration process of these materials [5].

Snoeck et al. [47] also affirm that the mixtures containing SAP had a lower capillary porosity and more gels cementitious than mortars without SAP. This condition is because the released water by the polymer stimulates continuous hydration, which decreases the porosity and densifies the cementitious matrix.

Therefore, the relative humidity increases inside the mortars due to the presence of the hydrogels resulting in a continuous hydration process, reducing the capillary porosity in older

ages [48]. As a result, the capillary pores become filled with hydration products until there is no more space for the precipitation of new products formed [49]. As a result, the pore structure tends to become thinner, and the connection between the capillary pores is decreased [37].

Senff et al. [50] presented similar behavior for cementitious mortars with 0.66 of w/c ratio produced with 0.3% of commercial SAP based on acrylic acid (Evonik®). However, for this mortar, there was a reduction of around 29% concerning the control sample. The authors attribute this behavior to the fact that the SAP particles create a heterogeneous microstructural arrangement involving larger and discontinuous voids that would limit the values capillarity of the material.

6.3.3 Weight loss

Weight loss is a complementary property to evaluate the water retention capacity of cementitious materials produced with hydrogels and their effectiveness as internal curing agents. In addition, it is used to explain the change in the amount of evaporation which is also related to the structure of the surface pores [51]. Figure 6.3 illustrates the relation between relative humidity variation and mass variation over time of mortars produced without or with nanocomposite hydrogels.

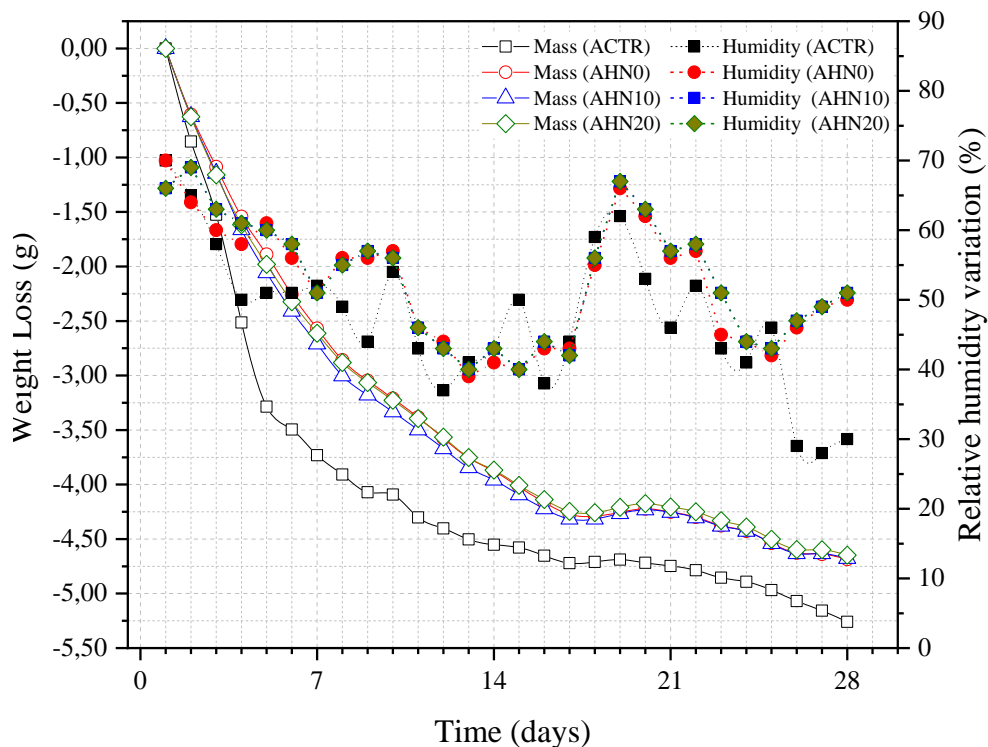


Figure 6.3 – Relation between relative humidity variation (%) and weight loss (g) of mortars produced without or with different nanocomposites hydrogels over time.

In general, all mortars produced with hydrogel had a lower weight loss than ACTR control mortar. This significant reduction confirms the hydrogel effectiveness as an internal curing agent that helps to maintain the internal relative humidity of the cementitious matrix [52].

In addition, the weight loss for all mortars up to 14 d follows a more pronounced linear behavior, and after this age, the variations become smaller.

Another behavior found was the relation of the weight loss with relative humidity variation of the environment where the samples were arranged. The relative humidity of the sample packing places decreases up to 14 d, in agreement with the weight loss in this period. As the hydrogels have a controlled water release capacity, the variation of local humidity in this time interval was higher than the control sample. This may be related to more significant water evaporation from AHN0, AHN10, and AHN20 mortars, because the hydrogels provide extra curing water to the moisturizing matrix [53], improving the local humidity.

After 14 d, the humidity variations are higher, observing an inflection point at 18 d in the weight loss. These behaviors are frequently attributed to the increase in external relative humidity (RH about 66%) presented in Figure 6.3, which allowed an increase in the packed humidity local and, consequently, a slight increase in the sample masses.

Ma et al. [54] obtained similar results for mortars produced with fly ash and commercial SAP based on polyacrylamide and poly(acrylic acid) as co-polymer. The authors verified that for the same w/c ratio, the water loss of the reference sample was higher, while the mortars with SAP were lower. This was attributed to the lower weight loss because the SAPs reduce the evaporation amount and improve the structure of surface pores.

This reduction in the weight loss observed in the mortars with hydrogels is interesting because it is evidence that the polymer acts as a hydroretentor agent. Furthermore, Wyrzykowski et al. [55] verified that the addition of SAP reduces the self-desiccation of cement materials with a w/c ratio under 0.40, avoiding reducing internal relative humidity and autogenous shrinkage process. These results are another indicator of the efficiency of the polymer as an internal curing agent because their presence the maintenance local packed moisture higher.

6.3.4 Dry shrinkage and mass variation

Cement-material shrinkage combines several types of shrinkage, such as chemical, autogenous, drying, and carbonation. In general, the phenomena result from water loss and

volume reduction of hydrated products compared with the reaction of the compound materials [56].

Thus, one of the important types of shrinkage to be controlled is the drying shrinkage which is a volumetric reduction caused by evaporation of the internal humidity [12, 37, 57], indicating a humidity transport, i.e., water leaving the interior of cement-material for the environment [58]. The importance of controlling the occurrence of this type of pathological manifestation is that drying shrinkage can be occasioned to several problems related to material durability, such as the risk of corrosion, sulfate attack, alkali-aggregate reaction, and unsatisfactory structural performance [59]. Thus, Figure 6.4 (a, b, and c) showed the drying shrinkage of the mortars without or with hydrogels in three different curing media.

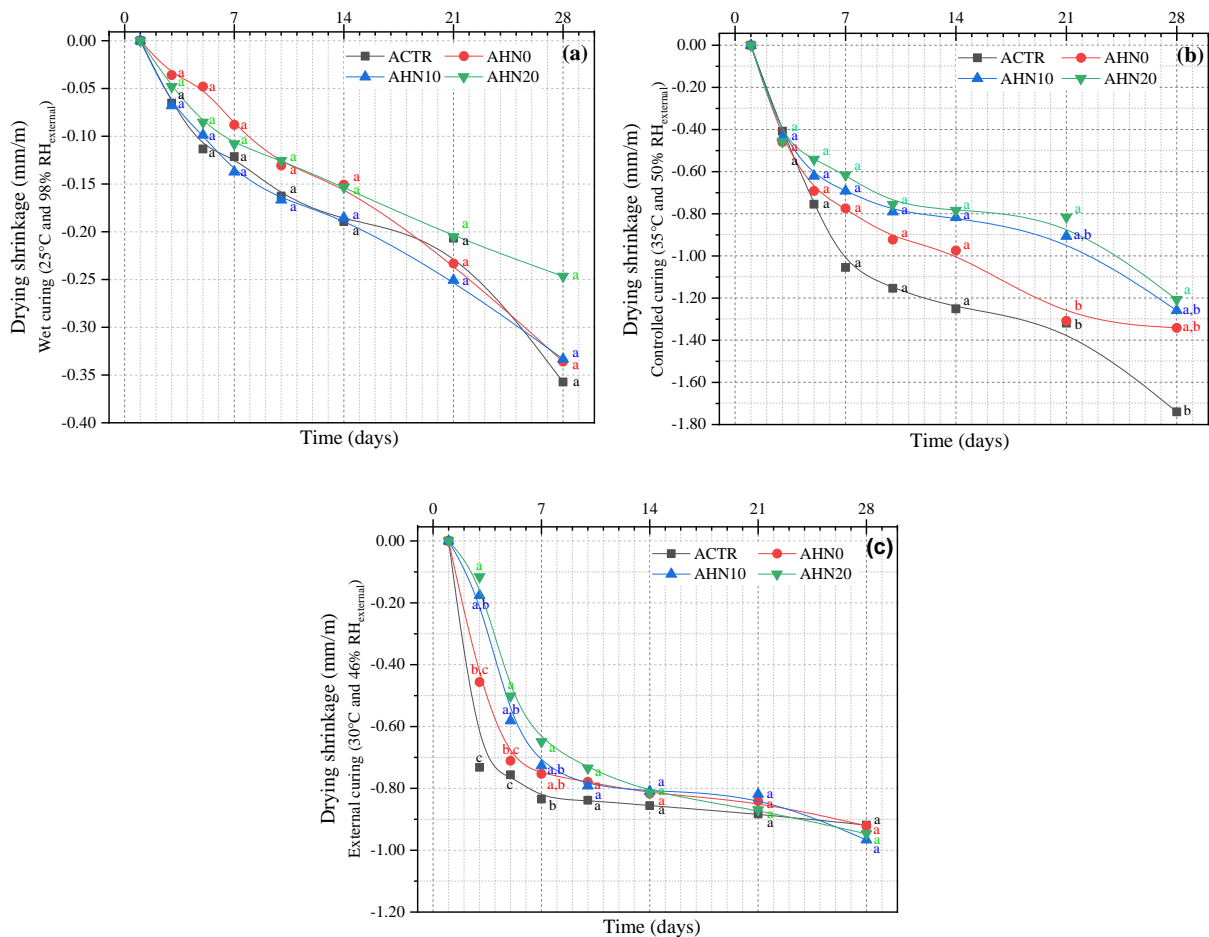


Figure 6.4 – Evolution of dry shrinkage (mm/m), over time, of cement mortars without and with hydrogel nanocomposites in different curing media (a) wet curing (35±2°C and 98% RH_{external}); (b) Controlled curing (35±2°C and 55% RH_{external}); (c) External curing (30±2°C and 46% RH_{external}). *Average followed by equal letters does not differ statistically from each other following the Tukey test with a 95% confidence level.

In general, all mortars showed shrinkage over time for the three curing conditions evaluated, as already expected. In contrast, these dimensional changes occurred due to factors like moisture evaporation from the cementitious material, continuous hydration of the cement particles non-hydrated that leads to self-dissection, and the surface water evaporation that causes the appearance of capillary pores, causing shrinkage cracking [60].

Figure 6.4a shows the volumetric variation behavior of mortars over time in a wet curing medium. The drying shrinkages for all mortars are statically similar; however, it is possible to verify that mortars with nanocomposite hydrogels have a decreasing trend to this type of shrinkage due to the controlled internal water release by the polymer. At 28 d, the drying shrinkage index to reference mortar ACTR was 0.36 ± 0.07 mm/m, while for mortars AHN0, AHN10, and AHN20, the average values were 0.34 ± 0.11 mm/m, 0.3 ± 0.04 mm/m, and 0.25 ± 0.07 mm/m, respectively.

One of the causes for the small variation in this curing medium is due to water diffusion conditions through the material, which directly depends on the prevailing atmospheric conditions [56] and aspects such as pore structure, size, and sample shape. As the curing was performed at high relative humidity (98%), the shrinkages become similar to all mortars, not verifying the influence of hydrogel as an internal curing agent.

Figure 6.4b illustrates the results for a controlled curing medium in an oven at 35 °C, and the relative humidity of 50% remained constant throughout the test. Under these conditions, the mortars with nanocomposites hydrogel showed lower drying shrinkage than the control sample. At 3 d, drying shrinkage was accentuated and similar for all mortars, and after 7 days, the effect of the hydrogel is evidenced. At 28 d, the reductions in drying shrinkage of mortars AHN0, AHN10, and AHN20 were 23%, 27.6%, and 30.5%, respectively, which indicates the efficiency of hydrogel release in maintaining of internal moisture of the sample.

These results corroborate those reported by Sun et al. [12], where cementitious materials containing SAP showed similar behaviors because during the setting time, as the internal humidity of the material decreases, the osmotic pressure increases. Therefore, the water in SAP is gradually released. Yang et al. [61] also state that due to water evaporation and hydration, the internal moisture of cementitious materials can often not be maintained in an appropriate range, which causes a negative pressure in the capillary pores and provides the shrinkage. The authors affirm that the SAP application is precisely performed to reduce the

shrinkage and crack, increasing the relative humidity of the material, compensating for self-drying.

From Figure 6.4c, it is possible to verify that the hydrogels have an efficient performance in early ages. At 5 d, the shrinkages were more significant, representing 6.0%, 23.2%, and 33.7% for AHN0, AHN10, and AHN20 mortars, respectively, compared to the reference. After 14 days, there are no significant variations in the shrinkage of all mortars, and at 28 d, the average value of drying shrinkage of these same mortars is around 0.94 ± 0.02 mm/m. These results correspond to observations realized by Beushasen et al. [62] where mortars produced with 0.45 w/c ratio and additions of 0.4% and 0.6% of commercial SAP (BASF®) had reductions in shrinkage force from 10 days when compared to a reference sample, indicating an overall positive effect of the SAP addition. Jensen et al. [63], applying acrylamide and acrylic acid-based SAP to cement-pastes also verified that this polymer could potentially be used to reduce the drying shrinkage, but the effect may be small.

The analyses performed by Tan et al. [57] showed that there was a reduction in drying shrinkage of mortars based on cement and sand (1:2 dosage and 0.42 w/c ratio) with polyacrylamide and poly(sodium acrylic) SAP. This condition was linked to the fact that the moisture in the mortar pores is maintained due to hydration by the water reserved inside the polymer filler. This study was performed by using presoak and dry SAP. They observed that the water stored by the presoak polymer could release water more efficiently and earlier to fill the pores than dry SAP powder. Therefore, the reduction of shrinkage caused by presoak SAP was more visible, demonstrating the efficiency of using presoak polymers.

However, Liu et al. [64] showed adverse results where mortars prepared with fume silica, fly ash, low w/c ratio of 0.18, and the addition of 0.3% and 0.6% of polyacrylamide and poly(acrylic sodium)-SAP had a drying shrinkage increased, justifying that SAP increases the surface porosity allowing higher evaporation of capillarity water.

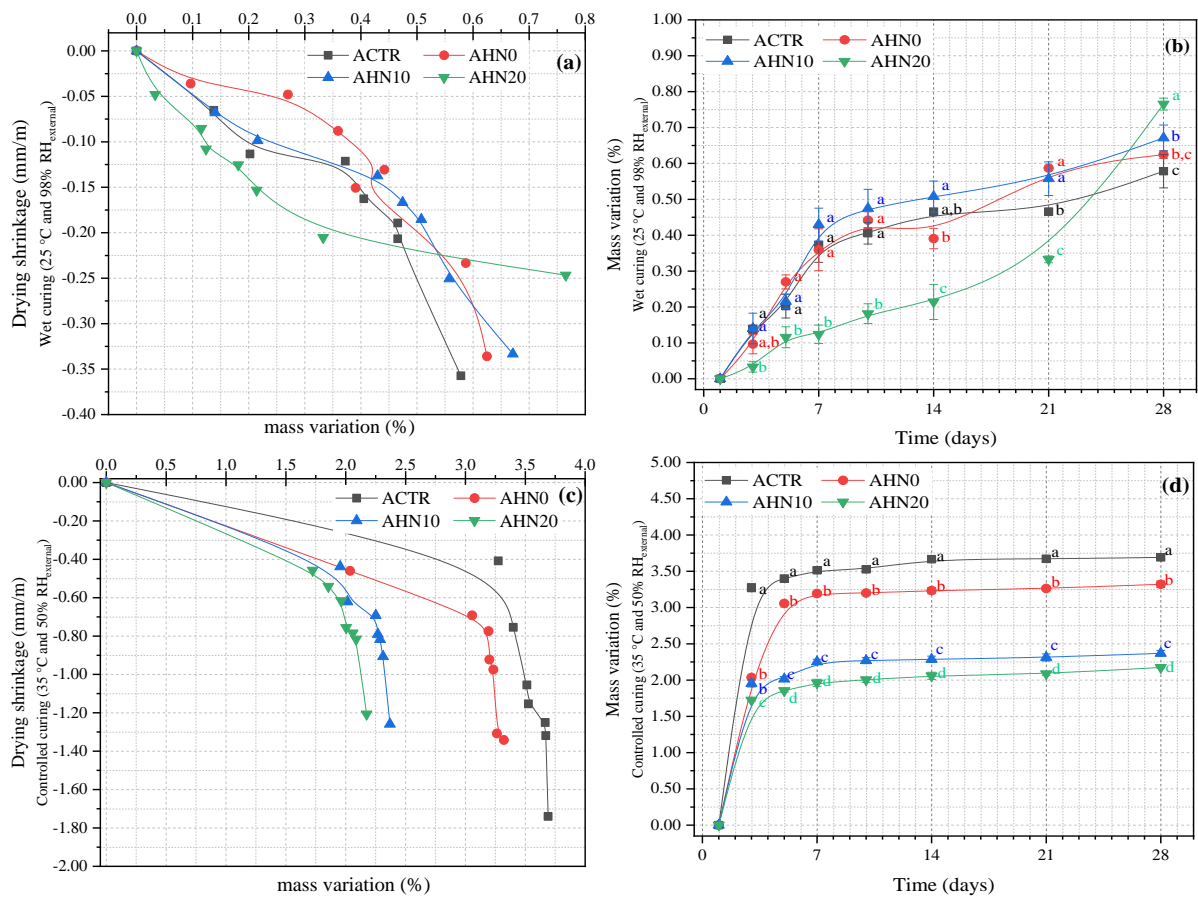
These results also were verified by Liu et al. [10] that mortars with 0.48 w/c ratio and produced with the addition of 0.4 wt% dry amphoteric hydrogel prepared from poly(acrylamide) and 4-(2-((carboxylatomethyl) dimethylammonium)ethoxy)24-oxobut-2-enoate increased the drying shrinkage the mortars. The authors attributed this behavior to the fact that the hydrogel density is lower than cement particles or sand. As a result, the polymer added to the mortars tended to rise and aggregate. This aggregation would cause the water released from the hydrogel to be poorly distributed in the mortars, which was not beneficial in reducing drying shrinkage.

This may indicate that the presoaked hydrogels used in the AHN0, AHN10, and AHN20 mortars of this study are evenly distributed in the mixture, thus avoiding surface evaporation as verified by both authors reducing shrinkage by drying.

In general, from the results presented, the behavior of mortars with and without hydrogel can be linked to reducing the w/c ratio total and the nanoclay concentration present in the nanocomposite matrix. The addition of hydrogel decreases the w/c ratio total of the mixture because part of the water is inside the polymer, reducing both capillary porosity and drying shrinkage [65].

On the contrary, the increase of Cloisite Na+ into polymer matrix decreases drying shrinkage, but more discretely. Furthermore, due to the more controlled release of water over time, provided by nanoclay, which decreases capillary porosity at later ages due to its continuous [47], conforming discussed previously.

Another important point to be discussed is the relation between drying shrinkage and the mass variation of the samples at different curing media for all mortars (Figure 6.5).



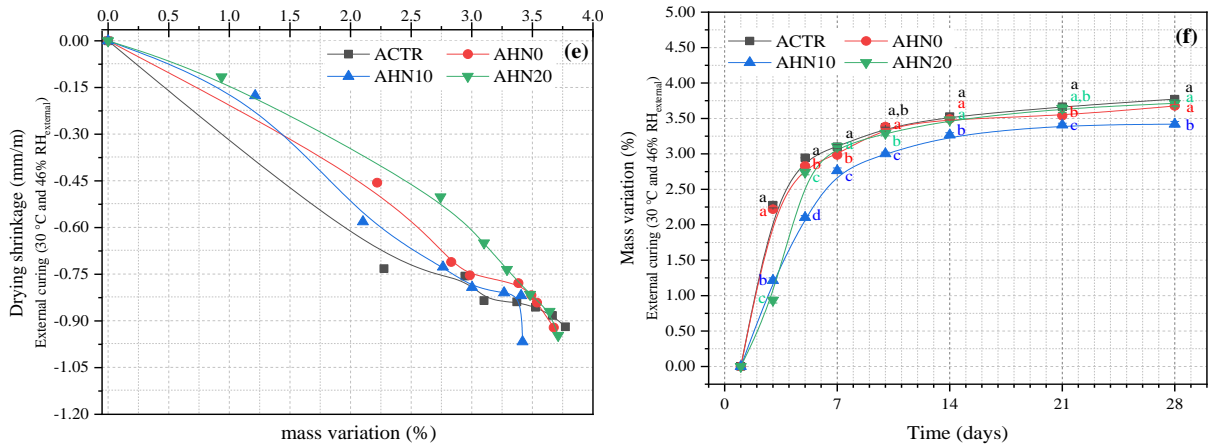


Figure 6.5 – Relation between drying shrinkage (mm/m) and mass variation (%) of the cement mortars without and with hydrogel nanocomposites in different curing media (a, b) wet curing ($35\pm 2^\circ\text{C}$ and $98\% \text{RH}_{\text{external}}$); (c, d) Controlled curing ($35\pm 2^\circ\text{C}$ and $55\% \text{RH}_{\text{external}}$); (e, f) External curing ($30\pm 2^\circ\text{C}$ and $46\% \text{RH}_{\text{external}}$). *Average followed by equal letters does not differ statistically from each other following the Tukey test with a 95% confidence level.

The results for all curing conditions show that shrinkage varies following the sample weight loss because the shrinkage modifies the material volume due to the internal moisture evaporation [20]. In wet curing, Figures 6.5 (a and b), the ACTR, AHN0, and AHN10 mortars presented similar mass variation among them, without significant statistical differences until 10 days. At 28 d, it was observed that the losses of mass were more significant for the mortars containing nanocomposite hydrogels. The most considerable mass variation was found for AHN20 mortar due to the nanoclay presence that causes slower release water.

In the controlled curing condition, Figures 6.5 (c and d), the mass loss curves are much more defined and different among them. For mortars with hydrogels, the losses of mass and shrinkage are smaller than the control mortar due to the water retention by the polymer, corroborating the results observed by Yao et al. [66]. It can be observed that as the cloisite- Na^+ concentration increases in the polymer matrix, the loss of mass decreases and the shrinkage.

In more severe temperature and low relative humidity conditions, the hydrogels action is satisfactory because the slight variation can be an indicator of better cementitious matrix hydration since the internal curing limited the shrinkage with the polymer, whose one of the functions is to avoid self-desiccation [55].

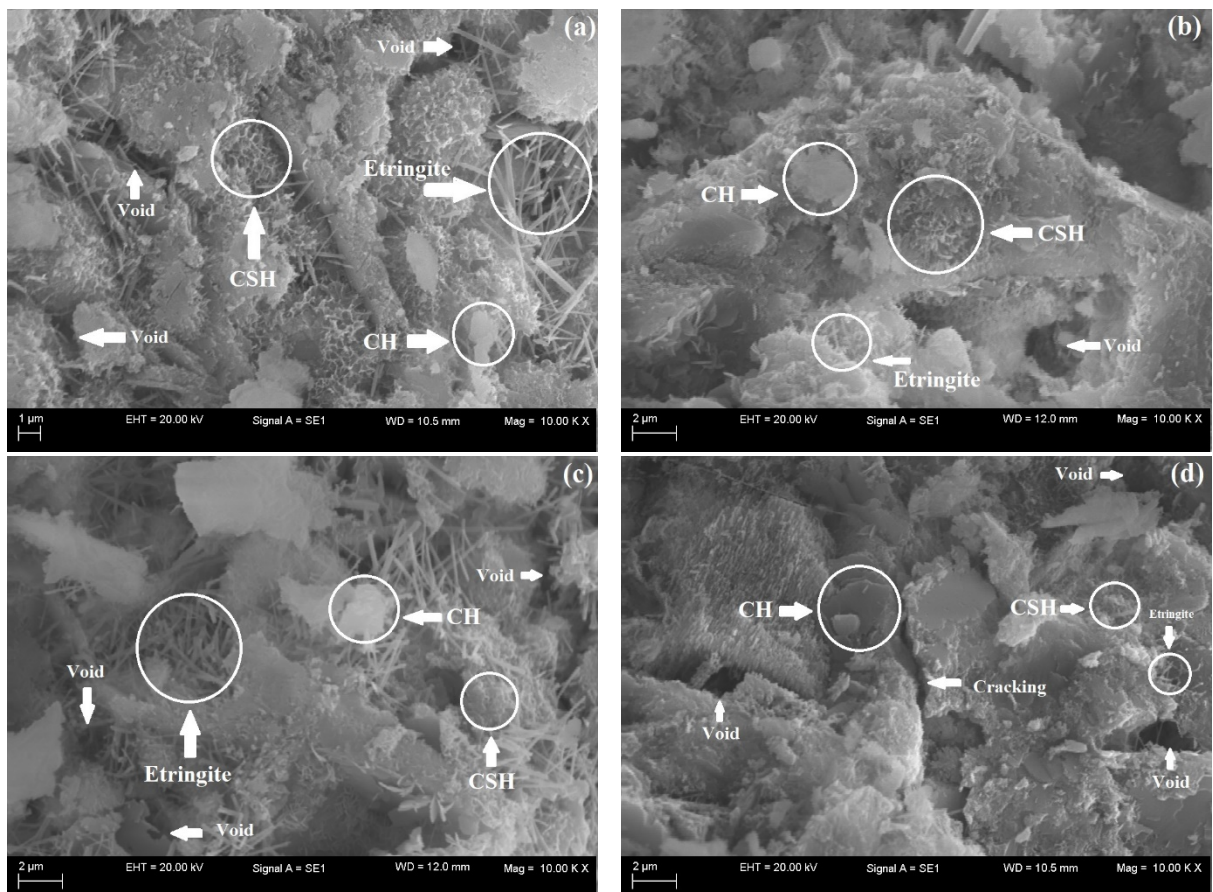
Figures 6.5 (e and f), the environment curing conditions the weight loss was very similar for all mortars. However, there is a tendency to reduce shrinkage and loss of mass for mortars with hydrogels due to them acting as internal curing agents.

In the three curing conditions, it is possible to relate such behaviors to w/c ratio reduction caused by nanocomposites hydrogels and the action of the Cloisite Na⁺ nanoclay in the water release process cementitious matrix. As part of the water is retained by the absorbent polymer, the total w/c ratio is reduced in the mortars produced with hydrogels, which causes a drying shrinkage reduction [67].

In addition, the water released by the polymer may restrict the amount of evaporation water, promoting greater cement particle hydration, as analyzed by Yao et al. [66], and avoid self-desiccation [55]. Therefore, the results indicate that the presoaked hydrogels present a satisfactory behavior for all curing conditions in drying shrinkage due to their release capacity, showing their efficiency as an internal curing agent.

6.3.5 SEM-EDX analysis

SEM analyses allow for characterization of the morphology of the microstructure of cementitious materials and thus evaluation of the effects of additions on the matrices of these materials. Therefore, to evaluate the impact of nanocomposite hydrogels on the microstructures of the cementitious mortars, SEM images were selected for samples of mortars with and without hydrogels at 7 and 28 d, as shown in Figure 6.6.



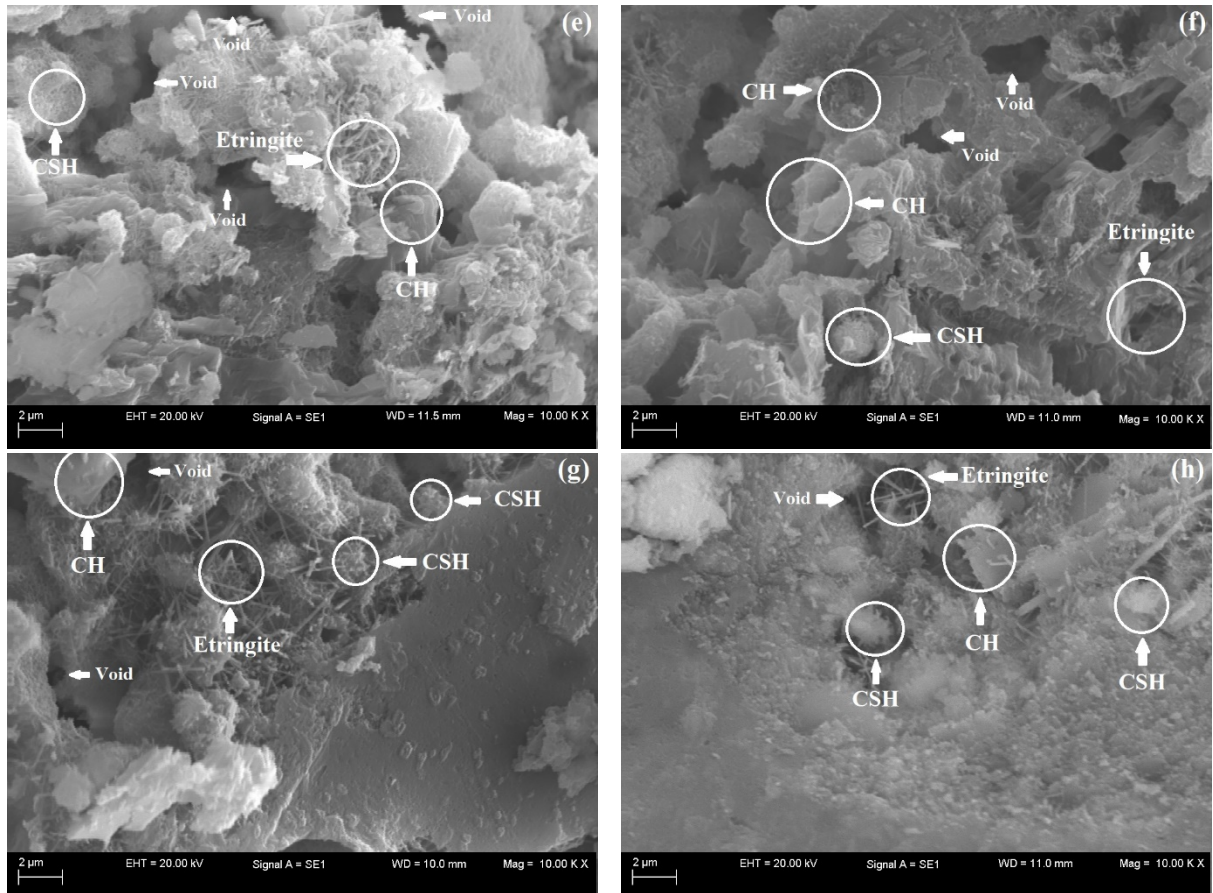


Figure 6.6 – SEM images of the cement mortars (a) ACTR (control) at 7 days, (b) ACTR (control) at 28 days, (c) AHN0 at 7 days, (d) AHN0 at 28 days, (e) AHN10 at 7 days, (f) AHN10 at 28 days, (g) AHN20 at 7 days and (h) AHN20 at 28 days.

At 7 d, all samples present hydrated products with the extensive presence of needle-like ettringite crystals with a large crystal of portlandite (C-H). C-S-H can also be observed in all the samples, and its morphology is similar to a fibrous sponge, in agreement with Pourjavadi et al. [68].

However, it was not possible to clearly identify the presence of hydrogels in AHN0, AHN10, and AHN20. This is possibly related to a low concentration of 0.5% wt of the presoaked hydrogel concerning the dry cement mass used in the mortar dosage.

Thus, as Santos et al. [69] described, despite the lack of identification of the organic phase in the images, the mortars did not present incompatibility or phase separation, which is satisfactory as it indicates possible homogenization of the polymer in the cement matrix of the material.

At 28 d, the micrographs in Figures 6.6 (b, d, f, and h) illustrate denser matrices with smaller ettringite formations. However, the presence of nanocomposite hydrogels provides the establishment of a densified matrix due to the more efficient hydration of cement particles, especially for AHN20, as analyzed by Pourjavadi et al. [70]. In contrast, AHN0 and AHN10

showed voids and the appearance of some microfissures that directly contribute to their mechanical behavior [57].

In general, the formation of ettringite, C-H, and C-S-H occurs in all cementitious matrices, both the control (without hydrogel) and the ones containing hydrogels, indicating that the hardening reactions of the cement were effective over time, in agreement with Cilli et al. [71].

Notably, at 7 d, the mortars with hydrogels present compressive strength lower than the control (Table 6.1) due to the formation of a more discontinuous matrix and the presence of voids observed in the micrographs presented in Figures 6.6 (c, e, and g). These characteristics may be related to the lower availability of free water at an early age, as part of the kneading water is reserved inside the polymer.

Table 6.1 - Average value and standard deviation to mechanical properties in the hardened state to different mortars. *Average followed by equal letters does not differ statistically from each other following the Tukey test with a 95% confidence level.

| Mortar | Consistency index (mm) | Compressive Strength (MPa) | | Density in the hard state (g/cm ³) | |
|--------|----------------------------|----------------------------|---------------------------|--|--------------------------|
| | | 7 d | 28 d | 7 d | 28 d |
| ACTR | 282.20 ± 0.75 ^a | 24.85 ± 0.94 ^a | 30.79 ± 0.60 ^a | 2.19 ± 0.02 ^a | 2.18 ± 0.02 ^a |
| AHN0 | 279.02 ± 1.52 ^b | 22.27 ± 0.64 ^b | 26.36 ± 0.70 ^c | 2.17 ± 0.02 ^a | 2.18 ± 0.03 ^a |
| AHN10 | 279.67 ± 1.36 ^b | 21.94 ± 0.85 ^b | 28.03 ± 0.73 ^b | 2.19 ± 0.03 ^a | 2.19 ± 0.01 ^a |
| AHN20 | 268.50 ± 0.45 ^c | 21.20 ± 0.61 ^b | 30.11 ± 0.77 ^a | 2.18 ± 0.01 ^a | 2.17 ± 0.01 ^a |

At 28 d, the cement matrix of mortar AHN20 (Figure 6.6 h) was more densified and similar to ACTR (Figure 6.6b), which is also seen in their similar mechanical behavior, according to Table 6.1, indicating the efficiency of the hydrogels in the internal hydration process. The denser microstructures with few pores result from hydration and consequently the formation of more effective hydrated products [72]. Figures 6.6 (d and f) also indicate that AHN0 and AHN10, at 28 d, presented microstructures with voids and some microcracking, which reduced their compressive strength.

Table 6.2 presents the results obtained by the application of the EDX technique, but it did not show significant changes for all the mortars studied. This technique was used to identify the presence of hydrogels in the cement matrix; however, the minimal or zero variation can be related to the low concentration of hydrogels used in the production of the mortars. At 28 d, it was possible to verify that AHN0, AHN10, and AHN20 presented a small increase in the carbon element concerning the ACTR mortar; however, this variation was

discrete, which does not allow us to conclude whether it is related to the presence of hydrogels or the occurrence of the carbonation process, as also observed by Santos et al. [69].

Table 6.2 - EDX analysis for mortars produced with and without nanocomposite hydrogel.

| Chemical Element | ACTR (% wt) | | AHN0 (%wt) | | AHN10 (%wt) | | AHN20 (%wt) | |
|------------------|-------------|-------|------------|-------|-------------|-------|-------------|-------|
| | 7 d | 28 d | 7 d | 28 d | 7 d | 28 d | 7 days | 28 d |
| C | 4.26 | 3.41 | 3.51 | 4.17 | 4.10 | 4.43 | 4.32 | 3.98 |
| O | 53.30 | 54.84 | 54.92 | 55.30 | 58.93 | 49.97 | 53.60 | 50.36 |
| Na | 0.23 | * | 0.31 | * | 0.31 | * | 0.35 | * |
| Mg | 1.68 | 1.85 | 2.44 | 1.82 | 1.84 | 1.36 | 2.12 | 1.54 |
| Al | 1.88 | 1.77 | 2.41 | 2.54 | 2.50 | 0.77 | 2.04 | 1.75 |
| Si | 7.19 | 8.99 | 6.59 | 7.76 | 7.89 | 37.04 | 7.81 | 8.07 |
| S | 0.96 | 0.86 | 1.09 | 0.86 | 1.14 | 0.43 | 1.03 | 0.86 |
| K | 0.51 | 0.58 | 0.94 | 1.07 | 0.60 | 0.55 | 0.86 | 0.89 |
| Ca | 28.84 | 26.44 | 26.39 | 25.22 | 21.54 | 14.63 | 26.46 | 31.17 |
| Fe | 1.16 | 1.28 | 1.39 | 1.26 | 1.15 | 0.45 | 1.40 | 1.39 |

*Undetected element

Thus, the presence of the other elements comes from the composition of cement and the result of the formation of the hydration products, indicating that such reactions were effective over time.

6.4 CONCLUSIONS

The application of nanocomposite hydrogels in cement materials is a promisor technology to improve their physical and mechanical performance due to their capacity to retain and release water over time into these matrices, acting as an internal curing agent. Thus, based on the presented analyses, the following conclusions can be formulated:

- At 28 d, the results pointed that hydrogel with 20% of Cloisite Na⁺ was efficient, and it reduced around 4.41% of the water absorption compared to the control sample. This behavior corroborates with mechanical properties discussed previously.
- The capillarity coefficient reduces extensively using nanocomposite hydrogels, and results corroborate with the water absorption index. The reductions were 51%, 61%, and 71% for AHN0, AHN10, and AHN20 mortars, respectively, compared with the ACTR mortar because the presoaked hydrogel applied removes part of the dosage water and consequently reduces the free water quantity and material capillarity.
- In general, all mortars produced with hydrogel had a lower weight loss if compared to the control.

- For the three curing conditions evaluated, all mortars showed a shrinkage over time, which was already expected. However, the controlled curing demonstrated that hydrogels cause a drying shrinkage in the mortars. Furthermore, the addition of hydrogel decreases the w/c ratio total of the mixture because part of the water is inside the polymer, which reduces the capillary porosity and causes the reduction of drying shrinkage. Therefore, the results indicate that the presoaked hydrogels present a satisfactory behavior for all curing conditions in drying shrinkage due to their release capacity, showing their efficiency as an internal curing agent.
- The SEM images of all mortars present hydrated products with the extensive presence of needle-like crystals of ettringite together with a large crystal of portlandite. Calcium silicate hydrate can also be observed in all samples, whose morphology is similar to a fibrous sponge. At 28 d, the micrographs represented denser matrices with smaller ettringite formations. However, the presence of nanocomposite hydrogel provides the establishment of a densified matrix due to more efficient hydration of cement particles, especially for AHN20.
- EDX did not show significant changes for all the mortars studied. However, minimal or zero variation can be related to the low concentration of hydrogel used to produce the mortars. At 28 d, it was possible to verify that AHN0, AHN10, and AHN20 presented a small increase in the carbon element concerning ACTR mortar; however, this variation was discrete, which does not allow us to conclude if it is related to the presence of hydrogel or the occurrence of the carbonation process.

Nanocomposites hydrogels may prove efficient as an internal agent despite the complexity of interactions between inorganic and organic matrices. Thus, this hybrid additive can be an innovative material for improvements in water control studies in cementitious materials construction technologies.

6.5 REFERENCES

- [1] S. Tang, J. Huang, L. Duan, P. Yu, E. Chen, A review on fractal footprint of cement-based materials, *Powder Technol.*, 370 (2020), 237-250.
- [2] S. Y. Chung, J. S. Kim, D. Stephan, T. S. Han, Overview of the use of micro-computed tomography (micro-CT) to investigate the relation between the material characteristics and properties of cement-based materials, *Constr. Build. Mater.*, 229 (2019), 1-13.

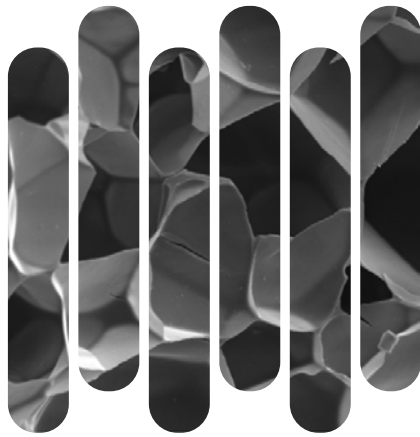
- [3] S. Guo, P. K. Forooshani, Q. Dai, B. P. Lee, R. Si, J. Wang, Design of pH-responsive SAP polymer for pore solution chemistry regulation and crack sealing in cementitious materials, *Compos. B. Eng.*, 199 (2020), 1-36.
- [4] P. Banfill, *Rheology of Fresh Cement, and Concrete*. London: CRC Press, Liverpool, United Kingdom, 1991.
- [5] J. Dang, J. Zhao, Z. Du, Effect of superabsorbent polymer on the properties of concrete. *Polymers*, 9, 12 (2017), 1-17.
- [6] V. Mechtcherine, Use of superabsorbent polymers (SAP) as concrete additive, *RILEM Technical Letters*, 10 (2016), 81-87.
- [7] A.M. Neville, *Properties of Concrete*, Wiley, Chichester, 2012.
- [8] H. F. Taylor, *Cement Chemistry (Vol. 2)*. London: Thomas Telford, 1997.
- [9] M. Valcuende, C. Parra, E. Marco, A. Garrido, E. Martínez, J. Cánoves, Influence of limestone filler and viscosity-modifying admixture on the porous structure of self-compacting concrete, *Constr. Build. Mater.*, 28 (2012), 122-128.
- [10] X. Y. Liu, C. H. Huang, C. H. Zhuang, K. C. Hsu, C. H. Huang, An amphoteric hydrogel: Synthesis and application as an internal curing agent of concrete, *J. Appl. Polym. Sci.*, 132 (2015), 1-9.
- [11] H. X. D. Lee, H. S. Wong, N. R. Buenfeld, Self-sealing of cracks in concrete using superabsorbent polymers, *Cem. Concr. Res.*, 7 (2016), 194–208.
- [12] B. Sun, H. Wu, W. Song, Z. Li, J. Yu, Design methodology and mechanical properties of Superabsorbent Polymer (SAP) cement-based materials, *Constr. Build. Mater.*, 204 (2019), 440-449.
- [13] M. Balapour, W. Zhao, E. J. Garboczi, N. Y. Oo, S. Spatari, Y.G. Hsuan, P. Billen, Y. Farnam, Potential use of lightweight aggregate (LWA) produced from bottom coal ash for internal curing of concrete systems, *Cem. Concr. Compos.*, 105 (2020), 1-12.
- [14] J. T. Kevern, Q. C. Nowasell, Internal curing of pervious concrete using lightweight aggregates, *Constr. Build. Mater.*, 161 (2018), 229-235.
- [15] C. Schröfl, D. Snoeck, V. Mechtcherine, A review of characterization methods for superabsorbent polymer (SAP) samples to be used in cement-based construction materials: Report of the RILEM TC 260-RSC, *Mater. Struct.*, 50, 4 (2017), 197-216.
- [16] D. Snoeck, D. Schaubroeck, P. Dubruel, N. de Belie, Effect of high amounts of superabsorbent polymers and additional water on the workability, microstructure and strength of mortars with a water-to-cement ratio of 0.50, *Constr. Build. Mater.*, 72, 24 (2014), 148–157.
- [17] K. Farzanian, A. Ghahremaninezhad, The effect of the capillary forces on the desorption of hydrogels in contact with a porous cementitious material, *Mater. Struct.*, 50, 5 (2017), 216.
- [18] L. De Meyst, E. Mannekens, M. Araújo, D. Snoeck, K. Van Tittelboom, S. Van Vlierberghe, N. De Belie, Parameter Study of Superabsorbent Polymers (SAPs) for Use in Durable Concrete Structures, *Mater.*, 12, 9 (2019), 1-15.
- [19] D. Sarbapalli, Y. Dhabalia, K. Sarkar, B. Bhattacharjee Application of SAP and PEG as curing agents for ordinary cement-based systems: impact on the early age properties of paste

- and mortar with water-to-cement ratio of 0.4 and above, *Eur. J. Environ. Civ. Eng.* 21, 10 (2017), 1237-1252.
- [20] D. Snoeck, L. Pel, N. de Belie, The water kinetics of superabsorbent polymers during cement hydration and internal curing visualized and studied by NMR, *Sci. Rep.*, 7, 1 (2017), 1-14.
- [21] D. Li, B. Chen, X. Chen, B. Fu, H. Wei, X. Xiang, Synergetic effect of superabsorbent polymer (SAP) and crystalline admixture (CA) on mortar macro-crack healing, *Constr. Build. Mater.*, 247 (2020), 1-12.
- [22] J. Browning, D. Darwin, D. Reynolds, B. Pendergrass, Lightweight Aggregate as Internal Curing Agent to Limit Concrete Shrinkage, *ACI Materials Journal*, Farmington Hills, 108 (2011), 638-644.
- [23] A. N. Lopes, E. F. Silva, D. C. Dal Molin, R. D. Toledo Filho, Shrinkage-Reducing Admixture: Effects on Durability of High-Strength Concrete, *ACI Materials Journal*, Farmington Hills, 110 (2013) 365-374.
- [24] American Society for Testing and Materials (ASTM), Standard test method for rate of water of masonry mortar. ASTM C1403-15. West Conshohocken, PA, 2015.
- [25] European Committee for Standardization. Methods of test for mortar for masonry - Part 8: Determination of water retentivity of fresh mortar. EN 1015-8. 1999.
- [26] Associação Brasileira de Normas Técnicas (ABNT), Argamassa para assentamento e revestimento de paredes e tetos - Determinação da absorção de água por capilaridade e do coeficiente de capilaridade, NBR 15259: 2005, Rio de Janeiro, RJ, 2005.
- [27] Associação Brasileira de Normas Técnicas (ABNT), Argamassa para assentamento e revestimento de paredes e tetos - Determinação da variação dimensional (retração ou expansão linear), NBR 15261: 2005, Rio de Janeiro, RJ, 2005.
- [28] American Society for Testing and Materials (ASTM), Standard Test Method for Drying Shrinkage of Mortar Containing Hydraulic Cement. ASTM C596-18. West Conshohocken, PA, 2015.
- [29] American Society for Testing and Materials (ASTM), Use of Apparatus for the Determination of Length Change of Hardened Cement Paste, Mortar, and Concrete. ASTM C490/C490M – 17, West Conshohocken, PA, 2017.
- [30] S. Cunha, J. Aguiar, V. Ferreira, A. Tadeu, Argamassas com incorporação de Materiais de Mudança de Fase (PCM): Caracterização física, mecânica e durabilidade, *Mater.*, 20, 1 (2015), 245-261.
- [31] J. M. P. Q. Delgado, V. P. de Freitas, A. S. Guimarães, Water movement in building walls: interfaces influence on the moisture flux, *Heat Mass Transf.*, 52, 11 (2016), 2415-2422.
- [32] R. J. Ball, G. C. Allen, G. C. The measurement of water transport in porous materials using impedance spectroscopy, *J. Phys. D.*, 43, 10 (2010), 1-7.
- [33] D. W. Nascimento, M. R. de Moura, L. H. Mattoso, F. A. Aouada, Hybrid biodegradable hydrogels obtained from nanoclay and carboxymethylcellulose polysaccharide: hydrophilic, kinetic, spectroscopic and morphological properties. *J. Nanosci. Nanotechnol.* 17, 1 (2017), 821-827.

- [34] A. Bortolin, F. A. Aouada, L. H. Mattoso, C. Ribeiro, Nanocomposite PAAm/methyl cellulose/montmorillonite hydrogel: evidence of synergistic effects for the slow release of fertilizers, *J. Agric. Food Chem.*, 61, 31 (2013), 7431-7439.
- [35] D. Snoeck, L. F. Velasco, A. Mignon, S. Van Vlierberghe, P. Dubruel, P. Lodewyckx, N. De Belie, The effects of superabsorbent polymers on the microstructure of cementitious materials studied by means of sorption experiments, *Cem. Concr. Res.*, 77 (2015), 26-35.
- [36] D. Snoeck, Superabsorbent polymers to seal and heal cracks in cementitious materials. RILEM technical letters, 3 (2018).
- [37] Z. He, A. Shen, Y. Guo, Z. Lyu, D. Li, X. Qin, Z. Wang, Cement-based materials modified with superabsorbent polymers: A review, *Constr. Build. Mater.*, 225 (2019), 569-590.
- [38] J. Justs, M. Wyrzykowski, F. Winnefeld, D. Bajare, P. Lura, Influence of superabsorbent polymers on hydration of cement pastes with low water-to-binder ratio, *J. Therm. Anal. Calorim.*, 115, 1 (2014), 425-432.
- [39] D. Snoeck, K. Van Tittelboom, S. Steuperaert, P. Dubruel, N. De Belie, Self-healing cementitious materials by the combination of microfibres and superabsorbent polymers. *J. Intell. Mater. Syst. Struct.*, 25, 1 (2014), 13-24.
- [40] H. AzariJafari, A. Kazemian, M. Rahimi, A. Yahia, Effects of presoaked super absorbent polymers on fresh and hardened properties of self-consolidating lightweight concrete, *Constr. Build. Mater.* 113, 13 (2016), 215-220.
- [41] SAP, RILEM TC. Application of Superabsorbent Polymers (SAP) in Concrete Construction. RILEM State-of-the-Art Report Prepared by Technical Committee, p. 165, 2012.
- [42] N. M. Alderete, Y. V. Zaccardi, N. De Belie, Mechanism of long-term capillary water uptake in cementitious materials, *Cem. Concr. Compos.*, 106 (2020), 1-50.
- [43] H. S. Wong, Concrete with superabsorbent polymer. *Eco-Efficient Repair and Rehabilitation of Concrete Infrastructures*, (2018), 467–499.
- [44] J. Yang, F. Wang, Z. Liu, Y. Liu, S. Hu, Early-state water migration characteristics of superabsorbent polymers in cement pastes, *Cem. Concr. Res.*, 118 (2019), 25-37.
- [45] E. Gruyaert, B. Debbaut, D. Snoeck, P. Díaz, A. Arizo, E. Tziviloglou... N. de Belie, Self-healing mortar with pH-sensitive superabsorbent polymers: testing of the sealing efficiency by water flow tests. *Smart Mater. Struct.* 25, 8 (2016), 084007.
- [46] P. K. Mehta, P.J.M. Monteiro, *Concrete Microstructure Properties and Materials*, McGraw-Hill Publishing, New York, 2006.
- [47] D. Snoeck, N. De Belie, The influence of superabsorbent polymers on the microstructure and permeability of cementitious materials. In *International Conference on Concrete under Severe Conditions-Environment and Loading*, Nanjing, September 23–25, 363–373, 2013.
- [48] S. Igarashi, A. Watanabe, Experimental study on prevention of autogenous deformation by internal curing using super-absorbent polymer particles, In: *Volume changes of hardening concrete: testing and mitigation*, Proceedings of an International RILEM conference, Lyngby, RILEM Publications S.A.R.L., 77-86, 2006.

- [49] J. Justs, M. Wyrzykowski, D. Bajare, P. Lura, Internal curing by superabsorbent polymers in ultra-high-performance concrete, *Cem. Concr. Res.*, 76 (2015), 82-90.
- [50] L. Senff, R. C. E. Modolo, G. Ascensão, D. Hotza, V. M. Ferreira, J. A. Labrincha, Development of mortars containing superabsorbent polymer. *Constr. Build. Mater.* 95, 21 (2015), 575-584.
- [51] P. K. Mehta, P. J.M. Monteiro, A. Carmona Filho, *Concreto: estrutura, propriedades e materiais*. Pini, 1994.
- [52] D. Snoeck, O. M. Jensen, N. De Belie, NThe influence of superabsorbent polymers on the autogenous shrinkage properties of cement pastes with supplementary cementitious materials. *Cem. Conc. Res.*, 74 (2015), 59-67.
- [53] M. J. Krafcik, N. D. Macke, K. A. Erk, Improved concrete materials with hydrogel-based internal curing agents, *Gels*, 3, 4 (2017), 46-64.
- [54] X. Ma, J. Liu, Z. Wu, C. Shi, Effects of SAP on the properties and pore structure of high-performance cement-based materials, *Constr. Build. Mater.*, 131(2017), 476-484.
- [55] M. Wyrzykowski, A. Assmann, C. Hesse, P. Lura, Microstructure development and autogenous shrinkage of mortars with CSH seeding and internal curing, *Cem. Concr. Res.*, 129 (2020), 1-12.
- [56] M. Valcuende, E. Marco, C. Parra, P. Serna, Influence of limestone filler and viscosity-modifying admixture on the shrinkage of self-compacting concrete, *Cem. Concr. Res.*, 42, 4 (2012), 583-592.
- [57] Y. Tan, H. Chen, Z. Wang, C. Xue, R. He, Performances of Cement Mortar Incorporating Superabsorbent Polymer (SAP) Using Different Dosing Methods. *Materials*, 12, 10 (2019), 1-13.
- [58] F. A. Neville, J. J. Brooks, *Tecnologia do concreto*. Bookman, Porto Alegre, RS, Brazil, 2013.
- [59] P. F. Reis, F. Evangelista Jr, E. F. Silva, Profile of internal relative humidity and depth of drying in cementitious materials containing superabsorbent polymer and nano-silica particles. *Constr. Build. Mater.*, 237 (2020), 1-9.
- [60] K. Venkateswarlu, S. V. Deo, M. Murmu, M. Overview of effects of internal curing agents on low water to binder concretes. *Mater. Today-Proc.* (2020).
- [61] J. Yang, Y. Guo, A. Shen, Z. Chen, X. Qin, M. Zhao, Research on drying shrinkage deformation and cracking risk of pavement concrete internally cured by SAPs, *Constr. Build. Mater.*, 227 (2019), 116705.
- [62] H. Beushausen, M. Gillmer, The use of superabsorbent polymers to reduce cracking of bonded mortar overlays, *Cem. Concr. Comp.*, 52 (2014), 1-8.
- [63] O. M. Jensen, P. F. Hansen, Water-entrained cement-based materials: II. Experimental observations, *Cem. Concr. Res.* 32, 6 (2002), 973-978.
- [64] J. Liu, N. Farzadnia, C. Shi, X. Ma, Shrinkage and strength development of UHSC incorporating a hybrid system of SAP and SRA, *Cement and Concrete Composites*, 97 (2019), 175-189.

- [65] A. Assmann, Physical properties of concrete modified with superabsorbent polymers, Dissertation of master degree. Stuttgart University, Germany, 2013.
- [66] Y. Yao, Y. Zhu, Y. Yang, Incorporation superabsorbent polymer (SAP) particles as controlling pre-existing flaws to improve the performance of engineered cementitious composites (ECC), *Constr. Build. Mater.*, 28, 1 (2012), 139-145.
- [67] N. L. Nunes, A. D. de Figueiredo, Retração do concreto de cimento Portland, *Boletim Técnico da Escola Politécnica da USP, Departamento de Engenharia de Construção Civil; BT/PCC/452EPUSP, São Paulo*, 1-59, 2007.
- [68] A. Pourjavadi, S. M. Fakoorpoor, A. Khaloo, P. Hosseini, Improving the performance of cement-based composites containing superabsorbent polymers by utilization of nano-SiO₂ particles, *Mater. Des.* 42 (2012), 94-101.
- [69] J. C. D. Santos, M. M. Tashima, M. R. de Moura, F. A. Aouada, Obtainment of hybrid composites based on hydrogel and Portland cement. *Química Nova*, 39, 1 (2016), 124-129.
- [70] S. H. Kang, S. G. Hong, J. Moon, Absorption kinetics of superabsorbent polymers (SAP) in various cement-based solutions. *Cem. Concr. Res.* 97, 7 (2017), 73-83.
- [71] S. L. Cilli, H. C. Silva, A. Watanuki Filho, M. R. D. M. Aouada, F. A. Aouada, Otimização de metodologia de obtenção de pastas cimentícias contendo hidrogéis. *J. Exp. Tech. Instrum.* 2, 1, (2019), 1-9.
- [72] R. Garg, R. Garg, M. Bansal, Y. Aggarwal, Experimental study on strength and microstructure of mortar in presence of micro and nano-silica, *Mater. Today*, (2020), 1-9.



CHAPTER 7

FINAL CONSIDERATIONS

*“Final considerations, future perspectives,
impacts and economic, social relevance”*

7.1 FINAL CONSIDERATIONS

Hybrid hydrogel nanocomposites based on polyacrylamide, carboxymethylcellulose, and different Cloisite Na⁺ concentrations (0%, 10%, and 20% wt/ wt of acrylamide+CMC) were successfully reproduced in their synthesis.

From FTIR and SEM techniques, it was possible to observe that the nanoclay was incorporated into the polymeric matrix and to verify some modifications in the hydrogel microstructure when swollen solution from the filtrate of the water+cement mixture. Some hydration products resulting from cement hydration were found impregnated on the hydrogel surfaces. The presence of groups of CO₃²⁻ confirmed them and SO₄²⁻ related to carbonatation and ettringite formation. XRD patterns also indicated the presence of these products in hydrogels swollen in solution from the filtrate of the water+cement mixture

Notably, XRD patterns indicated that the amorphous character of the hydrogel in the nanocomposites was discrete. In addition, the basal spacing of the nanoclay peak in the polymeric matrices was not observed, indicating that its platelets are probably exfoliated in the hydrogel chains when these hydrogels are swelled in a filtrated solution of water+Portland mixture. That confirms a satisfactory interaction between organic and inorganic compounds during the synthesis process.

The results also showed that the presence of Cloisite Na⁺ interferes directly with the absorption mechanism in both swelling media. Thus, comparing the hydrogels swollen in distilled water, the nanocomposites, when placed in water and cement solution, presented an increase of 22.02, 10.03, and 20.46% in the degree of swelling of the hydrogel with 0, 10, and 20% Cloisite Na⁺ concentrations respectively. This improvement can be related to the solvation process where some cement solution ions can associate with water molecules provoking an expansion of the hydrogels chain.

The physicochemical characterization of the hydrogels contributed to the development of the dosages used in this study. From the understanding of the swelling degree, it was possible to optimize the amount of water to maintain the w/c ratio constant. Moreover, the release kinetics also contributed to understanding their effect on the physical and mechanical properties of the mortars studied. For instance, the increase in the concentration of nanoclay into hydrogel caused greater water retention by the polymer, reflecting significant reductions in exudation and slump flow, corroborating the results of increased water retention of mortars in the fresh state.

Although these changes directly affect the workability of mortars, which could be solved with plasticizer admixtures, the water retention and release of water somewhat controlled by the polymer is satisfactory for maintaining the internal humidity of the cement matrix. This is very interesting for plastic shrinkage reduction, reduction of voids, and improvements in mechanical properties at later ages. In this sense, it was observed that the mortar produced with the highest nanoclay content (AHN20) was the one that presented the best performance concerning the others tested. These same mortars also showed mechanical strengths statistically similar to the control (ACTR), even under wet curing conditions that possibly kept the hydrogels swollen until the test was performed. This is a positive indication that the concentration of nanoclay in the polymeric matrix acts as a reinforcing agent, minimizing the effects of strength loss since presoaked hydrogels are low-strength inclusions in the mortar mixture.

The amount and percentage of voids in the AHN20 mortar were also statistically similar to the control, reflecting improved or similar mechanical properties to the reference. It can also verify similar behavior in the mass loss and plastic shrinkage properties. The greater water retention by the hydrogel represents a lower shrinkage by the mortar, corroborating with water retention and exudation results. This is a good indication that the nanoclay concentration indeed contributes to a more controlled release of water by the hydrogel.

In summary, from the results, it was possible to conclude that hybrid nanocomposite hydrogels have great applicability in the civil industry, especially as internal curing agents. This may bring benefits related to more effective curing procedures, improvements in cement hydration processes, and consequently increasing the performance and durability of these materials.

7.2 FUTURE PERSPECTIVES

To further contribute to the understanding of the study, the following future perspectives are presented:

- ✓ To synthesize, characterize, and apply hybrid nanocomposite hydrogels with natural clays. In addition, to use other reinforcement elements (ashes, fibers) to synthesize hydrogels and evaluate their effects on their hydrophilic properties.

- ✓ To evaluate the absorption and release kinetics of the hydrogels when applied in dry and swollen states into cementitious materials. In addition to understanding the internal hydration mechanisms carried out.
- ✓ To analyze the microstructure of cementitious materials using other techniques such as microtomography, permeability, porosity, among others.
- ✓ To evaluate the contribution of these hydrogels in the freeze-thaw properties
- ✓ To verify aspects of degradation and cycles of absorption and release over time within cementitious matrices.

7.3 IMPACTS AND ECONOMIC, SOCIAL RELEVANCE

This study showed that the hybrid nanocomposite hydrogel in construction could contribute considerably to the economic aspects. This type-material can reduce water consumption during cementitious matrices because the traditional curing process requires a large amount of water during the hardening stage. Another factor is the characteristics of the materials produced with these nanocomposites. The constructions can have improved durability and performance, extending their useful life since pathologies related to shrinkage can be minimized with their application.

The environmental relevance is based on the use of more biodegradable raw materials in the production of hydrogels, such as polysaccharides in their matrix. In this sense, we also highlight reducing water waste during the curing process since a small amount of polymer applied can ensure the necessary moisture to cure the cementitious material internally. Another aspect is the durability that also reflects on the environmental aspect in better performance of buildings because by extending its life, there is a lower generation of construction waste.

The social relevance is in disseminating and popularizing scientific studies since the application of new materials such as hydrogels in the construction industry. Additionally, improving traditional procedures by facilitating their execution can lead to the dissemination of new concepts to society, highlighting the importance of research and science to improve existing procedures. Therefore, the material developed and applied in this work has notable environmental, social, and economic relevance as a consequence.

ACKNOWLEDGMENTS

“This study was financed in part by the Coordenação de Aperfeiçoamento de Pessoal de Nível Superior – Brasil (CAPES) – Finance Code 001”.